LOW MOLECULAR WEIGHT PROTEINS OF MUSTARD SEED (*Brassica juncea*): STRUCTURE, FUNCTION AND INTERACTION WITH INTRINSIC LIGANDS

A THESIS SUBMITTED TO THE UNIVERSITY OF MYSORE FOR THE DEGREE OF DOCTOR OF PHILOSOPHY IN *BIOCHEMISTRY*

By

JYOTHI T. C.

Department of Protein Chemistry and Technology
Central Food Technological Research Institute
Mysore – 570020
India

May 2007

DECLARATION

I, Jyothi T. C. certify that this thesis is the result of research work done by me under the supervision of **Dr. A. G. Appu Rao** at **Department of Protein Chemistry and Technology**, **Central Food Technological Research Institute**, Mysore, India. I am submitting this thesis for possible award of ***Doctor of philosophy*** **(Ph. D) degree** in ***Biochemistry*** of the **University of Mysore.**

I further declare that this thesis has not been submitted by me for award of any other degree/diploma of this or any other university.

Signature of Doctoral candidate

Signed by me on 28th May 2007

Signature of Guide

Date: Counter signed by

Signature of Chairperson/Head of Department/
Institution with name and official seal

ABSTRACT

Napin from *Brassica juncea,* oriental mustard, is highly thermostable, proteolysis resistant and allergenic in nature. It consists of two subunits - one small (29 amino acid residues) and one large (86 amino acids residues) - held together by disulfide bonds.

The role of disulfide linkages, electrostatic as well as hydrophobic interactions on napin stability was investigated through spectroscopic methods. The subunits are hydrophilic in nature and possess extended structure. With the addition of 0.5 M NaCl, surface hydrophobicity of napin decreases, while the helical content increases by 25%. In presence of NaCl, emission maximum shifts towards shorter wavelength and the Stern-Volmer constant decreases from 6.5 M^{-1} to 3.4 M^{-1}, indicating compaction of napin. Na_2SO_4 has no significant effect on the structure due to lack of hydrophobic core. In presence of monohydric alcohols and trifluoroethanol, there is an increase in ordered structure. The study indicates that the structure of napin, which is hydrophilic in nature, is stabilized by electrostatic interactions, in addition to disulfide linkages.

Thermal unfolding is characterized by a three state transition with T_{M1} and T_{M2} at 50.5°C and 62.8°C, respectively; $\triangle C_{P1}$ and $\triangle C_{P2}$ are 2.05 kcal mol^{-1} K^{-1} and 1.40 kcal mol^{-1} K^{-1}, respectively. In the temperature range 37 – 45°C, the molecule undergoes dimerisation. Isothermal equilibrium unfolding by guanidinium hydrochloride also follows a three state transition, $N \leftrightarrows I \leftrightarrows U$ with $\triangle G_{1H2O}$ and $\triangle G_{2H2O}$ values of 5.2 kcal mol^{-1} and 5.1 kcal mol^{-1} at 27°C,

respectively. Excess heat capacity values obtained, are similar to those obtained from DSC measurements. There is an increase in hydrodynamic radius from 20 Å to 35.0 Å due to unfolding by guanidinium hydrochloride. *In silico* alignment of sequences and homology modeling of napin has revealed that the internal repeats (40%) spanning residues 31 to 60 and 73 to 109 are conserved in all *Brassica* species. The internal repeats may contribute to the greater stability of napin.

The factors responsible for the binding of sinapic acid, phytic acid and allyl isothiocyanate ligands with napin have been studied by spectroscopic methods. Sinapic acid and phytic acid binds to napin with a binding constant of 3.5×10^3 and 1.6×10^5 M^{-1} respectively. The available lysine content of napin – allyl isothiocyanate complex decreased significantly from 6 mole/mole to 1.8 mole/mole of napin. Phytic acid and allyl isothiocyanate induces the conformational change in napin structure. Microenvironment of tyrosine in napin changed upon binding to allyl isothiocyanate.

ACKNOWLEDGEMENTS

I am extremely grateful to my guide Dr. A. G. Appu Rao, Head, Protein Chemistry and Technology, CFTRI, Mysore, India for his helpful guidance and constant encouragement throughout the investigation. In particular his words of encouragement when things went wrong have been of great help.

My thanks are due to Dr. V. Prakash, Director, CFTRI, Mysore for providing the necessary facilities to carry out the research work in the institute and permitting me to submit the results in the form of a thesis.

It is my pleasure to thank Dr. Sridevi Annapurna Singh, for CD experiments, data analysis and also for her constant support during the course of investigation.

It is my sincere duty to acknowledge the help rendered by Prof. A. Surolia, MBU, IISc, Bangalore, for allowing me to use laboratory facilities. My thanks are also to Dr. Lalitha R. Gowda for helping me with HPLC, amino acid analysis and amino-terminal sequencing.

I wish to express my sincere thanks to all my colleagues, in the department, both past and present, for cooperation and ambient atmosphere all through my research.

My sincere duty to record my thanks to Mr. P. S. Kulasekhar for rendering help to make improvements to the presentation of the material in the thesis.

Finally I am deeply indebted to my parents, husband, in laws and brothers who were a constant source of support and encouragement in this endeavor.

CSIR, New Delhi, is gratefully acknowledged for the financial support in the form of fellowship.

JYOTHI T. C.

CONTENTS

ABBREVIATIONS

ΔC_P	Excess heat capacity
ΔG	Free energy
ΔH_C	Calorimetric enthalpy
ΔH_V	van't Hoff's enthalpy
AIT	Allyl isothiocyanate
ANS	8- aniline naphthalene sulfonic acid
ASA	Accessible surface area
CD	Circular dichroism
CPA	cis-Parinaric acid
CAPS	3-[cyclohexylamine]-1-propane sulfonic acid
DSC	Differential scanning calorimetry
DTT	Dithiothreitol
EDC	1-ethyl-3- (3-dimethyl amino propyl) carbodiimide
GdnHCl	Guanidine hydrochloride
HPLC	High performanance liquid chromatography
kcal	kilo calories
kDa	kilo Dalton
K_I	Inhibition constant
MALDI-TOF	Matrix Assisted Laser Desorption ionization-Time of Flight
Na_2SO_4	Sodium sulphate
NaCl	Sodium chloride
NBS	N-bromosuccinamide
PAGE	Poly acrylamide gel electrophoresis

PRODAN	6-propionyl-2- (N, N-dimethylamino) naphthalene
PVDF	Polyvinyl difluoride
RP	Reverse Phase
SDS	Sodium dodecyl sulphate
TCA	Trichloroacetic acid
TFA	Trifluoroacetic acid
TFE	Tri fluoroethanol
TI	Trypsin inhibitor
TLCK	tosyl lysine chloro methyl ketone
T_M	Transition temperature
TFE	Trifluoroethanol
TNBS	Trinitrobenzene sulfonic acid
TNS	2-p-toluidinylnaphthalene –6-sulfonate
TPCK	tosyl phenylalanine chloromethyl ketone

LIST OF TABLES

LIST OF FIGURES

INTRODUCTION

INTRODUCTION

Cereals and legumes are major part of the human diet all over the world. The population in developing countries depends on seed protein for their entire protein requirements. Seed storage proteins are chief dietary proteins for half of the world population (Mandal and Mandal, 2000). The proteins present in seeds are of two type: metabolic proteins, both enzymatic and structural, which are concerned in cellular activities including the synthesis. Second type, storage proteins, together with reserves carbohydrates or oils, is synthesized during seed development. They function during seed germination and provide nitrogen and carbon for the developing seedling. The storage proteins occur within the cell in discrete protein bodies. Seed proteins are deficient in lysine and sulfur containing amino acids (De Clercq, et al., 1990).

Storage proteins utilized during germination of the seed are known for their nitrogen reserves. They provide necessary amino acids and amide nitrogen to the growing plant during the initial stages of germination (Barciszewski et al., 2000) and account for about 50% of the total proteins in mature seeds. The amount of protein present in seeds varies from 10% (in cereals) to 40% (in legumes). Storage proteins are generally rich in asparagine, glutamine and arginine or proline. The globulins are deficient in the sulphur containing amino acids - cysteine, methionine and tryptophan while cereals generally lack lysine, threonine and tryptophan.

Seed storage proteins are commonly present in the mature seed in discrete deposits called protein bodies. All storage protein fractions are mixtures of components that exhibit polymorphism both within single genotypes and among genotypes of the same species (Shewry et al., 1995). Little is known about the organization of storage proteins within protein bodies. This arrangement is important in efficient use of storage space and facilitating mobilization of storage proteins during germination.

The seed storage proteins on the other hand, have the sole purpose of providing amino acids to the seedling growth (nitrogen and sulphur source). Seed storage proteins distinguish themselves from other proteins - they accumulate in high amounts in seed, during mid-maturation stage of seed development and are used up during germination. These are synthesized only in the seed (in cotyledon or in endosperm) and not in other tissues. They are deposited mostly in special storage organelles called protein bodies.

Seed storage proteins were among the earliest of all proteins to be characterized. Wheat gluten was first isolated in 1745, and Brazil nut globulin was crystallized in 1859. Storage proteins are classified on the basis of their sedimentation coefficient (S). The sedimentation coefficient (Svedberg units, S) of a macromolecule is calculated by dividing the speed of sedimentation to acceleration applied. Osborne (1924) grouped storage proteins on the basis of their extraction and solubility in water (albumins), dilute saline (globulins), alcohol/water mixtures (prolamins), and dilute acid or alkali (glutelins). The major seed storage proteins include albumins, globulins, and prolamins. Globulins (7S and 11S) and albumins (2S) are the storage proteins of dicots

(e.g., pulses), whereas prolamins and glutelins are major proteins in monocots (e.g., cereals).

Globulins are a widely distributed group of storage proteins. They are present not only in dicots but also in monocots and fern spore (Templeman et al., 1987). They can be divided into two groups based on their sedimentation coefficients, the 7S vicilin - type globulins and the 11S legumin-type globulins. Both groups show variation in their structures, attributable partly to post-translational processing. The globulin storage proteins have been studied in legumes, especially peas, soybean, broad bean and french bean. The 11S (legumins) proteins are the major storage proteins in legumes (*Brassica* and cucurbits) and cereals (oats and rice). The mature 11S protein consists of six non-covalently interacting subunits. Each subunit pair in turn consists an acidic subunit of M_r ~ 40,000 Da and a basic subunit of M_r ~20,000 Da, linked by a single disulfide bond (Shewry et al., 1995). While albumin and globulin storage proteins are widely distributed in flowering plants, the prolamins are restricted to one family, the grasses, which include the major cereals.

The 2S albumins are proteins grouped on the basis of their sedimentation coefficients ($S_{20.w}$) (Youle and Huang, 1981). They are widely distributed in dicot seeds. Recent interest in 2S albumins directed towards their exploitation in genetic engineering. Altenbach et al (1987,1992) used 2S albumin of Brazil nut, which is rich in methionine (Youle and Huang, 1981) to increase the methionine content of tobacco seeds up to 30%. Tabe and co-workers have used the methionine rich sunflower 2S albumin to increase the methionine content of forage grasses (Tabe et al., 1993).

The seed storage proteins are secretory proteins synthesized with a signal peptide and cleaved as the protein is translocated into the lumen of the endoplasmic reticulum (ER). Secretory proteins assume their folded conformations within the lumen of the ER, which is also the site of disulfide bond formation. Molecular chaperones of the HSP_{70}/BiP family may facilitate folding by binding transiently to the nascent polypeptides and may prevent the formation of incorrect inter- or intramolecular interactions. 2S albumins, 7S and 11S globulins of legumes are transported via the Golgi apparatus to the vacuole, which fragments to form protein bodies. The 7S and 11S globulins are present in the same protein bodies with no spatial separation. In other dicots, such as pumpkin, sunflower, *Brassica*, and castor bean, 2S albumins are stored together with 11S globulins (Shewry et al., 1995; Shewry and Halford, 2002).

Seed storage proteins are isolated by extracting crushed whole seeds or seed meals resulting from oil extraction with a low salt buffer. The fractionated proteins are further purified by a combination of methods such as heat and isoelectric precipitation, ammonium sulphate fractionation, gel filtration and ion exchange chromatography.

Mustard

Mustard belongs to the family of *Brassicaceae* (Cruciferae) and is a dicot and an herbaceous plant. Leaves are alternate and simple lobed. Inflorescence is raceme. Flowers are less conspicuous, bilaterally symmetrical and fruit is a silique (long) or a silicle (broad) (Figure 1). Mustard is an important oilseed of India (Table 1) and cultivated extensively in the

A

B

Figure 1. Mustard plant

A: Mustard plant **B:** Mature mustard seeds.

Table 1: Production of oilseeds in India

Oilseeds	Production (MMT)
Groundnut	4.4
Mustard	7.6
Soybean	8.7
Safflower	1.98
Sunflower	1.21
Sesame	1.23
Cotton	0.83
Castor	0.55

(***Source:*** *Ministry of agriculture, India, 2006 - 2007*)

states of Rajasthan, Uttar Pradesh, West Bengal, Madhya Pradesh and Punjab (Thiyam, 2003). India produces ~7.6 MMT of mustard and is the second major oil seed crop. *Brassica juncea* or Indian/oriental mustard is the major mustard variety grown in India.

Mustard seed contains about 35 - 40% oil and 20 - 25% protein (Table 2). The defatted meal contains 35 - 45% protein (Prakash and Rao, 1986; Batra et al., 2001). The high molecular weight protein fraction constitutes about 25% and low molecular weight constitutes about 70% of the total proteins (Aruna and Appu Rao, 1988). 2S albumins, widely distributed in dicot seeds, are especially abundant in the *Brassicaceae* family. The intrinsic ligands present in the mustard seeds are phenolic acids, phytic acid and glucosinolates. Interaction of intrinsic ligand with proteins reduces the nutritional quality.

The quality seed protein depends on how far its amino acid composition matches with the balanced amino acid composition. Mustard protein has a well-balanced amino acid profile and a favorable protein efficiency ratio of 2.64 compared to 2.19 for soybean, which is rich in essential amino acids (Delisle et al., 1984).

Reports are available in the literature on the biological activities of mustard seed proteins. Angiotensin converting enzyme (ACE) inhibitory peptides have been isolated from mustard protein digested with subtilisin as reported by Marczak et al (2003). Inhibitors for the human immunodeficiency virus (HIV) are obtained by hydrolyzing the mustard proteins isolate with endoprotease alcalase (del Mar Yust et al., 2004).

Table 2. Composition of whole Mustard

Component	Content (%)
Oil	35 – 40
Protein	20 – 25
Moisture	6 – 8
Crude fibre	12 – 17
Ash	7 – 8
Protein (Defatted meal)	35 – 45
Phenolic acid	0.6 – 1.3
Phytic acid	0.6 – 0.95
Glucosinolates	0.2 – 0.6

(*Prakash and Rao, 1986*)

Major seed storage proteins are often given names after the genus/species/family, in which they occur, e.g., zein in maize, hordein in barley and helianthinin in sunflower (Crouch et al., 1983). The seed storage proteins of mustard are cruciferin (12S globulin) and napin (2S albumin).

Cruciferins

Cruciferin (12S globulin) is a large, neutral, oligomeric protein synthesized in *Brassica* seed during seed development (Rödin and Rask, 1990). Cruciferin (molecular weight of 300 kDa) is an oligomeric protein with six subunits. Each subunit is composed of an acidic and a basic subunit, linked by a disulfide bond. The Stokes radius (by quasi-elastic light scattering) is found to be R_S = 5.7 nm (Schwenke et al., 1980). These proteins are situated in rough endoplasmic reticulum. Cruciferin subunits are rich in aromatic amino acids with 5 tryptophan and 10 tyrosine residues per molecule, and with a molecular weight of ~54 kDa (Figure 2). A conserved sequence (of 42 amino acid residues) spanning from 119 to 160, rich in glycine and glutamine is present in each subunit (Shaw and Ryan, 1989).

The secondary structure of cruciferin is characterized by a low (11%) content of α - helix and a relatively high (31%) content of β - structure. Myrosinase, responsible for the pungent odor of mustard, is associated with the high molecular weight 12S protein (Gururaj Rao, 1980).

Cruciferins are susceptible to trypsin, chymotrypsin and papain hydrolysis. These proteins can be dissociated either by urea or guanidinium

```
    1          11         21         31         41        51
  1 MARLSSLLSF SLALLTFLHG STAQQFPNEC QLDQLNALEP SHVLKAEAGR IEVWDHHAPQ 60
 61 LRCSGVSFVR YIIESKGLYL PSFFSTARLS FVAKGEGLMG RVVLCAETFQ DSSVFQPSGG 120
121 SPFGEGQGQG QQGQGQGHQG QGQGQQGQQG QQGQQSQGQG FRDMHQKVEH IRTGDTIATH 180
181 PGVAQWFYND GNQPLVIVSV LDLASHQNQL DRNPRPFYLA GNNPQGQVWI EGREQQPQKN 240
241 ILNGFTPEVL AKAFKIDVRT AQQLQNQQDN RGNIIRVQGP FSVIRPPLRS QRPQEEVNGL 300
301 EETICSARCT DNLDDPSNAD VYKPQLGYIS TLNSYDLPIL RFLRLSALRG SIRQNAMVLP 360
361 QWNANANAVL YVTDGEAHVQ VVNDNGDRVF DGQVSQGQLL SIPQGFSVVK RATSEQFRWI 420
421 EFKTNANAQI NTLAGRTSVL RGLPLEVISN GYQISLEEAR RVKFNTIETT LTHSSGPASY 480
481 GGPRKADA
```

Figure 2. Amino acid sequence of High molecular weight cruciferin (gDNA) from *Brassica napus* (CRUA_BRANA: Acc. No. P11090). Cruciferin alpha subunit (23-298) and cruciferin beta subunit (299-480). The disulfide bridge Cys_{105} and Cys_{305}. Signal peptide (1-22)

(*Shaw and Ryan, 1989*)

hydrochloride and the extent of dissociation depends on the concentration of the denaturant. Unfolding follows multi-state transition and protein aggregates at 80°C with T_M ~61°C. Cruciferin acquires compact structure at lower SDS concentration and dissociates at higher SDS concentration (Gururaj Rao and Rao. 1983).

Napins

Mustard napins are expressed, during seed development, as precursors and translocated into the endoplasmic reticulum where the intra chain disulfide bonds are formed (Gehrig et al., 1996; Muntz, 1998; Muren et al., 1996). Proprotein is then transported via the secretory pathway to the vacuole where the proteolytic cleavages occur, resulting in matured protein. Mature napin (molecular weight ~ 14 kDa) consists of two subunits (~ 4.5 kDa small subunit and ~10 kDa large subunit) held together by disulfide bonds.

The small subunit is composed of about 40 amino acids and the large subunit has about 90 amino acids residues. These two subunits are connected with two interchain disulfide bonds (Baszcynski and Barciszewski, 1999; Gehrig et al., 1996; Mandal et al., 2002). Napin is rich in - lysine and sulfur containing amino acids. These proteins are characterized by their strong basicity (Isoelectric point pI~11) mainly due to basic and amidated amino acids (Schmidt et al., 2004).

Napins are particularly interesting as they represent an excellent model for studying both expression of the particular family of plant genes and protein maturation processes in plant cells (Neumann et al., 1996[a]; Muren et al.,

1996; Mandal and Mandal, 2000). Understanding the structure, stability of these proteins, their biophysical and functional properties, is important before they become candidate for genetic engineering. Hence basic research is required for large-scale application of this protein.

Napin (14. 0 -14.7 kDa) belongs to multigene family encoded by 10 -16 genes and its primary structure is similar to each other. Napins (2S seed storage proteins), TIs, and allergenic seed proteins are products of distinct members of a multigene family evolved from a common ancestral gene (Mandal et al., 2002). An extremely high degree of homology among napin variants renders their separation and purification very difficult. The multigene proteins are identified by amino acid sequence analysis and mass spectrometry (Gehrig et al., 1996).

The polypeptide chain corresponding to cDNA sequence suggests that the initial translation product is a 20 kDa pre-cursor protein containing both the polypeptides of mature napins. First, an N-terminal signal peptide is cleaved off from the precursor, which is consequently cleaved in four other sites, yielding mature napins (Muntz, 1998).

Secondary structure of napin, exhibits ~50% α - helix with very a low β - structure content (Schmidt et al., 2004). Napin is fundamentally an all α - helix protein. The tertiary structure, determined by circular dichroism, has two positive and two broad negative bands. The UV - spectrum of napin has maxima at 278 nm with a shoulder at 288 nm (Menendez-Arias, 1986).

Interestingly, napin was found to have a structure similar to two other plant proteins, hydrophilic seed protein from soybean and nonspecific lipid transport protein found in maize, wheat & barley. Internal hydrophilic cavity could not be observed in napin similar to the lipid transport proteins. The high sequence homology among the napins and the similarity of their secondary structures confirmed by almost overlapping CD spectra, it was suggested that all napins and napin-like proteins belong to the same superfamily with a very similar three dimensional structure (Rico et al, 1996; Pantoja-Uceda, et al., 2004).

Napins are polymorphic proteins as they originate from multigene families. Their isolation from seeds renders micro-heterogeneous material not suitable for three-dimensional structure determinations by x - ray. Recently, NMR studies of napin like protein have been carried out. The small and large subunit molecular mass were determined to be 3.8 and 8.4 kDa respectively.

The NMR structure of *Brassica napus* napin as reported by Rico et al., (1996), reveals the presence of five amphipathic helices arranged in a right-handed super helix, which is also a characteristic folding motif found in all prolamin family proteins. The analysis of ^{1}H –assigned resonances of napin type 2S albumin showed that the small subunit is split into two α-helices (I & I^{l}) connected by non - helical region formed by two-four amino acid residues. This fragment bends to fit the helices III and IV of large subunit. The α-helix II of large subunit runs parallely with I & I^{l}. The short loop between helices III and IV is rich in glutamine residues.

Napin has 15 positive and 8 negative charges at neutral pH, including the two N- and C- termini. Nine positive charged side chains and four negative charges are conserved in all known low molecular weight napins. Polar residues, including the overabundant glutamines, are exposed to the solvent and hydrophobic residues are buried in the interior of the protein (Rico et al., 1996). Presence of single tryptophan in the small subunit and tyrosine in the large subunit of napin is shown in the figure 3B. The α-helices of large subunit forms a cleft in which the two helices of the small subunit fit relatively well. The global fold of the protein consists of four - helical motifs, whose helices are arranged in a right - handed super helix (Figure 3A).

Napins consist of two polypeptide chains, linked by interchain disulfide bonds (Ericson et al., 1986; Crouch et al., 1983). Despite differences in their subunit structure and synthesis, all the 2S albumins are compact globular proteins with, conserved cysteine residues (Figure 4).

Napins are composed of two intra and inter disulfide linkages with a motif:

.... $Cys_{(S)}$ .... $Cys_{(S)}$ .... /.... $Cys_{(L)}Cys_{(L)}$ .... $Cys_{(L)}$ x $Cys_{(L)}$ .... $Cys_{(L)}$ .... $Cys_{(L)}$....

Small subunit Large subunit

Two intermolecular disulfide bonds connecting small and large subunits are formed between the cysteines $Cys_{(S)}$ – $Cys_{(L)}$ and two-intra disulfide bonds are formed $Cys_{(L)}$ – $Cys_{(L)}$ (Pantoja-Uceda et al., 2004). This eight-cysteine motif is conserved in all the *Brassicaceae* family napins. The disulfide bridges in napin are similar to the other 2S albumins. The deduced amino acid sequence of *Brassica juncea* napin (figure 5) shows high sequence homology

A

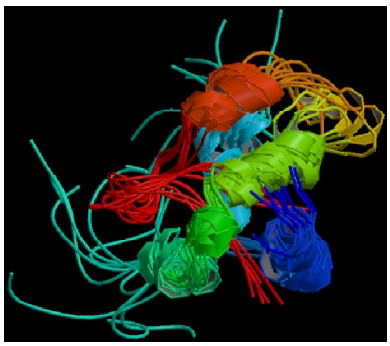

B

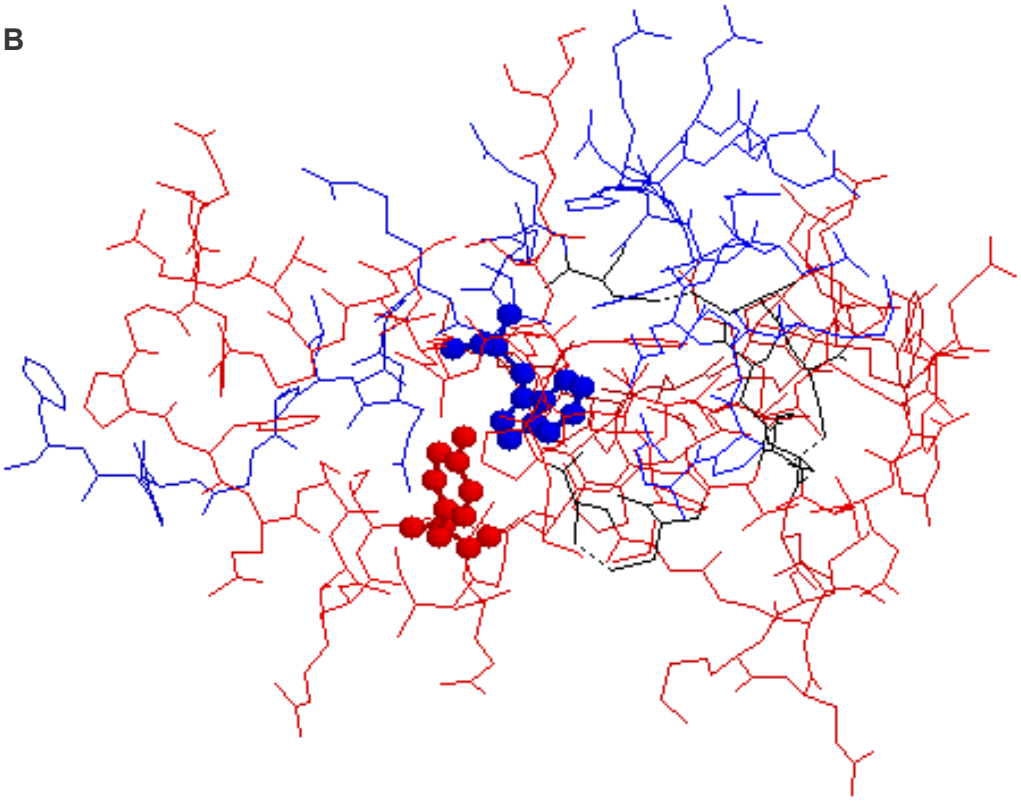

(*Rico et al., 1996*)

Figure 3. A: Solution Structure of mustard napin from *Brassica napus*. Ribbon structure of biological napin molecule, Pdb id: 1pnb **B:** Stick model of napin showing single tryptophan and tyrosine in small and large subunit respectively. The disulfide bonds are shown in black color. Rasmol 2.7.3 was used for the structure visualization of napin.

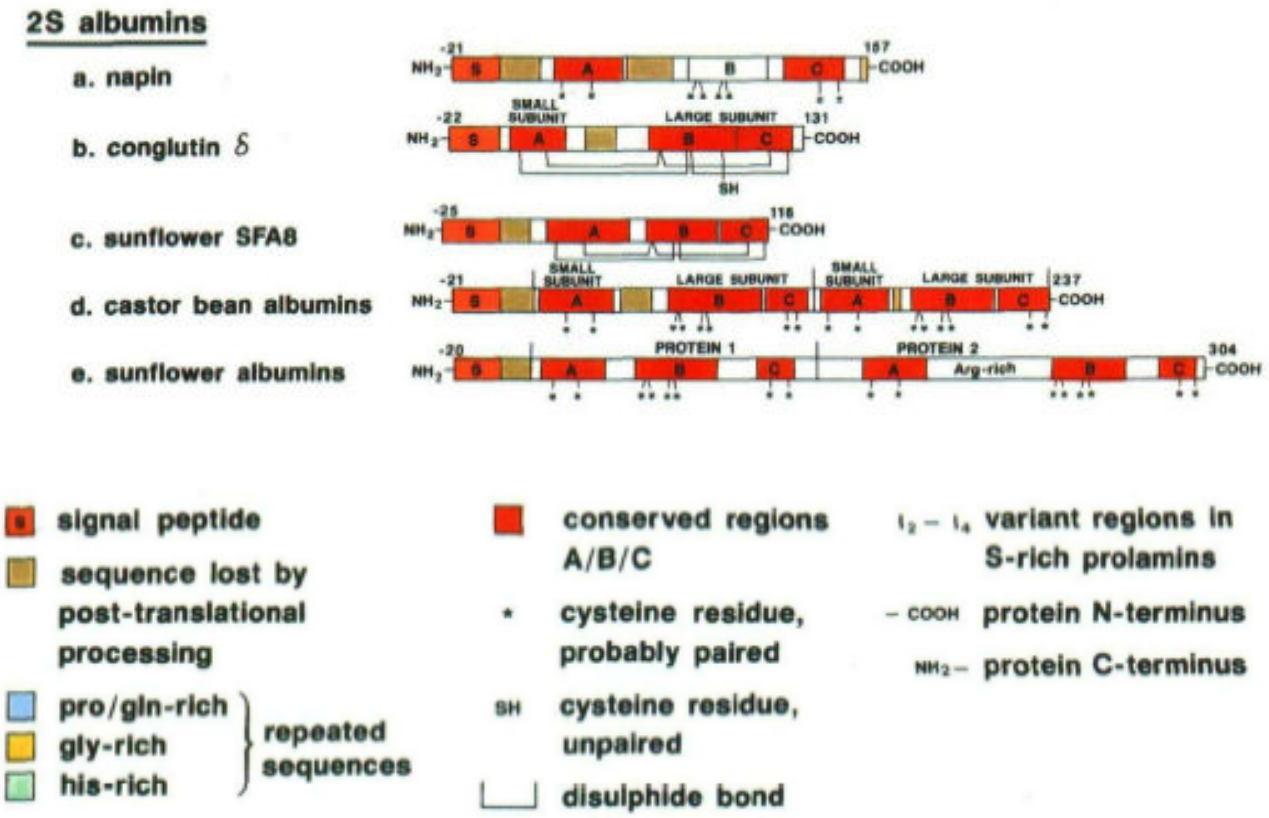

Figure 4. Schematic structures of the albumin family proteins (*Shewry, 1995*)

Small subunit

IPKCRKEIQQ AQHLRVCQQW LHKQAMQSG

LARGE SUBUNIT

SQGPQQRPPL LQQCCNELHQ EEPLCVCPTL

KGASKAVKQQ IQQQGQQQGK QQMVSRIYQT

ATHLPKVCNI PQVSVCPFQK TMPGPS

Figure 5. Deduced amino acid sequence of *Brassica juncea* napin.

GenBank Acc. No. - CAA46785.

(*Dasgupta et al., 1995*)

with other *Brassicaceae* napins (Dasgupta et al., 1995). The low molecular weight napin sequence shows ~ 85% homology among *Brassica* family (*B. campestris*, *B. oleracea*, *B. nigra*, *B. carinata*, *B. juncea*, *B. excelsia*, *B. napus*) and considerable homology with other napins

of castor bean, brazil nut, hazel nut, sunflower, cottonseed, peanut and trypsin inhibitor from barley. *Brassica* napin was cloned using oligodeoxyribonucleotide primers and polymerase chain reaction. The cloned sequence had 90% homology among the *Brassica* napin sequences (Dasgupta et al., 1993).

Napins contain 6% lysine and 9% cysteine. The deficiency could be remedied by use of napins in human nutrition. However, allergenicity of napin limits their utilization in food (Barciszewski et al., 2000).

Allergenic proteins

Allergenic proteins are thermally stable and resist digestion, retain sufficient structural integrity, to stimulate immune reactions. Resistance to proteolysis by digestive enzymes (at low pH) is one of the typical features of allergenic proteins (Astwood et al., 1996; Fuchs and Astwood, 1996).

Atopic allergy is a clinical disorder, which causes severe symptoms (skin rash, itching, sneezing, asthma, rhinitis) in human beings. More than 10% of the world population suffers from atopic Type I (very fast allergic response) allergy (Monsolve et al., 1993: Astwood et al., 1996). Stability to the enzyme hydrolysis may be a requirement to sensitization for these

important food allergens (Astwood et al., 1996). Proteins, which are resistant to proteolysis, (simulated by gastric fluid) are able to reach the gut immune system intact (Pantoja-Uceda et al., 2004). The napin storage proteins are one of the most important plant allergens that sensitize via the gastrointestinal tract.

Three major allergens Ara h 1 (64.5 kD), Ara h 2 (17.5 kD), Ara h 3 (14 kD), are abundant proteins in the peanut. Glycinin and β-conglycinin are the major allergenic proteins of soybean, which are involved in food hypersensitivity reactions (Breiteneder and Ebner, 2000; Breiteneder and Radauer, 2004). Plant allergenic proteins and their biological functions are tabulated in the Table 3.

Napins from mustard, castor bean, brazil nut, sunflower, peanut, and english walnut have shown to be type I allergy inducers, suggesting that this family of storage proteins is intrinsically allergenic (Monsolve et al., 1993). Allergy to peanut 2S is a significant health problem because of the high frequency of systematic allergic reactions.

The presence of more glutamine residues in the napin could also be one of the reasons for its allergenic potency. Kinnunen et al., have shown that the substitution of glutamine for other amino acids, increased allergenicity of the proteins and peptides (Kinnunen et al., 2003).

Monsalve et al., identified an allergenic epitope (Monsalve et al., 1993) region on *B. juncea* napin, which comprises 14 amino acid residues “QGPHVISRIYQTAT”. The hypervariable segment present in the napin

Table 3. Plant allergens with known biological functions

Protein classification	Allergen source/ allergen
Inhibitors of proteases and α-amylases	Soybean: Kunitz trypsin inhibitor family; cereals: trypsin/α-amylase inhibitors
Peroxidases	Wheat, barley
Profilins	Peanut *Ara* h 5, soybean, hazelnut, apple, pumpkin seeds
Seed storage proteins	
2S albumins	Oriental mustard: *Bra* j 1; yellow mustard: *Sin* a 1; Brazil nut: *Ber* e 1; English walnut: *Jug* r 1
Vicilins	Peanut: *Ara* h 1; English walnut: *Jug* r 2
Conglutins	Peanut: *Ara* h 2, *Ara* h 6, *Ara* h 7
Glycinins	Peanut: *Ara* h 3, *Ara* h 4; soybean
β-conglycinins	Soybean
Lectins	Peanut: agglutinin

(*Breiteneder and Ebner, 2000*)

structure constitutes an important antigenic region. This region is present in the segment connecting helices III and IV in napin, which forms an unstructured loop and the residues present in the loop are exposed to solvent.

The hypervariable region of

2S Ricin: ....VRVQGQHGPFQS….

2S Peanut: ....DRLQGRQQEQ…..

2S *Brassica*: …..QGPHVISRIYQTAT…..

(*B. juncea* napin)

The antigenic determinant in *B. juncea* involves the single tyrosine residue of the molecule, located on the large chain (Menendez-Arias et al., 1990). The immuno-dominant portion - hypervariable region - of napin is shown in the figure 6.

The important types of allergens of legumes and cereals are 2S albumin seed storage proteins and protease inhibitors (Breiteneder and Radauer, 2004). All plant food allergens are either protective or storage proteins. Bio-computational methodology can be used as a tool to identify protein allergenicity and non-allergenicity of amino acid sequences. This method compares the query sequence with the known allergenic amino acid sequences of protein.

It is important to study the physicochemical and structural characteristics that make protein an allergen. The compactness and stability

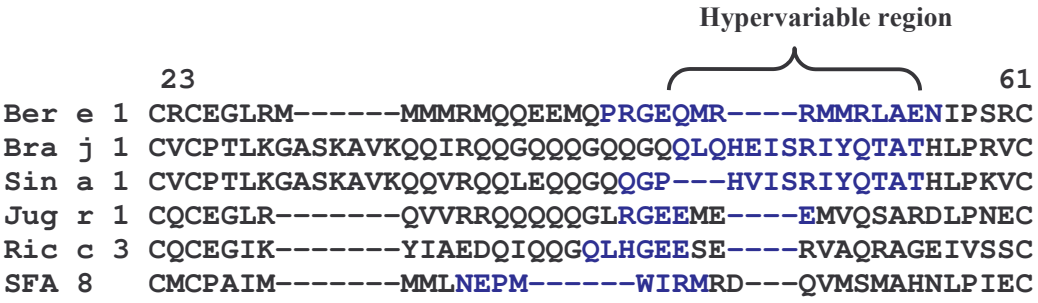

Figure 6. Hyper variable and epitope regions present in different 2S albumins. 2S albumin sequence from Ber e 1 – Brazil nut; Bra j 1-*Brassica juncea*; Sin a 1 – *Sinapis alba*; Jug r 1 – English walnut; *Ric* c 3 – Castor bean; SFA 8 – Sunflower, the amino acid residues in blue color represents the epitope region.

(*Moreno et al., 2005*)

are relevant aspects for the protein to be allergenic. Therefore, protein structure and stability can be interrelated to the allergenicity.

Oriental mustard (*B. juncea*) and yellow mustard are the food allergens, which can elicit allergenic reaction when ingested. The napin allergen is found to remain ~25% intact after the *in vitro* simulated gastric juice digestion. A peptide from the large subunit together with the disulfides and allergen epitope is found to remain even after 2h of digestion (Moreno et al., 2005). Moreno et al., has shown that the large subunit is more resistant to proteolytic attack than the small subunit as the intra disulfide bridges play an important role in holding the core protein structure together, even after extensive proteolysis. Proteolysis is not affected by preheating at 100°C, acid or neutral pH (Pantoja-Uceda et al., 2004; Moreno et al., 2005).

Brassica napus and Brazil nut napins have been shown to be resistant to pepsin in simulated gastric juice at pH 1.2 for longer than 60 and 15 min, respectively. The major 2S allergen from brazil nut is reported to be highly resistance to digestion by simulated gastric fluid (SGF). The digestion of napin with pepsin is not affected by preheating in either in acidic or neutral pH (Moreno et al., 2005). Protein remains undigested and conserves the antigenic epitopes of *B. napus* napin after the digestion with pepsin for an hour.

The accessibility of cleavage sites for pepsin, chymotrypsin and V8 protease was studied with napin precursor and matured napin from *B. napus*. A large number of the cleavage sites identified on the precursor, were

exposed to the exterior of the protein. However, mature napin exhibited resistance towards proteolysis (Muren et al., 1996).

The native napins can act as trypsin inhibitors. However, their inhibitory activity disappeared after reduction (Neumann et al., 1996[a] and 1996[b]; Gehrig 1996). Rapeseed napin inhibits trypsin with an IC_{50} value of 3 ± 1.5 μM. Dithiothreitol abolishes trypsin inhibitory activity, suggesting that subunits are poor inhibitors.

Brassica juncea napin is a seed storage albumin. Its precursor protein is a trypsin inhibitor (TI). The TI activity of the precursor is lost after being processed and converts into mature napin. The *B. juncea* coding sequence, has been expressed in *E. coli* cells, and produced the pronapin (precursor of napin). This produced pronapin also expressed TI activity like seed extract (Mandal et al., 2002).

The deduced amino acid sequence of the *Brassica juncea* gene shows the presence of soybean Kunitz TI active site-like motif GPFRI. The structure of mature *B. juncea* suggests TI- active GPFRI motif is location is on surface loop near the junction of the prosequence and the small subunit. During maturation this prosequence is cleaved and precursor loses TI activity. *B. juncea* TI gene has been introduced into tobacco and tomato plants, the expression levels of TI are comparable with the reported transgenic expression of soybean Kunitz TI, cowpea and barley TI. Napins can be expressed in seed crops at high levels in the non-seed parts and in seeds up to late maturation stage when insect damage is maximal, thus providing field

protection. Hence, this novel TI gene can be used as a highly effective insect control protein (Mandal et al., 2002).

In *Brassica* seeds, during the dehydration i.e., maturation stage, the TI would get processed to inactive storage protein, to yield a final low-level safer protein for human and animal consumption. The residual low-level TI activity remaining in the seeds may be enough to protect the dehydrated seeds (Mandal et al., 2002).

Napin stability

High solubility and stability of the napin are also the important factors for a protein to be allergenic (Astwood et al., 1996). The most intriguing, yet confronting question is how a protein folds into its compact, ordered and functionally active form (Sinha et al., 2005). To understand the structure and stability of napin, it is important to understand the nature of unfolding (Nicholson and Scholtz, 1996; Pradeep and Udgaonkar, 2004).

Studies on protein stability explore the sequence – structure – stability relationship. Sequence defines structure, whose interactions with each domains/subunits afford stability to the protein (Razvi and Scholtz, 2006; Grimsley et al., 2003). The effect of temperature and denaturants on the protein structure is useful in determining the stability of protein. Precise revelation of thermodynamic stability and conformational stability contribute to the prediction of napin structure.

The analysis of thermal unfolding data provides an estimate of the conformational stability of a protein. Analysis of denaturant induced unfolding

data provides the stability of a protein in a solution. Equilibrium denaturation studies have been very useful in understanding the structure, stabilization and folding of proteins.

The stability of napin from *B. juncea* was studied in denaturing agents such as in 10 M urea, 1% SDS and also over a wide range of pH (3 - 11) and temperature. The study reveals that napin is stable in denaturing agents and over a wide range of pH and temperature (Mandal et al., 2002; Schmidt et al., 2004).

The structural stability of *Brassica napus* napin (in solution) was studied by microcalorimetry (Krzyzaniak et al., 1988). The thermodynamic data showed that the napin is very stable since its transition temperatures at pH 6 and 3 are 100.3°C and 80°C, respectively. The two consecutive transitions were attributed to two different folding domains. Napin underwent limited thermal unfolding as followed by circular dichroism (Krzyzaniak et al., 1988). All the secondary structure could be recovered after cooling back to 20°C, indicating its high thermal stability (Krzyzaniak et al., 1988). No significant change in the secondary structure of the napin was observed in the pH range 3-11 also solubility of napin was not affected in the range (Schmidt et al., 2004).

Napins are structurally homologous and heterodimeric (small and large subunits of ~ 4 kDa and 9 kDa respectively) proteins. The cysteine residues are conserved - which form four disulfide bonds and hold two subunits together and contribute to their stability. This rigid structure may be responsible for the stability of napin to proteolytic attack. The effect of pH (3 -

11) on tertiary conformation of napin has been studied by fluorescence spectroscopy. No obvious changes in the fluorescence emission maxima are observed in the test pH range and it can be concluded that the structure of napin is not sensitive to pH (Schmidt, et al., 2004).

There are a few quantitative study of heterodimer protein unfolding. Unfolding of heterodimeric protein is challenging over monomeric proteins (Sinha et al., 2005). The unfolding of monomer proteins involves only intrasubunits interactions, whereas heterodimer proteins are stabilized by intra and intersubunit interactions (Neet and Timm, 1994). The thermodynamic stability of heterodimer protein has been determined by differential scanning calorimetric and equilibrium unfolding measurements. The unfolding of these proteins establishes the role and the contribution of intersubunit interactions to their stability.

Differential scanning calorimetry (DSC) of proteins provides information on the cooperativity of thermal unfolding and energy of stabilization. The thermodynamic parameters ΔH (enthalpy change) T_M (mid point of transition) may be obtained directly for the protein thus, enabling the calculation of free energy (ΔG) of stabilization. Cooperative units participating in unfolding can be analyzed by comparing the calorimetric enthalpy (ΔH_C) measurements with the corresponding van't Hoff enthalpy (ΔH_V) (Becktel and Schellman, 1987; Lopez and Makhatadze, 2002).

Unfolding of protein may follow two-state or three-state transition. The two-state and three-state has been shown by energy landscape (Figure 7)

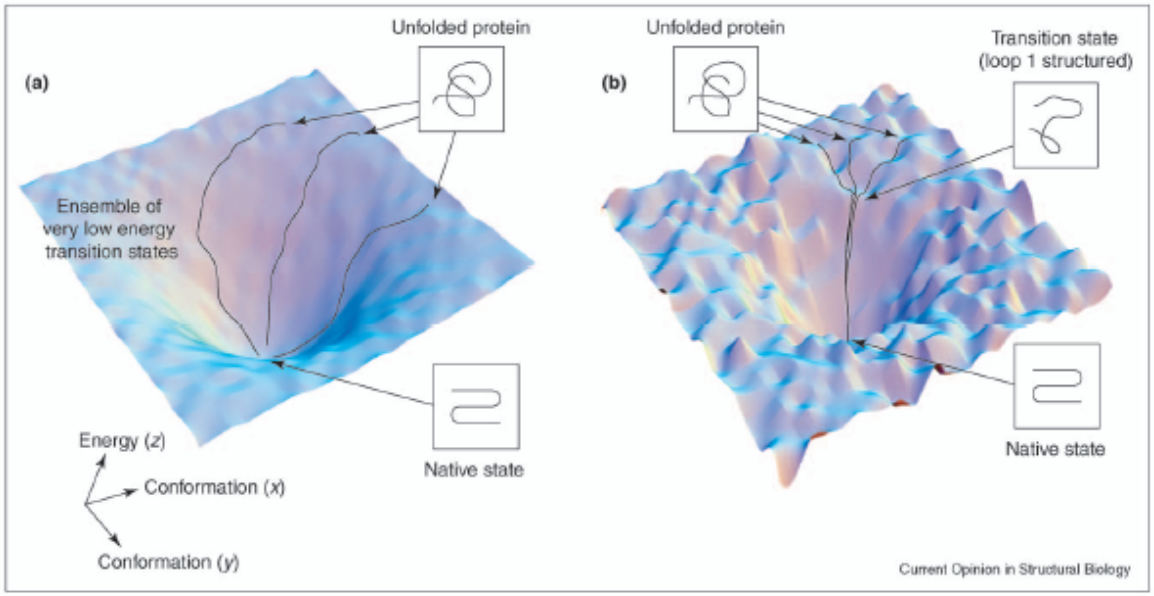

Figure 7. Energy landscape/funnel hypothesis diagram. The x- and y- axes represent hypothetical conformational coordinates. The z-axis represents energy. (**a**) Two-state unfolding (**b**) Three state unfolding

(*Deechongkit et al., 2006*)

or folding funnel hypothesis (Deechongkit et al., 2006). During thermal denaturation, protein may undergo unfolding or association. In case of heat shock protein, Hsp27, it has been reported that with increasing temperature, the molecule undergoes change in state of association of the molecule (Lelj-Garolla and Mauk, 2006).

Three-dimensional structures of proteins are often helpful in understanding the protein stability. Disulfide bonds stabilize the native structures of proteins (Anfinsen and Scheraga, 1975; Creighton, 1988). The disulfide bond engineered lysozyme variant unfolds at a temperature 23.4°C higher than wild type (Matsumura et al., 1989). The disulfide bridges in BBI play a prominent role in the stabilization of their reactive site configuration (Singh and Appu Rao, 2002).

Disulfide bridges of napin may play an important role on their conformation stability, since they must be stored for long periods of time, at least until the onset of germination. The various factors, other than disulfide bridges, contribute to the stability of proteins are domain- domain interactions, protein – protein interactions and internal repeats.

Even though the primary structure lacks disulfide linkages, lipoxygenase is found to be stable. The structure of soybean lipoxygenase consists of two domains, a smaller N-terminal and a major C-terminal domain. The domain interactions play essential role in the activity, stability and folding of lipoxygenase (Sudharshan and Appu Rao, 1999). Napin is a heterodimer, where the structure is stabilized by intersubunit interactions. The unfolding of

napins may throw light on the role as well as the contribution of intersubunit interactions to their stability.

Bowman - Birk inhibitors (BBIs) are small serine proteinase inhibitors with conserved array of seven disulfide bridges. The self-association of horse gram inhibitors is due to the interaction between the ε- amino group of Lys24 of one monomer and the carboxy-side chain of Asp76, of the other monomer. The self-association to form dimers, leads to the increased thermal stability and greater resistance to enzyme attack by stabilizing the conformation of BBI (Kumar et al., 2005).

Role of internal repeats in protein stability

Repetitions of amino acid sequence or structure in a protein are known as internal repeats. Detection of repeat in the protein is an arduous task. Internal repeats can vary from short amino acid (polyglutamine tracts of Huntington's disease) to large repetitions containing multiple domains. Repeats may be motifs or domains. The protein repeats based on their structural types can be classified into

1. All - β (WD40 – human protein)
2. All - α (Ankyrin, human erythrocyte protein)
3. Mixed α / β (leucine rich repeats)

Number of repeat proteins are involved in the protein – protein interactions. In some proteins, the presence of internal repeats helps in the functioning of antifreeze protein (Andrade et al., 2001).

Argos et al., had first identified the repeats in the plant storage protein of maize called 'zein' (Argos et al., 1982). The structure of the repeat bears little relation to its function, since it is the unusual composition of nitrogen rich amino acids, which is required for its seed germination properties. The amino acid repeats are arranged in a layer of helices packed in a hexagonal arrangement (Mastsushima et al., 1997). The internal repeats in the protein can be identified using web-based bioinformatics tools. Some of the internal repeats identified in proteins are tabulated in Table 4.

Insect and plant proteins protect themselves from freezing using repeats that impede ice formation (Liou et al., 2000). On the other hand, bacterial proteins use different types of repeat to favor the formation of ice as a mechanism of weakening an infected plant (Gurian – Sherman and Lindow, 1993). In case of TPR and ANK proteins, stability increases with increasing the number of repeat structures in the molecules (Main et al., 2005).

Structure of the protein is also stabilized by non-covalent interactions, apart from the disulfide bridges. The four non-covalent forces involved in the conformation are (Kyte, J., Structure in Protein Chemistry), van der Waals forces, hydrogen bonds, hydrophobic interactions and ionic interactions (electrostatic)

van der Waals interactions are the most important interaction, energetically and structurally, between molecules. All atoms and molecules attract each other, even in the absence of charged groups. This reciprocal interaction induces weak polarization effects and short-range interactions. Hydrogen bonds are formed when two electronegative atoms compete for the

Table 4: Internal repeats function and distribution

Repeat	Length	Structure	Function	Distribution
Ankyrin	33	α - Helix	Protein - Protein interaction	Eukaryotic-bacterial-viral
Bacterial glycosyl transferase	35	Unknown	Enzyme, Small molecules binding	Bacterial
Adenovirus fiber protein	15	Triple β- spiral	Protein - Protein interaction, bind s to host receptor	Viral
Major vault protein	52	Unknown	Multi-drug resistance	Eukaryotic
Flocculin	45	Unknown	Regulatory of flocculation	*S. cerevisiae*
Zein	20	α- Helix	Plant seed storage protein	Plants

(*Andrade et al., 2001*)

same hydrogen atom. The two types of hydrogen bands present in the molecules are inter and intra hydrogen band.

Hydrophobic and electrostatic interactions are also important parameters, which affect the proteins structures. In defining protein structure-function relationships, hydrophobic interactions play a major role due to its close correlation with protein stability (Schmidt et al., 2004; Nakai and Li-Chan, 1993).

Hydrophobic effect and hydrogen bonding mainly stabilize the protein structure. Hydrophobic interactions result in a tendency of non-polar atoms to interact with each other. Hydrophobicities of the individual amino acid side chains have been measured experimentally in a variety of ways. Because of the varying hydrophobicities of amino acid side chains, the neutral term 'hydropathy' is often used to describe their relative hydrophobicity (Jack Kyte, Structure in Protein Chemistry, 2007). Hydrophobicity of proteins is defined as the tendency of non-polar residues to adhere to one another in aqueous environment (Murphy, et al., 1990). Hydrophobic interactions in proteins play a major role in dictating conformation, solubility, ligand binding, aggregating properties etc., Some of hydrophobic residues in a protein may be buried in the interior, while others may be exposed at the surface, because of its specific folding pattern (Murphy, et al., 1990; Nakai and Li-Chan, 1993).

A number of studies have been carried out to understand protein hydrophobicity. The buried hydrophobic group of the protein is not accessible to surroundings; hence, effective hydrophobicity or surface hydrophobicity has

been proposed, in order to obtain better correlation with protein functionality (Alizadeh-Pasdar and Li-Chan, 2000).

Various methods have been used for experimental determination of protein hydrophobicity, which includes binding of hydrocarbons to proteins, reverse phase HPLC, and fluorescent probe method. Fluorescent probe methods are widely applied for rapid, routine determinations of surface hydrophobicity (Chaudhari et al., 1993).

The role of electrostatic interactions in structure stabilization or destabilization is studied by interaction of the protein with salt. It is difficult to compare the relative role of electrostatic interactions and hydrophobic interactions to the protein stability.

The effect of salts on the stability of proteins can be described in terms three different mechanisms, 1.The Hofmeister effect, 2. Debye - Hückel screening, and 3. Anion binding model. Protein stability also depends on the kosmotropic (stabilizes water structure) or chaotropic (disrupts water structure) nature of the salt. At low concentrations of salt, solubility of the proteins increases slightly (salting in). But at high concentrations of salt, the solubility of the protein drops sharply (salting out).

Organic solvents like monohydric alcohols induce protein denaturation by binding to hydrophobic groups of proteins (Herskovits et al., 1970). The addition of alcohols to protein solution induces α - helix structures, favors clustering of hydrophobic groups and more compactness in proteins (Arakawa and Goddette, 1985; Usha et al., 2006). Organic solvents including

monohydric alcohols induce protein denaturation by binding to hydrophobic groups of proteins (Herskovits et al., 1970). In the native state, alcohols bind to the surface of the protein molecule to some extent because protein contains mosaic of regions with different degree of hydrophobicity (Kuntz and Kauzmann, 1974). The progressive addition of alcohols to an aqueous protein solution induces α-helix with minimum residual globular structures (Arakawa and Goddette, 1985).

TFE is known as an intra-molecular hydrogen bond enhancer and protects solvent exposed hydrophobic residues from aggregating (Kentsis and Sosnick, 1998). The monohydric alcohol and TFE will enhance helix formation and is a frequent tool to study protein stability. TFE, a monohydric alcohol, at higher concentrations, destabilize protein tertiary structure and preserve protein secondary structure. At lower concentrations, it increases the propensity to form alpha helices in polypeptide chains. Latest studies have shown that low concentrations of TFE and other monohydric alcohols act by a kosmotropic mechanism which promotes desolvation of the polypeptide backbone, instead of directly strengthening hydrogen bonds or stabilizing helical structures. Monohydric alcohols like methanol and TFE induce higher helical structures in unfolded proteins than in folded states.

Biological function of napin

The major function of napins is storage and defense (Polya, 1997). Proteins such as glutamine-rich storage proteins display significant antimycotic and antibacterial activities (Neumann et al., 1996). The

mechanism of their activities consists of interaction with membrane active α- and β- thionins and producing fungal membrane damage (Polya, 1997).

The antifungal activity of the napin could be due to the permeabilization of fungal membranes. Strong interactions with phospholipid bilayers of mustard napins lead to fungal/bacterial membrane permeabilization (Terras et al., 1992; Terras et al., 1993).

Napins as well as their separated subunits were shown to be calmodulin- antagonists-inhibiting, calmodulin – dependent plant kinases. This is probably caused by the fact that calmodulin and the small subunit of napin contain similar α - helix – hinge - α- helix motif in their structures (Neumann et al., 1996[a]). It seems that competitive inhibition due to the binding of the small subunit of napin to kinases could be responsible for this phenomenon (Neumann et al., 1996[a] and 1996[b]). Calmodulin antagonist activity of *R. sativus* seeds disappears during seed germination.

Brassica napus napin prevents Ca^{2+} dependent fluorescence enhancement of calmodulin and also inhibits calmodulin-dependent myosin light-chain kinase (Neumann et al., 1996[b]).

Napins play a role in the regulation of its high level of synthesis, because of their DNA-binding properties. Presence of short track of basic amino acids in napin can be correlated to nuclear localization proteins (Gerace, 1995; Schneuwly et al., 1986; Gerber et al., 1994). Glutamine rich domains present in the napin are characteristic of transcription factors (Gehrig et al., 1996).

Napins from radish seed and *Brassica parachinensis* showed the antimicrobial and translation – inhibitory (IC_{50} - 6.2 nM) activity respectively (Terras et al., 1992; Ngai and Ng, 2003). Radish napin inhibited the growth of large spectrum of fungi in the IC_{50} range 3 - 200 μg/mL (Terras et al., 1992; Terras et al., 1993). Napin Heating at 100°C for 10 min did not affect the antifungal properties. The more basic nature of napin explains its higher specific antifungal activity.

The non-essential amino acid glutamic acid and glutamates are taste-active molecules that often occur in plant or animal proteins that humans use as foods. Napin has potential as a flavor enhancer due to the presence of 26% glutamine residues in the protein (Halpern, 2000**)**.

The events that occur during the processing, of pronapin to napin, could be compared to insulin. The elimination of the peptide segment linking the small and the large subunits on the precursor was catalyzed by maturation proteinases. However, the strong tendency to form the intra disulfide bond in the small subunit suggests that the proteolytic activity occurs after the correct arrangement of the inter disulfide bridges. Otherwise, the napin becomes the substrate of protein disulfide isomerase, which is found in both smooth and rough endoplasmic reticulum (Monsalve et al., 1991).

Bell and Rakow analyzed seed meals from 124 different cultivars of oil seed *Brassica* belonging to several species and found *B. juncea* strains to have the lowest levels of TIs. *B. juncea* appears to have evolved somewhere in central Asia, and the Indian subcontinent has been the home for

diversification of many *B. juncea* genotypes (Bell and Rakow, 1996; Prakash and Hinata, 1980).

Many biological activities were identified in napin. Also various other roles of napin are continuously investigated. Intrinsic ligands associated with mustard proteins, limit its application in food and feed.

Intrinsic ligands

Mustard napin constitutes about 70% of the total proteins (Aruna and Appu Rao, 1988) and has a well-balanced amino acid profile. However, its use as a food protein is limited due to the presence of undesirable compounds such as phenolics, glucosinolates, and phytates (Thiyam, 2003, Naczk et al., 1998).

Phenolic acids and their derivatives are commonly occurring compounds in the plant world (Naczk et al., 2006). Their presence in seeds causes deterioration in the taste, odor and color of protein concentrates. Oxidized phenolic compounds bind with essential amino acids such as lysine or methionine, forming complexes, which are inassimilable in the digestive tract of animals and man.

Phenolics interacts/binds with protein chiefly by (a) hydrogen bonding, (b) ionic interactions, (c) hydrophobic interactions and (d) quinones (oxidation product phenolic acid) forms covalent bond with protein (Spencer et al., 1988). Phenolic compounds cause discoloration of proteins, besides reducing the nutritional value and digestibility of the proteins. Phenolic compounds are

colored and are co-extracts during extraction of protein, which in turn interacts with protein.

Sinapic acid

The total phenolic acids content in mustard/rapeseed flour ranges from 6.2 - 13 g/kg dry weight, which is higher (10 – 30%) than other oleaginous seeds (Table 5). The specific mode of interaction of rapeseed/mustard phenolics with proteins/mustard is still not well understood (Naczk et al., 1998). Therefore, a better knowledge of factors which influence the interaction between phenolics and proteins would be beneficial in developing more efficient technologies for production of phenolic-free protein isolates.

The content of phenolic acids in mustard/rapeseed meal is five times higher than soybean meals. Therefore phenolics are important factors when considering mustard/rapeseed meal as a source of human food-grade protein because they contribute to the dark color, bitter taste, and astringency of protein products. Phenolics and their oxidized products can form complexes with essential amino acids and protein, thus lowering the nutritional value of rapeseed products (Spencer et al., 1988; Naczk et al., 1998).

Phenolic acids in mustard/rapeseed are present in the free, esterified and insoluble-bound forms and are derivatives of benzoic and cinnamic acids. The total content of phenolic acids in rapeseed meals is up to 18.4 g / kg, on a dry weight basis of defatted meal. Phenolic compounds have been identified as possible inhibitors of iron absorption. Sinapic acid (Figure 8) is the

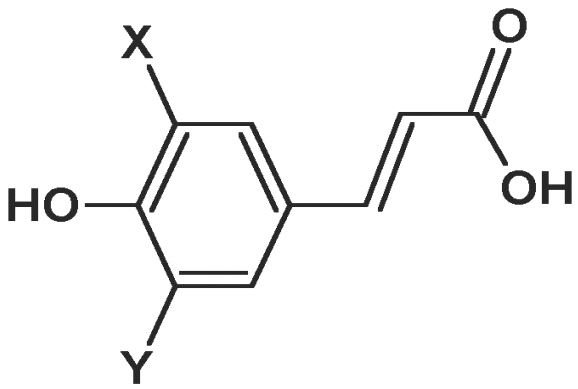

(*Naczk et al., 1998*)

Phenolic acid	X	Y
p-Coumaric	H	H
Caffeic	H	OH
Ferulic	H	OCH_3
Sinapic	**OCH_3**	**OCH_3**

Figure 8. Chemical structure of sinapic acid. Sinapic acid is the predominant phenolic acid present in *Brassica* seeds

Table 5. Total phenolic acids content in some oilseed

Oil seed	g/kg dry weight basis
Soybean flour	0.23
Cotton seed	0.57
Peanut flour	0.63
Rapeseed/canola flour	6.4 - 12.8
Canola meal	15.4 – 18.4
Soybean meal	4.6

(Naczk et al., 1998)

predominant phenolic acid present in the rapeseed meal (Vuorela et al., 2004; Shahidi and Naczk, 1992). Interaction of sinapic acid, a major antinutritional compound of *Brassica* species, is important when considering mustard as a source of food - grade protein (Velasco and Möllers, 1999).

Phenolics can form complexes with proteins, lowering their nutritional values. Phenols complex with proteins reversibly by hydrogen bonding between the hydroxyl groups of phenols and the carbonyl groups of peptides bonds or irreversibly by oxidation to quinones. Phenol - protein complex formation is the result of formation of hydrogen bonds and hydrophobic interactions (Naczk et al., 1998). Binding of phenolic acid to the protein can be measured by following the tryptophan fluorescence. Rapeseed sinapic acid is a potent antioxidant comparable to the α - tocopherol (Vuorela et al., 2004).

Presence of glucosinolates in plants appears limited to certain families.

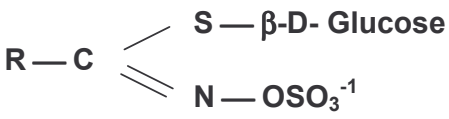

If R is,

—CH—CH = CH_2	**→ Sinigrin**
3-Pentenyl	**→ Glucobrassicanapin**
3-butenyl	**→ Gluconapin**
4-hydroxy-3-indolylmethyl	**→ Glucobrassicin**

They are predominant in *Cruciferae* family. These compounds are distributed throughout the plant, they occur predominantly in the mature plant. General formula of glucosinolates

Allyl isothiocyanate

Sinigrin is a major glucosinolates found in cruciferous family and is considered as a major precursor of the sulfurous flavors. Upon injury or mechanical disruption of plant tissue, myrosinase (β-thioglucosidase) hydrolyzes sinigrin and produces glucose and four distinct compounds viz., allyl isothiocyanate, allyl thiocyanate, allyl cyanide, & nitriles (Fenwick et al., 1983). The released hydrolytic products (Figure 9) are physiologically active compounds and goitrogenic in nature (Joseffson, 1972). They are also responsible for the biting taste of important condiments and contribute to the characteristic flavors of many plants whose leaves, flower bud, stem, root are consumed as vegetables.

Allyl isothiocyanate is a hydrolytic product of predominant glucosinolate sinigrin (about 93% of mustard glucosinolates are sinigrin) and is used as a flavoring agent (Kishore Kumar Murthy and Rao, 1986; Shahidi and Gabon, 1990; Pecháček et al., 1997; Cejpek et al., 2000).

During the processing of mustard/rapeseed oil, isothiocyanate participate in chemical reactions with protein and transform into indigestible/cytotoxic protein (Kawakishi and Kaneko, 1987). Kishore Kumar and Rao (1986) reported that the cruciferin - allyl isothiocyanate complex was

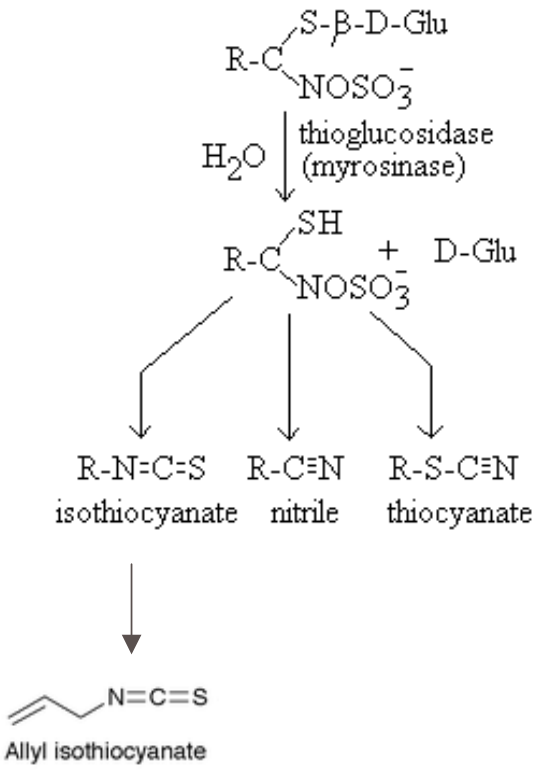

(*Fenwick et al., 1983*)

If R= —CH—CH═CH$_2$ ⟶ Allyl isothiocyanate

Figure 9. Schematic representation of glucosinolate hydrolysis by myrosinase.

poorly hydrolyzed by trypsin however chymotrypsin digestion was not affected.

Interaction of the mustard proteins with nascent AIT during oil extraction and isolation of the protein is limited since the pH of the seed material is about 6.0. Allyl isothiocyanate (AIT) is a strong electrophile and reacts with nucleophiles such as amino acids, amines, alcohols, etc. Among the hydrolytic products of sinigrin, AIT is an efficient inhibitor of bacteria and yeast (Shofran et al., 1998). Binding of AIT to cruciferin was followed by absorption, availability of lysine, electrophoretic mobility. AIT has recently been identified as an anti-carcinogenic agent in foods, and is a very reactive and unstable compound in an aqueous solution (Ohta et al., 1999).

Phytic acid

The second major anti-nutritional (intrinsic ligand) factor present in mustard is phytic acid (Myoinositol hexa-phosphoric acid). Phytic acid is the major phosphorus storage compound present in cereals and legumes. The biosynthesis pathway of phytic acid in plants is shown in figure 10. They are present in embryonic tissue and cotyledons as a calcium and magnesium salt. Because of its unique structure phytic acid has a high order of chelating potential (Cheryan, 1980; Carnovale et al., 1988).

Phytic acids carries negative charge, and has a strong ability to chelate multivalent metal ions, especially Zn, Ca and Fe. The binding results in the formation of insoluble salts with poor bioavailability minerals. Phytic acid precipitates protein upon interaction with them.

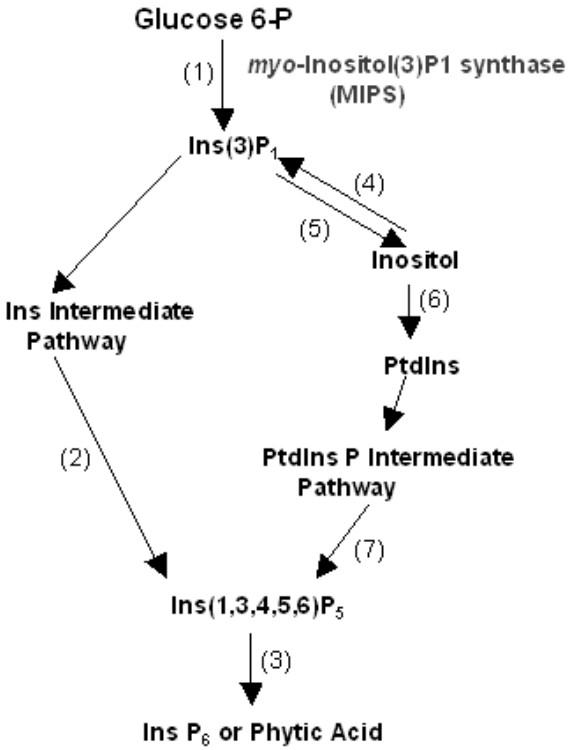

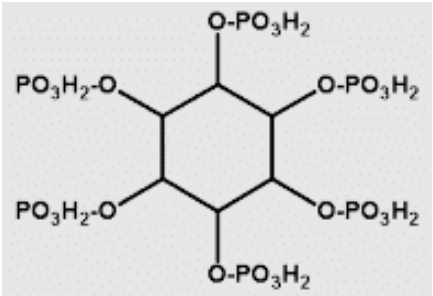

(*Cheryan, 1980*)

Figure 10. Plant biosynthetic pathway leading to Phytic acid

Binding can be studied by precipitation, fluorescence, and CD measurements. Phytic acid content in mustard seeds ranges from 6 – 9.5 mg/g (Mothes et al., 1990) and upon interaction it precipitates protein (Cheryan, 1980; Thompson, 1987; Rajendran and Prakash, 1993[a]; Rajendran and Prakash, 1993[b]; Maga, 1982).

The protein – intrinsic ligand interaction study helps in the identification of amino acids on proteins involved in interaction and also gives the information about the structural changes upon interaction with ligand. Chemical modification can also helps in identification of residues involved in ligand binding. The amino acids chosen for chemical modification are - amino groups of lysine, guanidine moiety of arginine, carboxyl groups of aspartic and glutamic acids, imidazole group of histidine, disulfide and sulphydryl groups of cystine and cysteine respectively. Interaction study of modified protein with the ligand would give us information about the role played by individual residue in binding.

Mustard napin is rich in sulfur containing amino acids and lysine that are lacking in other cereals and legumes. Its high content of glutamine also highlights its potency as flavor potentiator. However, in spite of its attractive amino acid profile, napins are under utilized in food. Its stability towards digestibility as well as temperature is responsible for its allergenicity. Association of intrinsic ligands present in mustard seed further limits its utility.

AIM AND SCOPE OF PRESENT INVESTIGATION

Seed proteins provide major share of dietary proteins for human and animal nutrition. These are classified into storage, structural and biologically active proteins. Seed storage proteins play an important role in the survival of plants by providing nutrition during seedling stage, protecting the seeds from microbes and insects and in maintaining the viability of seed.

Mustard is the second major oilseed crop of India and the Indian or oriental mustard (*Brassica juncea*) is the chiefly grown variety. Defatted mustard meal contains 35 - 45% proteins. Mustard has a well-balanced amino acid profile, compared to grains and legumes. The major storage proteins of mustard are high molecular weight cruciferin (12S) and low molecular weight napin (2S).

Napin is rich in lysine (available lysine- 6.7%) and sulfur containing (cysteine and methionine) amino acids. It consists of small and large subunits (of 29 and 86 residues) linked through two disulfide bonds. A single tryptophan and tyrosine are present in the small and large subunit, respectively. Napin has potential for enhancing food flavor due to the presence of high glutamine content (24%). The secondary structure arrangement of napin reveals that these proteins are tightly packed in the seed. However, allergenicity as well as resistance to proteolysis limits the utilization of napins in food.

The napin (2S albumin) family is highly stable to proteolysis as well as thermal denaturation. The structure of napin is not altered at high

temperatures and wide range of pH from 3 –11. In case of 2S albumin from Brazil nut, the intrachain disulfide bond of large subunit plays an important role in holding the core structure together against proteolysis. The two intra and two inter disulfide linkages, are the major contributors of stability and compact structure. Understanding the mustard napin structure is an important factor to explain its thermal stability and resistance to proteolysis. Also, apart from disulfide linkages, hydrophobic and electrostatic interactions are the important parameters affecting protein structure.

Mustard napin, as a food protein is limited due to the presence of undesirable compounds associated with it. The presence of intrinsic ligands like sinapic acid, phytic acid and allyl isothiocyanate compromises the nutrition quality and bioavailability of essential amino acids present in the napin. The total phenolic acids content in mustard/rapeseed flour is 10 – 30% higher than other oleaginous seeds. Glucosinolates occur in the seeds of *Brassica* species. They are hydrolyzed to isothiocyanates, glucose and sulfate by the action of enzyme myrosinase. The hydrolytic products of glucosinolates such as isothiocyanates, and nitriles, are toxic in nature. Phytic acid is the major phosphorus storage compound of seeds. Its presence in food decreases the bioavailability of many essential minerals and protein by forming complexes. Phytic acid content in mustard seeds ranges from 6 – 9.5 mg/g. Interaction studies of napin with intrinsic ligands helps in identification of amino acids involved in binding and also gives the information about the structural changes upon interaction.

The main objective of the present investigation is to utilize the low molecular weight protein fraction from mustard as a functional ingredient. Understanding the implications of interactions of low molecular weight mustard proteins with intrinsic ligands for digestibility and availability of essential amino acids.

With the above objectives the following studies were undertaken

1. Fractionation and characterization of napins and physicochemical characterization. Contribution of hydrophobicity and electrostatic interactions to the stability.
2. Mechanism of thermal and isothermal unfolding of napin: Role of dimerisation and internal repeats in structural stability.
3. Interaction of sinapic acid, phytic acid and allyl isothiocyanate with napin.

With the above studies an attempt has been made to understand the interactions and forces responsible for the stability of napin. These studies have been carried out by spectroscopic, calorimetric and ligand binding measurements.

The proposed work aims to answer the following questions: Why napins are hydrophilic in nature and what are the forces responsible for the stability of napin apart from disulfide bridges. Why napins are thermally stable? Will the modification of amino acids affects the binding of sinapic acid, phytic acid and allyl isothiocyanate.

The result obtained from the present study would help us to understand the contribution of relationship between the structure and stability.

MATERIALS AND METHODS

MATERIALS and METHODS

MATERIALS

Molecular biology grade guanidine hydrochloride (GdnHCl), Sephadex G - 50 superfine, blue dextran, alcohol dehydrogenase, bovine serum albumin, carbonic anhydrase, soybean trypsin inhibitor, cytochrome C, CAPS, TPCK treated α - trypsin (Lot - 121K7692), TLCK treated α - chymotrypsin (Lot - 109H7485), sinapic acid, phytic acid from rice, allyl isothiocyanate, dithiothreitol (DTT), iodoacetamide, acrylamide, bis-acrylamide, sodium dodecyl sulfate, tris base, TNS, TNBS, EDC, BHT, DTNB, succinic anhydride, and urea were from Sigma Chemical Company (St. Louis, MO, USA). Bio - Gel P-30 was from BIO-RAD laboratories (Richmond, CA). CM-Sephadex C - 50 was from Pharmacia Fine Chemicals, Uppsala, Sweden. Ampholine PAGplate and isoelectric focusing standards of broad pI (3.5 - 9.3) were from Amersham Biosciences, UK. 8 - anilino - 1 - naphthalene sulfonic acid (ANS) was from Aldrich Chemical Co., Milwaukee, USA. *cis* - Parinaric acid and PRODAN was from Molecular probes. Standard low molecular weight electrophoresis marker kit was from Genei, Bangalore. Solvents used were of HPLC grade. Milli-Q grade water was used for preparing reagents. All other chemicals were of analytical grade.

Mustard seeds (*Brassica juncea*) 'Argani' variety, was procured from National Seed Corporation (NSC) Ltd, Mysore, India, were finely ground, defatted with hexane, dried and stored at 27°C. All experiments were carried out in 0.02 M phosphate buffer pH 7.0 (buffer A).

Isolation and Purification

Purification of napin

Napin was purified as reported earlier with minor modifications (Aruna and Appu Rao, 1988). Purification was carried out using 0.02 M phosphate buffer pH 7.0 (buffer A) unless indicated. The protein from defatted *B. juncea* meal (5 g) were extracted with buffer A containing 1.0 M NaCl for 60 min (1:10) at 10°C. The suspension was centrifuged for 20 min to recover supernatant (2980 x g, 10°C), which was subjected to ammonium sulfate precipitation. The ammonium sulfate pellet (15 – 40%) was dissolved in buffer A containing 0.1 M NaCl and dialyzed against the same buffer. The dialyzed protein was loaded onto a Sephadex G - 50 (1.5 x 200 cm, 350 mL) pre-equilibrated with buffer A containing 0.1 M NaCl. The peak corresponding to 2S protein (170 - 185 mL) was pooled dialyzed against buffer A and fractionated on a CM-Sephadex column (2.1 x 7 cm, 25 mL). Bound protein was eluted with a linear gradient of 0 M – 0.5 M NaCl in buffer A at a flow rate of 20.0 mL/h. Protein concentration was determined by measuring the absorbance at 280 nm using a value of $E^{1\%}_{1cm}$= 4.8 (Aruna and Appu Rao, 1988).

Determination of homogeneity and molecular weight of napin

Electrophoresis

Homogeneity of the preparation was ascertained by non-reducing and reducing SDS–PAGE on a 15% vertical slab gel in presence of 0.1% SDS

according to the method of Laemmli (Laemmli, 1970). β- Mercaptoethanol was added to reduce the protein.

Native gel

Native-PAGE (10%) was run in 0.2 M glycine-HCl buffer, pH 4.0 and stained with 1% amido black in 7% acetic acid. The polarities were reversed during the run. Methylene green was used as the tracking dye.

Gel permeation chromatography using HPLC

Gel filtration was performed on Waters HPLC system (Waters, Milford MA), equipped with a 1525 binary pump and Waters 2996 photodiode array detector. Gel filtration was carried out using TSK-Super SW2000 (4.6 mm x 300 mm, 4.0μ) column. The column was pre equilibrated with buffer A, and 20 μg of protein was injected. The elution of the sample was carried out isocratically using the same buffer. The flow rate was maintained at 0.2 mL/ min at 25°C and detected at 230 and 280 nm by PDA detector. The analysis of the data was done by Waters Millennium software provided by the manufacturer. The column was calibrated with standard proteins (Cytochrome C-12,500 Da, Insulin- 5800 Da, Soybean trypsin inhibitor-20,000 Da, Carbonic anhydrase-29,000 Da, BSA-66,000 Da).

RP-HPLC

Homogeneity was also ascertained by reversed phase HPLC using symmetry shield ^{TM} RP_{18} (5.0 μ, 4.6 mm X 250 mm) Waters column, with solvent A (0.1% TFA in water) and solvent B (100% acetonitrile containing

0.1% TFA). The column was washed with solvent A for 10 min. Protein sample containing 20 µg / 20 µl was injected at a flow rate of 1 mL/min. The bound protein was eluted by a shallow gradient of acetonitrile from 0-50% over time span of 70.0 min. The eluted protein was monitored at 230 and 280 nm. Gel filtration chromatography was carried out using the above column, in presence of 0.1 and 1 mM DTT. The column was equilibrated with buffer A containing DTT. All other conditions were as given above.

Mass spectrometry

The molecular weight of the napin protein was analyzed by MALDI-TOF after RP-HPLC. The peak fraction was collected, concentrated under vacuum (speed vac Sawant, Mumbai) and analyzed. Matrix Assisted Laser Desorption Ionization Mass Spectroscopy (MALDI MS) analyses were performed on a Bruker Daltonics Ultraflex MALDI TOF/TOF system (Bruker-Daltonics, Bremen, Germany) in the reflective positive ion mode, equipped with a nitrogen laser of 337 nm. The samples were prepared by mixing equal volumes of samples (prepared in H_2O/TFA 100:0.1 and dialyzed against H_2O) and saturated matrix prepared separately in CH_3CN/H_2O/TFA (80:20:0.1) α-cyano-4-hydroxycinnamic acid (Sigma Aldrich Chemie GmbH). The amount of protein loaded on the probe slide was ~ 10 pmol. The samples were then dried at 25ºC under atmospheric pressure. Data was collected between 0-60,000 Da.

Western blotting

PVDF membrane preparation: The membrane was cut to the required size and soaked for 2 min in methanol. Membranes are transferred into buffer containing 10% methanol and equilibrated for 10min. Napin was reduced and loaded onto 15% SDS - PAGE. Gels were washed 4 - 5 times to remove glycine after the completion of electrophoresis. The gel was equilibrated in CAPS buffer for 10-15 min. Electrophoretic transfer (Mini Trans-Blot ®; Bio-Rad) was [in 10 mM 3-[cyclohexylamine]-1-propane sulfonic acid (CAPS) (pH 11.0) with 10% (v/v) methanol] carried out in a semi-dry blotting apparatus for 4 h using a current of 0.8 mA / cm^2 of the filter paper, at 100 V and 25°C. The membranes were stained with Ponceau stain, subunit bands excised and subjected to N- terminal sequencing by automated Edman degradation on an Applied Biosystems Procise® 4.0 sequencer.

N - terminal sequencing

The cut membrane was placed directly onto the fibre disc. The coupling reaction was carried out with Edman reagent phenyl isothiocyanate in presence of gaseous trimethylamine. Excess reagents were removed and cleavage was carried out with gaseous TFA. Free ATZ - amino acids (Anilino thiazolinone) were converted to PTH - amino acids with 25% TFA. These are separated on RP - HPLC and recovery was calculated using CR4A system. The results were recorded.

Trypsin inhibitor assay

Trypsin inhibition assay was carried out according to Smith et al., (Smith et al., 1980) using synthetic substrate BAPNA. To 1 mL of trypsin solution (4 mg/100 mL in 0.001N HCl), different amounts of napin were added and the volume is made upto 2 mL with water. This was incubated at 37°C for 5 min. Freshly prepared BAPNA solution (40 mg/mL) in tris-HCl buffer of pH 8.0 containing 0.05 M $CaCl_2$ was added and the resulting mixture was incubated for 10 min at 37°C. The reaction was terminated by the addition of 1 mL of 30% acetic acid and the absorbance was measured at 410 nm against the reagent blank. Trypsin was added after the addition of all other regents for blank. A trypsin standard was run in absence of inhibitor. Inhibition was tested for napin, subunits and peptide.

Tryptophan estimation in napin

The tryptophan content in napin was determined according to Spande and Witkop. Protein solution (1.2 mg/mL) at pH 4.0 was titrated with 10 mM NBS in water. Titration was continued until minimum optical density at 280 nm was observed. A molar extinction coefficient of ε_{280} for tryptophan – 5500 $M^{-1}cm^{-1}$ was used for the calculation (Spande and Witkop, 1967)

Cysteine estimation

Cysteines were estimated according to the method of Riddles and Blackley. Napin was dialyzed against 0.1 M phosphate buffer pH 7.2 (1 mM EDTA) with 5 - 6 changes for 24h at 8°C. Stock solution of Ellman's reagent in

buffer was added to reference and sample cuvette. Increase in the absorbance was monitored at 412 nm. Molar extinction coefficient of ε_{412} – 14150 M^{-1} cm^{-1} was used for the calculation of total number of cysteines (Riddles et al., 1983).

Tyrosine ionization

Tyrosine ionization was carried out according to the method of Donovan (1973). Ionization of phenolic group increases with increasing the pH. Napin solution (1% w/v) in glycine - HCl varying pH (8 – 11.5) was prepared by dialyzing against respective pHs. Absorbance was read at 280 nm after centrifugation. The number of hydroxyl group ionization was calculated using molar extinction coefficient of ε_{295} = 2480 $M^{-1}cm^{-1}$. A titration curve was constructed by plotting the number of phenolic group ionized as a function of pH (N-acetyl tyrosine ethyl ester).

Amino acid composition

The peak fraction of gel filtration purified napin and concentrated peptide fraction from HPLC were analyzed directly for total amino acids. The composition was determined according to the method of Bidlingmeyer et al., (1984) using Waters Pico-tag amino acid analysis system. Napin (5 mg/mL) was hydrolyzed for 24 h at 110°C with dry 6N HCl containing 1 % (v/v) phenol, in test tubes that had been sealed under vacuum. The total cysteine content in the protein was also determined by performic acid oxidation (Hirs, 1967). Performic acid was prepared by mixing formic acid, methanol and hydrogen

peroxide in the ratio of 9.6: 0.2: 1. The resultant solution was mixed well allowed to stand for 2h at room temperature, cooled and stored at 4°C in dark.

Protein was dissolved in formic acid mixture and cooled on ice for 30 min. Performic acid oxidation was allowed to precede for overnight (12h) at -5°C. The solution was diluted with water and freeze-dried. The freeze-dried protein was digested with 6N HCl for 24 h at 110°C. The standard amino acids as a mixture (Pierce H) containing 25 nmol of each amino acids were placed samples were dried under vacuum along with hydrolyzed protein. The samples were redried after treating (10 - 20 μL) with ethanol: water: triethanolamine (2 : 2 : 1). Amino acids were derivatised with phenyl isothiocyanate. The phenyl thiocarbomyl amino acids were analyzed by RP - HPLC using specific PICO-TAG ^{TM} amino acid analysis column (15 x 3.9 cm) with binary gradient. Temperature was maintained at 37 ± 1°C with column heater. The solvents used were 0.14 M sodium acetate containing 0.5 mL trimethylamine and titrated with glacial acetic acid to get pH 6.4 and 6% acetonitrile (Solvent A) and 60% acetonitrile in water (Solvent B). A gradient was run from 0-46% in 10 min at a flow rate of 1 mL/min. The peaks were detected at 254 nm.

Stability: Contribution of electrostatic & hydrophobic interactions

Isoelectric focusing

Isoelectric focusing was carried out according to the method described elsewhere (Jyothi et al., 2005). Isoelectric focusing of the napin and separated subunits was performed at 10°C on an Amersham Biosciences multiphor II

apparatus. The polyacrylamide gel, Ampholine PAGplate with a pH range 3.5 – 9.5 was used. The electrode wicks for the anode and cathode were soaked for 4 – 5 min in 1.0 M phosphoric acid and 1.0 M sodium hydroxide, respectively, and the excess electrolyte was removed. Broad pI kit (3.5 – 9.3) was used as standard. Protein (3 mg/mL) and separated subunits (2 mg/mL) along with markers were loaded directly onto the gel with sample application pieces. The gel was electrofocused for 90 min at constant 15W with a maximum of 1500V and 50 mA. The electrofocused gel was stained with coomassie brilliant blue R – 250.

Conformational studies using proteolytic enzymes

Conformational studies were carried out using TPCK treated α- trypsin. Napin was digested with trypsin using an enzyme to substrate ratio of 2 : 100. The digestion was performed in 0.05 M ammonium bicarbonate buffer (pH 8.1) at 37°C. Samples were drawn at regular intervals of 15 min and the degree of hydrolysis estimated by TNBS method (Nissen, 1979).

The hydrolytic behavior of trypsin on napin was also monitored by SDS – PAGE and RP - HPLC.

Peptide purification

Trypsin digested napin was loaded onto CM - Sephadex column (0.8 x 6 cm, 12 mL) which was pre-equilibrated with buffer A. Bound peptides were eluted with 0 - 0.5 M NaCl in buffer A gradient. Also for N - terminal sequencing of peptide purification was carried out using RP-HPLC, symmetry shield ^{TM} RP_{18} (5.0 µ, 4.6 mm x 250 mm) Waters column. Solvent 0.1% TFA in

water and 100% acetonitrile containing 0.1% TFA were used for gradient elution. The column was washed with Solvent 0.1% TFA in water for 10 min. Trypsin digested napin (5 mg/mL) was injected at a flow rate of 1 mL/min. The bound protein was eluted by a shallow gradient of acetonitrile from 0 - 50% over time span of 70.0 min. The eluted peptide was monitored at 230 nm and peak fraction was collected and concentrated under vacuum.

The amino terminal sequence of the purified peptide was carried out on Applied Biosystems Procise® 4.0 instrument. Molecular weight of the peptide was analyzed by MALDI - TOF. The purified peptide was spectroscopically characterized using CD, fluorescence and absorption.

Separation of subunits

The large and small subunits were separated according to reported procedures (Menendez-Arias et al., 1987) with a little modification. Napin was denatured with 8.0 M urea for 30 min and reduced by 0.1 M dithiothreitol at 27ºC for 2 h. Free cysteines were blocked using 0.2 M iodoacetamide in dark for an hour. Subunits were separated on G - 50 Sephadex gel filtration column (140 x 0.5 cm, 110 mL). Purity of the two separated peaks (Elution volume: 40 - 48 mL, 60 - 66 mL) was ascertained by 17% SDS-PAGE and gel filtration on HPLC. Further structural characterization of separated subunits was carried out by absorption, fluorescence and CD spectroscopy. Purity of the separated subunits was ascertained by 17% SDS-PAGE and gel filtration HPLC.

Hydropathy plot

Hydropathy plot was constructed according to Kyte and Doolittle (1982). The plot was constructed using the available amino acid sequence (*Brassica juncea* CAA46785). Scores assigned for the most hydrophobic and for most hydrophilic amino acid were +4.5 and -4.5, respectively.

Surface hydrophobicity measurements

Napin surface hydrophobicity was measured using ANS, TNS, CPA and PRODAN. Hydrophobicity was calculated according to Cardamone and Puri (1992). The binding constants were determined using Scatchard plot. A stock solution of ANS (ε_{350} 4.95 x 10^3 M^{-1} cm^{-1}) (Cardamone and Puri, 1992) and TNS (ε_{366} 4.3 x 10^3 M^{-1} cm^{-1}) (McClure and Edelman, 1967) was prepared in buffer A whereas CPA (ε_{303} 7.6 x 10^4 $M^{-1}cm^{-1}$), and PRODAN (ε_{360} 1.8 x 10^4 $M^{-1}cm^{-1}$) were prepared in ethanol and methanol (analytical grade), respectively. For CPA, 10 μg of butylated hydroxyanisole (BHA) was added per mL of ethanol, to prevent oxidation. The stock solution was transferred into a brown bottle and stored at 4°C (Alizadeh - Pasdar and Li-Chan, 2000). All reagents were prepared fresh.

Excitation wavelengths were 375, 366, 325 and 365 nm for ANS, TNS, CPA and PRODAN, respectively. The emission spectra were collected from 400 - 500 nm using a 1 cm path length cell. The excitation and emission slit widths were 5 and 5 nm, respectively. Appropriate blanks in the corresponding solvents were subtracted to obtain the fluorescence enhancement caused by the fluorescent probe. Binding constants for the

above ligands with napin were also determined in presence of NaCl and Na_2SO_4. The association constant was calculated using Scatchard plot (Scatchard, 1949)

The ligand concentration after additions given by,

$$[L]_T - \frac{SV_t}{V_i+V_t}$$

Where,

S = the stock concentration of ligand

Vt = the net volume of ligand added

Vi = the initial volume of protein

After each addition, the sample was mixed, allowed to equilibrate at 27ºC and the fluorescence emission intensity was recorded. Values of ΔF were also corrected for the sample dilution arising from successive ligand additions.

$$\frac{[L]_B}{[L]_F} = K\,n\,p - K\,[L]_B \qquad (1)$$

p = Protein concentration

n = No of ligand binding sites

K =Association constant

$[L]_B$ =ligand bound per mole of protein

$[L]_F$ = Concentration of free ligand

$$Q = \frac{\Delta F_{max}}{[L]}$$

$[L]_F = [L]_T - [L]_B$

Fluorescence quenching measurements

To determine the solvent exposure of tryptophan residues, fluorescence-quenching measurements were made with the progressive addition of acrylamide and potassium iodide in absence or presence of 0.5 M NaCl and 0.2 M Na_2SO_4. Protein solutions were centrifuged at 10,000 rpm for 30 min before the scans. Titration was carried out with excitation and emission slit widths of 5 and 10 nm respectively. Napin concentration was fixed at 0.1 mg/mL.

Sodium thiosulfate was added (0.1mM) to KI solution to prevent I^{-3} formation. Since the absorption of the KI at the excitation wavelength is not detectable, no correction was given for the inner filter effect. The absorption of acrylamide at 280 nm was corrected using the Lehrer and Leavis equation.

$$F_{corr} = F_{obs} \times 10^{A/2}$$

From the recorded titration spectra, the accessibility of tryptophan was calculated using Stern- Volmer equation (Eftink, 1991) namely,

$$(F_o/F) - 1 = K_{SV}.[Q] \qquad (2)$$

F_o and F are the fluorescence intensities in the absence and in the presence of acrylamide quencher. The K_{SV} is the Stern – Volmer constant. The slope of F_o/F vs. [Q] gives K_{SV}. The experiment was also carried out for the separated subunits.

Circular dichroism measurements

CD measurements were performed with Jasco-810 automatic recording spectropolarimeter calibrated with d (+)-10-camphor sulfonic acid. Dry nitrogen was purged continuously into the instrument before and during the experiment. The light path length of the cell used was 1 mm in the far-UV region (260 - 190 nm) and 10 mm in the near - UV region (320 - 240 nm). All measurements were made at 27°C and the mean residue ellipticity was calculated using a value of 110. Average of three scans at a speed of 10 nm/ min, with a bandwidth of 1 nm and response time of 1s, were recorded. Protein concentration of 0.4 mg/mL and 2.5 mg/mL was used for far and near UV measurements, respectively.

The effect of sodium chloride (0 – 1 M) or sodium sulfate (0 – 0.2 M) on the secondary and tertiary structure of napin were carried out after incubation of the protein in salt for a period of 30 min. Changes in the secondary structure of napin, upon interaction with different concentrations of monohydric alcohols (methanol, ethanol, propanol and butanol), were

followed in the range 2 – 18 M (alcohol concentration), at 222 nm. The studies were also made in presence of 3 – 12 M trifluoroethanol (TFE).

Gel filtration chromatography

Gel filtration was carried out on a Bio-gel P-30 column (0.6 x 35 cm) with a flow rate of 4.0 mL/ h. The column was calibrated with marker proteins whose Stokes radius were known (R_S). Blue dextran (1 mg/mL) was used for determining the void volume (void volume, V_O = 12 mL). The protein sample (4.0 mg/mL) was centrifuged at 10°C, 10000 rpm for 20 min before loading onto the column pre-equilibrated with buffer A. The experiment was repeated in presence of 0.5 M NaCl and 0.2 M Na_2SO_4. The column was equilibrated with required salt concentration in buffer A for the above.

Thermal stability

Thermal stability of napin, in presence or absence of 0.5 M NaCl, was followed by CD. The change in secondary structure, as a function of temperature, was monitored at 222 nm. Protein was heated in the temperature range 27 – 75°C, at 1°C/min using a peltier attachment (PMH 356WI). Protein concentration used for the study was 0.4 mg/mL in buffer A.

DNA - binding studies

Gel retardation assay

The studies on binding of napin to bacterial DNA were studied by DNA gel retardation assay. The napin (5 μg/mL) was incubated with bacterial DNA (100 μg/mL) in 10 mM Tris, 1 mM EDTA buffer, pH 8.0 for 30 min and the

mixture was loaded on to a 0.8% agarose gel. The electrophoresis was run in TBE buffer at constant voltage of 100V for 60 min. The DNA in the gel was visualized by staining with ethidium bromide (Hsu, et al., 2005).

Amphipathic plot: Helical wheel diagram was generated using BioEdit Sequence Alignment Editor software (ver.7.0.5.3).

Methylene blue assay was done as per the method of Greiner-Stoeffele et al., (1996). Protein stock solution of 10 mg/mL was used for the assay. RNA solution was prepared by dissolving 100 mg yeast RNA in 10 mL Mops buffer (0.1 M Mops – HCl, pH 7.5, 2 mM EDTA). Methylene blue buffer was prepared by dissolving 1mg Methylene blue buffer in 100 mL Mops buffer and the absorbance at 688 nm was adjusted to 0.5 $\pm$ 2% using Mops buffer. Due to light sensitivity of the dye, the Methylene blue buffer was stored in dark. DNA solution (100 μL) was mixed with varying concentration of napin and methylene blue buffer to a final volume of 1 mL in cuvette of 1 cm light path. The sample was preincubation at 25°C for 10 min in the spectrophotometer in the dark. RNA methylene blue complex causes an absorbance decrease at 688 nm. The decrease in the absorbance was monitored for 1 min (Greiner-Stoeffele et al., 1996). The IC_{50} and K_I were calculated.

The K_I is calculated according to the method of Sluyterman and Wijdenes (1973). In the Line Weaver - Burk plot the lines of various inhibitor concentration intersect in the first quadrant. This is due to the association between substrate and inhibitor.

Thermodynamic and structural stability of napin

Proteolytic digestion

Purified napin protein (4.0 mg/mL) was extensively dialyzed against 0.05 M, pH 8.15 ammonium hydrogen carbonate buffer, for 12 h at 8ºC. Dialyzed protein was centrifuged at 12000 rpm for 30 min. Prior to digestion protein and α-trypsin stock (10 mg/mL) were kept at 37ºC for four minutes to attain the temperature. The protein was digested with α-TPCK treated trypsin and α-TLCK treated chymotrypsin at 1:100 enzymes to protein. Aliquots were drawn for every fifteen minutes and the extent of hydrolysis was measured by trinitrobenzene sulfonic acid (TNBS) method (Nissen, 1979). The same procedure has been repeated for α-chymotrypsin digestion. The proteolytic digestion was also carried out at 27 and 60ºC and the digest was loaded onto 15% non reducing SDS-PAGE.

Thermal unfolding of napin

Circular dichroism studies

Circular dichroism spectra in the far UV (260-200 nm) and near UV (240-320 nm) region were recorded on a Jasco-810 spectropolarimeter (Jasco, Tokyo, Japan) calibrated with d-10 camphor sulfonic acid. Protein was heated in the temperature range 27 – 75°C using a peltier attachment (PMH 356WI). Dry nitrogen was purged before and during the measurements. The light path length of the cell used was 1mm in the far-UV region and 10 mm for near UV region. All the samples filtered through 0.22 μ membrane (millipore) filter before taking the spectra. During the course of measurement concentration of the protein was kept constant. An average of three scans at a

speed of 10 nm/min with a bandwidth of 1nm and a response time of 1s were recorded. The mean residue ellipticity, $[\theta]_{MRW}$ was calculated using a value of 110 for napin through out the CD experiment. Buffer base line was subtracted in each scan and the change in structure as a function of temperature was measured at $[\theta]_{222\ nm}$. The concentration protein used for the study was 0.4 mg/mL in buffer A. DTT (1 mM) was used for following thermal denaturation under reducing conditions. For all the CD measurements structural analysis were made according to Yang et al (1986)

Fluorescence measurements

Fluorescence emission spectra were recorded on a shimadzu RF-5000 automatic recording spectrofluorimeter in the temperature range of 15 - 70°C. The temperature of the cell was maintained by circulating water (Huber, Germany). The excitation and emission slit widths were set at 5 and 10 nm respectively. The excitation wavelength was fixed at 280 nm, and emission spectra were recorded from 300 - 400 nm. Samples were incubated at the test temperature for fifteen minutes before recording the fluorescence intensity. Unfolding was monitored at the emission maxima 343.0 nm. All the unfolding and refolding measurements were made at 27ºC with 0.16 mg/mL protein in buffer A.

DSC studies

Change in the heat capacity as a function of temperature was measured on the ultrasensitive differential scanning calorimeter, VP-DSC (Microcal Inc.). The scans were performed as a function of protein concentration (10 - 106

μM), pH (3.0 - 10.0) and rates (10 - 60 K/h). All DSC measurements were carried out with a protein concentration of 50 μM (0.8 mg/mL) in buffer A. The sample and dialysate were filtered through 0.22μ filter and degassed prior to loading the DSC cell. Glycine–HCl buffer (pH 3.0) 0.05 M, sodium acetate buffer (pH 3.5 - 5.5) 0.05 M, phosphate buffer (pH 6.0 - 7.0) 0.02 M, Hepes (pH 8.0 - 9.0) 0.05 M and glycine-NaOH (pH 10.0) at 0.05 M concentration were used for the pH dependent calorimetric scans of samples.

Napin was dialyzed against buffer A containing 1 mM DTT (5 changes over 24 h) before DSC, to understand the effect of reduction on thermal denaturation. At desired pH, buffer and the protein samples were dialyzed extensively with four intermittent changes (1:500, 8ºC). The 0.5 mL of protein and dialysate buffer was introduced in to sample cell and reference cell. The calorimeter was up scanned at a constant rate of 60 K/h. Using origin software supplied along with the instrument, the data were accumulated and analyzed. For the analysis of data the calorimeter is interfaced with microcomputer. The analysis of normalized data using progress base line, connection of pre and post transition base line of the DSC thermogram yielded the van't Hoff enthalpy (ΔH_V), midpoint of transition (T_M). The ratio of number of moles in the cell yields the calorimetric enthalpy (ΔH_C). The ratio of ΔH_V and ΔH_C yields the cooperativity of transition (Privalov and Khechinashivli, 1974).

Thermal unfolding of napin in presence and in absence of 1 mM DTT was carried out on Carry Bio100. The T_M was calculated using the software supplied along with the instrument.

Gel filtration chromatography for following the state of association

Gel filtration was carried out on a water-jacketed Sephadex-G50 superfine column (0.48 x 135 cm, 98 mL) at a flow rate of 8.0 mL/h in the temperature range 10 - 70°C ± 2°C. The column was calibrated with known molecular weight proteins (Sigma Chemical Co., St. Louis, USA). 0.8 mL fractions were collected and the absorbance measured at 280 nm. Blue dextran (1 mg/mL) was used to determine the void volume (V_o = 30.1 mL). Ovalbumin (43,000), carbonic anhydrase (29,000), trypsinogen (24,000) and RNase (14,500) were run independently at 27°C. Protein samples (8.0 mg / mL) were centrifuged for 20 min at 10,000 rpm and 27ºC before loading onto the column pre-equilibrated at the test temperature in buffer.

Cross-linking of napin by carbodiimide

Cross-linking of napin was carried out according to Enami et al., (1998). Protein (130 μM) was heated at 45°C for 15 min and the protein was cross linked by incubating in the presence of 1mM EDC (1-ethyl-3-(3-dimethyl aminopropyl) carbodiimide) for 12 h. The reaction was stopped by adding 100 mM sodium acetate. The cross-linked protein was extensively dialyzed against 0.02 M phosphate buffer with four changes. The pH of the solution was adjusted to 9.5 and dialyzed against 0.02 M phosphate buffer pH 7.0. The cross linking of the napin was confirmed by non - reducing SDS - PAGE. The 15% gel was stained by coomassie brilliant blue R - 250.

Isothermal unfolding of napin

Isothermal equilibrium unfolding induced by guanidinium hydrochloride

Preparation of GdnHCl

Stock solutions of GdnHCl (8.2 M) were prepared fresh, in buffer A containing 0.002% sodium azide. The pH of stock solution was adjusted by adding 0.01 M NaOH. Concentration of GdnHCl was determined by measuring refractive index (RI) of solution (Nozaki, 1972).

The equilibrium unfolding was monitored with the help of fluorescence spectrometer, circular dichroism and gel filtration chromatography as a function of guanidinium hydrochloride. Protein samples were equilibrated for 12h at 27ºC. (Where there is no further increase in the fluorescence intensity). During the course of incubation, there was no precipitation of napin as confirmed by recording the absorption spectra from 300 - 600 nm. The temperature of the CD and fluorescence cell was maintained at 27ºC. The stock solutions of GdnHCl and protein were prepared using buffer A, containing 0.002% sodium azide. The concentration of the protein was kept constant during the measurement. All fluorescence-unfolding measurements were made with 0.12 mg / mL protein.

Excitation and emission slit widths were set at 5 and 10 nm respectively. The excitation wavelength was fixed at 280 nm, and emission spectra were recorded from 300 - 400 nm. Unfolding was monitored at the emission wavelength 343.0 nm. Each data point is an average of five individual experiments. GdnHCl induced isothermal denaturation curves were collected in the temperature range 15 - 55ºC. A circulating Huber water bath was used to maintain the temperature of the sample within ± 0.5 ºC of the set temperature.

Similarly far-UV and near UV CD spectra were recorded for napin in GdnHCl (0 - 7 M). The data points are an average of three scans at a speed of 10 nm/min. Corresponding base lines were subtracted and the change in structure was measured at $[\theta]_{222\ nm}$. The protein concentration was 0.4 mg/mL and 2.5 mg/mL for far and near UV, respectively.

Reversibility of napin unfolding

The reversibility of unfolding was checked by refolding the unfolded protein by dialyzing against buffer A for 24h with five changes and diluting with the same buffer. Refolding was confirmed by measuring secondary, tertiary structure, fluorescence emission spectra, gel filtration, and hydrophobicity.

The hydrophobic surface exposure of native, denatured and refolded protein (25 μM) were measured by incubation in dark with the hydrophobic probe ANS (Engelhard and Evans, 1995). A concentrated stock of ANS was added to get a final concentration of 25 μM. The excitation wavelength was 375 nm and emission spectra collected from 400 - 550 nm using 1cm path length cell. The excitation and emission slit widths were 5 and 5 nm. Appropriate blank spectra of ANS were used for correcting the protein bound ANS spectra obtained.

Unfolding of napin by gel filtration chromatography

Gel filtration was carried out on a Bio-gel P-30 column (0.6×35 cm) with a flow rate of 4.0 mL/h. The column was calibrated with known molecular weight proteins for which stokes radius is known (Rs). Blue dextran (1 mg/mL) was used for determining the void volume (void volume V_o = 12 mL). Alcohol

dehydrogenase (1,50,000 Da, R_S = 44.3 Å), bovine serum albumin (66,000 Da, R_S=33.5 Å), cytochrome C (12,500 Da, R_S=17 Å) and soybean trypsin inhibitor (20,000 Da, Rs=20 Å) were run independently (Uversky, 1993). The protein samples (4.0 mg/mL) were incubated for 12h in various concentrations of denaturant (0-7.0 M) at 27ºC and centrifuged for 20 min at 10000 rpm. The incubated protein was loaded onto the column which was pre equilibrated with the desired concentration of the denaturant in buffer A. The void volume (V_o) correction was given for each increase in the denaturant concentration. The elution volume was calculated (Uversky and Ptitsyn, 1994).

Elution volume= $(V_e - V_o) / (V_t - V_o)$

Where, V_e = Elution volume of the protein V_o=Void volume

V_t=Total bed volume

Dynamic light scattering measurements

The dynamic light scattering measurements were done using Dyna Pro-MS800 dynamic light scattering equipment (Proterion, Protein solutions, Wyatt Technology, Santa Barbara, CA). The protein concentration used was 1.0 mg/mL in buffer A.

Computational analysis of the sequence for the internal repeats

Internal repeat regions in the sequence of napin were identified using the software 'RADAR', (**R**apid **A**utomatic **D**etection and **A**lignment of **R**epeats; http://www.ebi.ac.uk/Radar/index.html, *European Bioinformatics Institute*). The software uses an automatic algorithm, for segmenting the interested

sequence into repeats. It identifies short composition biased as well as gapped approximate repeats and complex repeat architectures involving many different types of repeats in sequence (Heger and Holm, 2000). This program identifies both sequence similarities and duplications in the sequence.

Sequence alignment

Brassica family napin sequences were aligned using CLUSTAL W version 1.83 from *European Bioinformatics Institute*. Sequences of napins used in the alignment were taken from GenBank as well as protein databank databases and include *Brassica juncea* (CAA46785), *Brassica oleracea* (CAA46783), *Brassica compestris* (CAA46782), *Brassica nigra* (CAA46784), *Brassica carinata* (CAA52813), *Brassica rapa* (CAA46171) and *Brassica napus* (1pnb).

Homology modeling

A model of napin was constructed based on the NMR structure of *Brassica napus* protein (PDB code: 1PNB). The Swiss-model software was used for this purpose was obtained from the website (http://swissmodel.expasy.org//SWISSMODEL.html).

Intrinsic ligands

Preparation of phenolic acid free napin

1. Activated charcoal: Purified napin was treated with 1% activated charcoal and was incubated at 27°C for 15 min, the resulting mixture was centrifuged.

2. Napin was treated with 1% PVP and fractionated on Sephadex G-50 column, pre-equilibrated with buffer A.

3. Protein bound sinapic acid (15 mg) was removed by increasing the pH to 10, followed by gel filtration on LH-20 (partly hydroxy propylated Sephadex G-25) column (140 x 0.5 cm, 110 mL). Protein was centrifuged at 10000 rpm for an hour, before loading onto the column. The column was pre - equilibrated with 0.02 M Glycine – NaOH buffer (pH 9.5) and protein was eluted from the column with same buffer. Protein fractions corresponding to napin were pooled and used for interaction studies.

Fluorescence measurements

Interaction of sinapic acid, phytic acid and allyl isothiocyanate with napin has been monitored following the quenching of relative fluorescence intensity of napin. Fluorescence measurements were carried out using Shimadzu RF 5000 spectrofluorimeter attached with thermostated circulating water bath. The solution in the cuvette was stirred using a Hellma cuv-o-stir®. Excitation and emission slit widths were set at 5 and 10 nm, respectively. Measurements were made using a 10 mm pathlength cuvette with the sample in buffer A. Fluorescence quenching of napin was followed at 27 ± 1°C. All samples were centrifuged at 10000 rpm for an hour to remove any aggregates. Inner filter effect was corrected by following the quenching of N-acetyl tryptophanamide, equivalent in absorption of napin at 280 nm. The

binding constant was calculated using established procedures (Appu Rao and Cann, 1981).

The binding constant K is given by

$$K = \beta / (1-\beta).\ 1/C_f, \qquad (3)$$

where $\beta = Q/Q_{max}$ and $C_f = C_T - n\beta T$, in which Q is the corrected percentage quenching; Q_{max}, the maximum quenching, C_f, the molar equilibrium concentration of unbound sinapic acid; C_T, the molar constituent concentration of sinapic acid; T, the molar constituent concentration of napin; and n is the binding stoichiometry (Lee et al., 1975).

The value of K (binding constant) is given by the slope of a plot of $\beta/(1-\beta)$ against C_f. Q_{max} has been determined by extrapolation of a double reciprocal plot of 1/Q vs. 1/C, to 1/C = 0. In both cases, the data are fitted to a straight line by the method of least squares.

Sinapic acid- binding

Determination "ε" for Sinapic acid

Molar extinction coefficient was determined by measuring the absorbance of sinapic acid (0 - 150 μM) in ethanol. The absorbance spectrum of sinapic acid is having maxima at 321, 238 and 204 nm.

Stock solution of sinapic acid was prepared in ethanol (10 mM) using $\varepsilon_{321\ nm} = 2.2 \times 10^4\ ML^{-1}$, and added in increments of 5 μL to napin (7μM) in

buffer A. The excitation and emission wavelengths were set at 295 nm and 340 nm respectively. The effect of temperature in the range 17 - 47°C, on the binding constant was determined by fluorescence quenching studies. Effect of ionic strength on the binding constant of sinapic acid with napin was determined by increasing the concentration of sodium chloride (0 - 200 mM) in buffer A. The effect of salt on the Stokes radius of napin was studied by gel filtration. Gel filtration measurements were carried out using TSK super SW 2000 (300 x 4.6 mm) column. The absorbance was detected at 280 nm. Standard proteins from a molecular weight marker kit for gel filtration (Sigma) with known stokes radius were used for calibrating the column. Blue dextran (1 mg/mL), was used for determining the void volume.

Determination of intrinsically bound sinapic acid by HPLC

Intrinsically bound sinapic acid to napin was quantitated by HPLC method. Purified napin (40 mg) was extracted with 80% methanol for 3h at 70 °C, centrifuged at 10000 rpm for an hour and concentrated under nitrogen. Dried napin was redissolved in 2 mL mixture of ammonium di hydrogen phosphate (75% v/v) and methanol (25% v/v). An aliquot of 20 µL was directly injected to symmetry shield ^{TM} RP_{18} (5.0 µ, 4.6 mm x 250 mm) Waters column equipped with a C_{18} guard column. The solvent system used was, solvent A: 0.02 M ammonium di hydrogen phosphate buffer (pH 2.15)/methanol (75:25), solvent B: methanol. The gradient was 5% solvent B (0 - 15 min), 5 - 35% solvent B (15 – 20 min), 35 – 100% B (35 – 45 min), 100 – 5% B (45 – 50 min), 5% B (50 – 52 min) with an 18 min post run period at 5% solvent B. Elution profile was monitored at 325 nm with a flow rate of 1 mL/min at 27°C

(Vuorela et al., 2004). A standard curve was constructed by injecting standard sinapic acid (0 – 0.1 mg). The amount of intrinsically bound ligand was calculated from the curve.

Phytic acid – napin interaction

Stock solution of phytic acid was prepared in buffer A. Protein solution of 1 mg/mL was taken and the desired pH was adjusted (1 – 7) and known amount of phytic acid solution was added. After 30 min of incubation at room temperature, napin was centrifuged and protein in the supernatant was measured at 280 nm. Napin at respective pH were taken as controls. The precipitation was also followed as a function of phytic acid concentration.

Inorganic phosphate was estimated according to the method of Chifflet et al (1988). Supernatant solution of protein-phytic acid complex, after precipitation with 3% TCA was used for the determination of inorganic phosphorus. To 50 µl napin (10 mg/mL), 50 µl of 12% SDS was added and mixed. The color developing was started after the addition of 100 µl mixture of 6% ascorbic acid in 1N HCl and 1% ammonium molybdate solution. The samples were left at 27°C for 10 min and terminated by the addition of 150 µl stopping solution (2% Sodium citrate, 2% Sodium metaarsenite, 2% acetic acid). This mixture was incubated at room temperate for 20 min at 27°C and absorbance was read at 850 nm. All the reagents were prepared freshly. NaH_2PO_4 (0 - 15 µM) was used to construct standard curve.

Determination of binding constant of phytic acid by HPLC

Quantitative estimation of phytic acid binding to napin was carried out on RP-HPLC. The amount of free phytic acid in the napin-phytic acid complex was determined by this technique. Protein - phytic acid complex (2 mg/mL) was precipitated with 3% TCA and centrifuged after 30 min at 10000 rpm. The supernatant was filtered through 0.22 μ membranes (Millipore) filter. An aliquot of 20 μL was injected directly to the symmetry shield ^{TM} RP_{18} (5.0 μ, 4.6 mm x 250 mm) Waters column. Bound phytic acid was Isocratically eluted using 0.005 M sodium acetate for 15 min at a flow rate of 1 mL/min. The eluted phytic acid was monitored at 254 nm (Tangendjaja et al., 1980). A standard curve of phytic acid was constructed (0 – 0.2 mg). The amount of free phytic acid calculated from the standard curve. Binding constant was calculated from Scatchard plot (Scatchard, 1949).

Circular dichroism measurements

Circular dichroism spectra in the far UV (260 - 200 nm) and near UV (240 - 320 nm) region were recorded. All the samples filtered through 0.22 μ membranes (Millipore) before taking the spectra. An average of three scans at a speed of 20 nm/min, with a bandwidth of 1 nm and response time of 1s, was recorded. The mean residue ellipticity, $[\theta]_{MRW}$ was calculated using a value of 110 for napin.

The spectra were recorded for napin and napin–phytic acid (0.07 and 0.3 mM phytic acid) and napin-AIT complex (0.1 and 0.3 mM AIT). Secondary structural analysis was performed according to Yang et al (1986).

Modification of amino acids

Lysine modification by Succinylation

Modification of lysine was carried out according to the method of Hass et al (1964). To a 2 mL of 10 mg protein 100 mg of solid succinic anhydride was added. The solution was stirred continuously at pH 8.0 for 2 hr. The pH was adjusted with 1N NaOH. Resultant solution was dialyzed extensively against buffer A (24 hr at 4°C). Extent of modification was measured by estimating "available lysine".

Modification of Tryptophan residue

The tryptophan residue on napin was modified using N – bromosuccinamide (NBS) according to the method of Spande and Witkop (1967).

AIT- binding

Stock solution of AIT was prepared in ethanol (10 mM) concentration was determined by using $\varepsilon_{240\ nm}$ = 770 $M^{-1}cm^{-1}$ (Schwimmer, 1961). Intrinsically bound AIT to napin was determined by RP – HPLC according to Matthäus and Fiebig (1996). AIT was extracted from pure napin with 80% ethanol for 3h at 60°C. Resulting mixture was centrifuged and injected on to RP C_{18} column. Mobile phase used was water and 100% acetonitrile, for a total run time of 60 min. The column was pre equilibrated for 8 min with 20% acetonitrile. Gradient was started from 40% acetonitrile to 60% acetonitrile in 27 min. The column was equilibrated at 20% acetonitrile for 25 min. The gradient elution of AIT was monitored at 240 nm.

Binding of AIT - napin complex was studied by measuring the available lysine content. AIT concentration was varied from 0 to 0.6 mM at napin concentration 100 μM. After 2 h incubation at 27°C the available lysine content was measured. The experiment was also carried out in the pH range 4 – 10 and concentration 10 – 200 μM (napin).

Change in the electrophoretic mobility of napin and napin – AIT (1 mg/mL) complex was carried out on 10% native – PAGE. Glycine – HCl buffer (0.2 M) at pH 4.0 was used as running buffer. Methylene green was the tracking dye. Gels were stained in 0.5% amido black in 7% acetic acid and destained using 7% acetic acid. Electrophoretic mobility was calculated using the software (Software Syngene tools from Synoptics technologies, UK).

Available lysine

Available lysine was estimated according to Sashidhar et al (1994). To 1 mL of Napin (1 mg/mL) solution, 4% $NaHCO_3$ (1 mL, pH 8.5) and 1 mL of freshly prepared 0.01% TNBS were added. The mixture was incubated at 40 ± 2°C for 2h and terminated by adding 1 mL of 10% SDS followed by 0.5 mL of 1N HCl. The absorbance of the solution was monitored at 335 nm against appropriate blanks. A standard lysine (0 – 25 μg) curve was constructed.

Effect of AIT concentration was studied by measuring the available lysine content. AIT concentration was varied from 0 – 0.6 mM, and napin concentration was kept constant (100 μM). After 2h incubation available lysine was measured. Also, interaction of AIT (0.3 mM) with napin (100 μM) was

studied as a function of temperature in the range 17 – 47°C. After two hours of incubation available lysine content was measured.

Effect of tyrosine ionization on napin and napin – AIT complex was studied in the pH range 7.0 –11.9. The pH of the napin solution was adjusted by the addition of 0.1 M NaOH. The sample was centrifuged and absorbance read at 280 nm.

RESULTS AND DISCUSSION

RESULTS AND DISCUSSION

Napin of *B. juncea* is a basic protein is allergenic in nature. There are four aromatic residues - one tyrosine, one tryptophan and two-phenylalanine residues -in the molecule (Dasgupta et al., 1995). Spectroscopic methods can be used conveniently to follow conformational changes of this molecule due to the unique presence of one tyrosine and one tryptophan in the large and small subunits, respectively. The structural stability of napin was probed, by DSC, CD, fluorescence and size exclusion chromatography, after thermal and chemical denaturation.

Napin was purified to homogeneity by gel filtration followed by ion - exchange chromatography. The purity was ascertained by SDS-PAGE under reducing and non-reducing conditions (Figure 11A) and size exclusion chromatography on HPLC (Figure 11B). Molecular mass of napin was determined by MALDI -TOF (Figure 11C) to be 14724 Da. Hydrodynamic radius of the napin, by dynamic light scattering was determined to be 2 nm (Figure 12A). The intensities of reduced napin are similar (Figure 12B). In the present study, the N-terminal amino acid sequence of napin (first eight residues of both large and small subunits) was identical to the reported sequence of *Brassica juncea* napin (Dasgupta et al., 1995).

Amino acid composition of napin is shown in the table 6. Napin contains single (n_{Trp} = 1.29) tryptophan and no free cysteines. The measured TI activity of napin is found to be 9-units/mg protein.

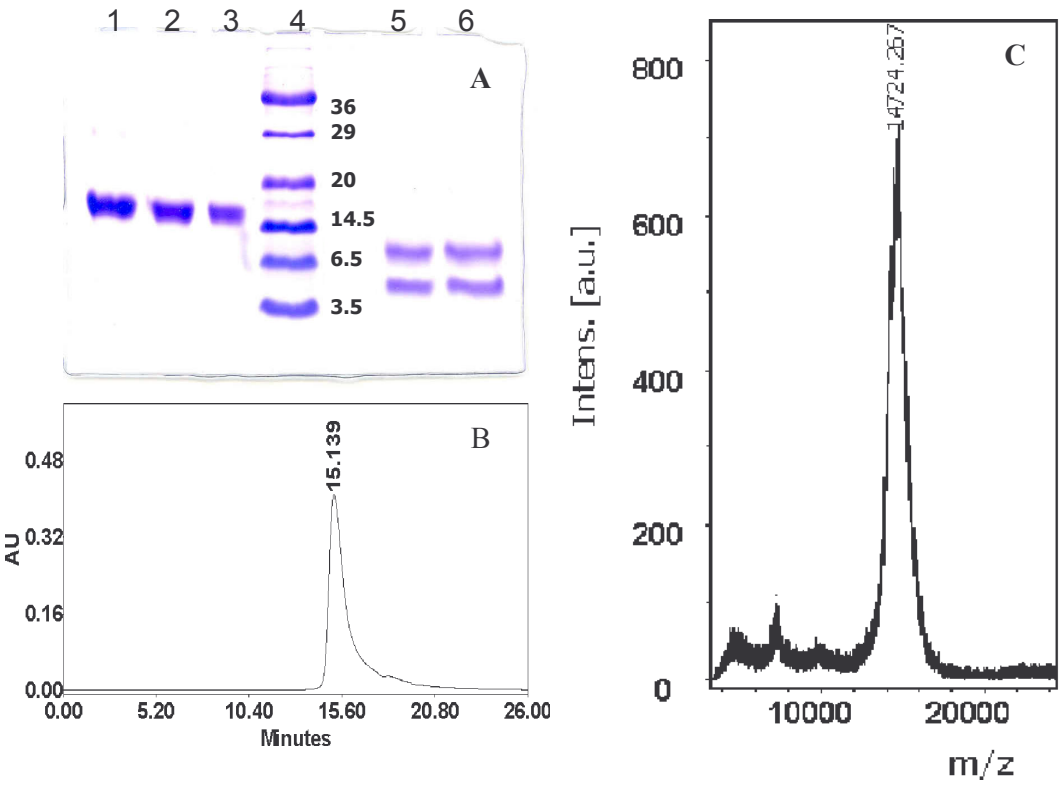

Figure 11. Establishing the homogeneity of *Brassica juncea* napin

A: SDS-PAGE pattern under non-reducing (lanes 1-3) and reducing (lanes 5 and 6). The gel (15%) was stained with coomassie brilliant blue R-250. Molecular weight markers in the range 36,000 – 3500 Da were run along with the protein (lane 4). The concentration of protein loaded was 1 mg/mL. **B:** Size exclusion chromatography on HPLC. Detection was at 280 nm using a photo diode array detector. Protein concentration was 1μg/μL. **C:** MALDI-TOF spectra of napin. The spectrum indicates an apparent molecular mass of 14,724 Da. RP-HPLC purified napin was used for determination of mass.

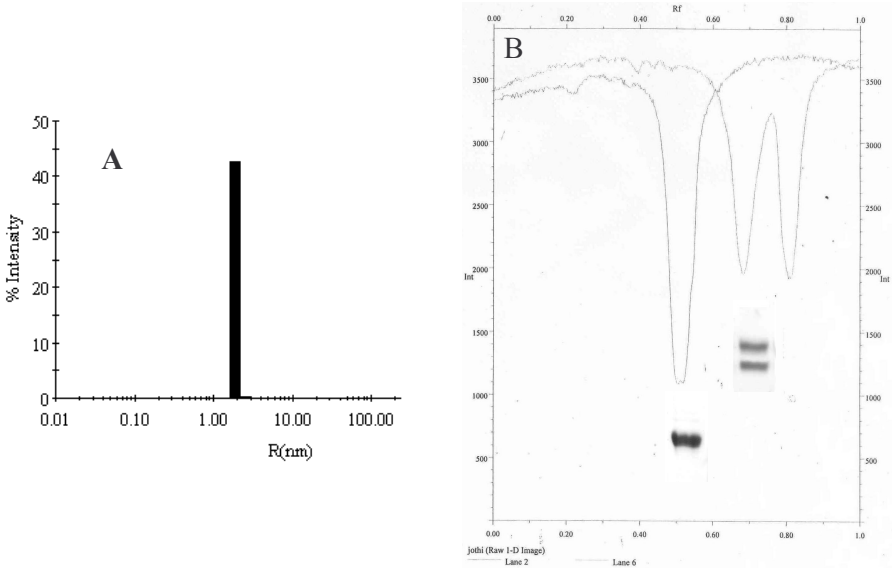

Figure 12. Hydrodynamic radius and intensity documentation of napin

A: Determination of hydrodynamic radius of napin using dynamic light scattering. A protein concentration of 1 mg/mL was used for the experiment.

B: Intensity documentation of napin and reduced napin of Napin and subunits.

Table 6. Amino acid composition of *Brassica juncea* napin

Amino acid	Mole (%)
Asx**	1.5
Glx***	25.1
Ser	4.3
Gly	7.5
His	2.9
Arg	7.34
Thr	2.89
Ala	5.43
Pro	10.72
Tyr	0.24
Val	5.07
Met	3.6
Iso	3.4
Leu	6.8
Phe	1.98
Lys	5.13
Cys	6.1

Cysteines are estimated as cysteic acid
** includes both Asp and Asn
*** includes both Glu and Gln

Section A: Contribution of electrostatic & hydrophobic interactions to the stability

Hydrophobic interactions play a major role in protein conformation (Privalov and Gill, 1988). Hydrophobicity of proteins helps in understanding and predicting the effects of manipulation of protein sequence. There are limited reports on the hydrophobicity of mustard napin. The surface hydrophobicity of napin using aliphatic and aromatic fluorescent probes has been calculated. The increase in the fluorescence emission intensity upon binding to accessible hydrophobic surface regions of proteins is used as a measure in the calculation of surface hydrophobicity. ANS, TNS and CPA are charged probes, whereas PRODAN is a neutral probe used to eliminate the contribution of electrostatic interactions during fluorescence measurements (Alizadeh-Pasdar and Li-Chan, 2000).

Organic solvents like monohydric alcohols induce more ordered helical conformation relative to native state of the protein (Herskovits, 1970). The addition of alcohols to the protein solution, apart from inducing α-helix structures, favors clustering of hydrophobic groups and better compactness in proteins (Arakawa and Goddette, 1985; Usha et al., 2006). We have used NaCl, Na_2SO_4, monohydric alcohols and TFE to explore the underlying forces that stabilize the napin molecule.

The pI (Iso electric point) of purified napin was found to be pH > 10.5 (shown in Figure 13A).

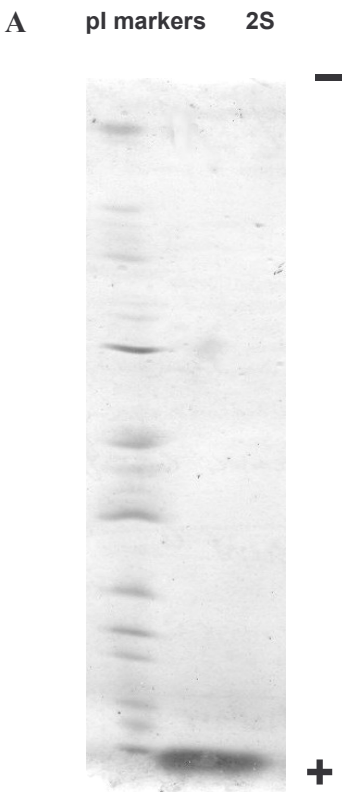

B

Amino terminal sequence

Small subunit– IPKXRKEF...
Large subunit– SQGPQQRP...

Figure 13. Isoelectric focusing and amino terminal sequence of purified napin. A: Isoelectric focused gel of napin. A concentration of 50 µg of napin was used for the experiment. The samples are loaded along with the standard pI markers. **B:** Amino terminal sequence of large and small subunit of napin.

The N - terminal sequence of reduced napin (Figure 13B) was identical to the deduced amino acid sequence from *B. juncea* (Dasgupta et al., 1995).

Limited proteolysis

Limited proteolysis of napin was carried out, using trypsin as a tool, to study the exposure of basic amino acid residues. The release of peptides as a function of time is shown in figure 14 inset. Digestion of napin by trypsin was feeble after 3 – 4 h of digestion. The protein digest, after RP-HPLC, showed a major peptide peak at retention time of 42 min (Figure 14). Molecular weight of the peptide was determined as ~ 6589 Da by MALDI –TOF (Figure 15). The peptide was found to be rich in cysteines and glutamines as determined by amino acid composition.

The structural studies by fluorescence (Figure 16) and CD (Figure 17A and 17B) shows the conformation of peptide is aperiodic. The peptide shows the emission maxima at 352 nm, which is a characteristic of solvent exposed tryptophan.

Hydrophobicity of napin

The hydrophilic/hydrophobic nature of napin was determined using Kyte and Doolittle Hydropathy plot (Figure 18). Sequence of napin used for the plot was from GenBank database (*Brassica juncea* CAA46785). The plot confirmed the hydrophilic nature of napin.

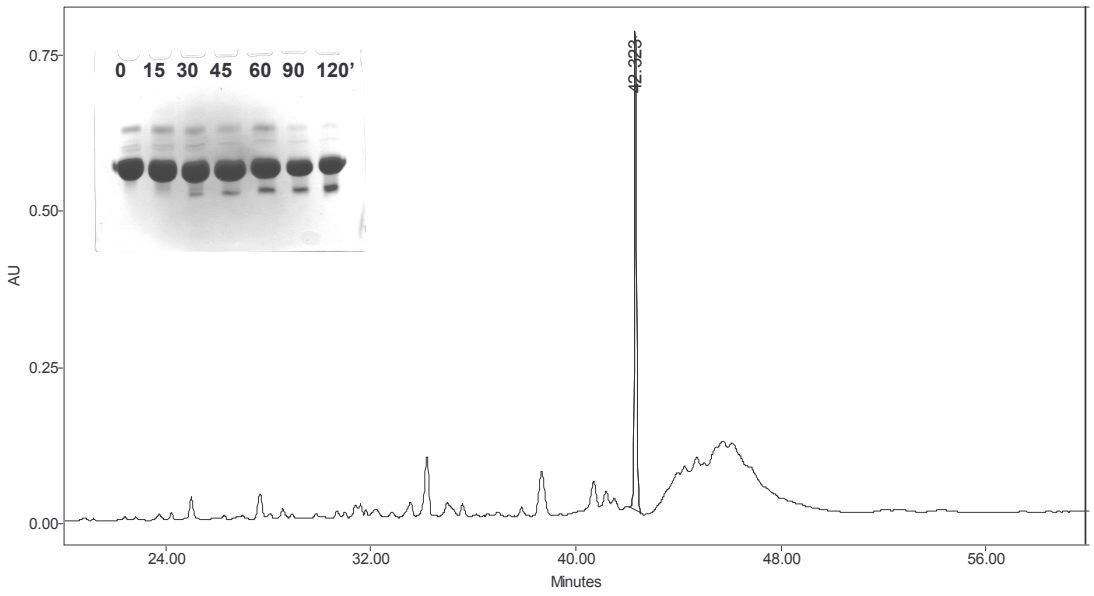

Figure 14. Trypsin digestion of napin

Purification of tryptic digests on RP HPLC. RP-HPLC was carried out using a symmetry shield ^{TM} RP_{18} (5.0 µ, 4.6 mm X 250 mm) Waters column. The bound protein was eluted by a shallow gradient of acetonitrile from 0-50% over time span of 70.0 min. The eluted protein was monitored at 230 and 280 nm. **Inset:** Napin (4.0 mg/mL) was digested with α-TPCK treated trypsin at 2:100 enzyme to protein ratio in 0.1 M ammonium hydrogen carbonate buffer (pH 8.2) at 37ºC. At different time intervals (min) the digest was drawn and loaded onto 15% non-reducing SDS-PAGE. Adding 10 µM TLCK The digestion was terminated.

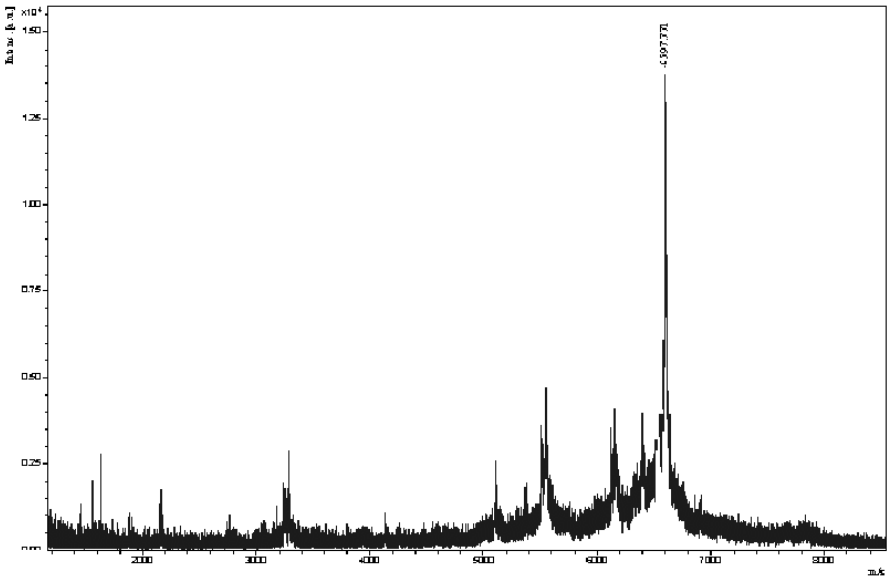

Figure 15. Mass spectra of purified peptide

Peptide MALDI-TOF spectrum indicates an apparent molecular mass of 6,597 Da. RP-HPLC purified peptide was used for the determination of mass.

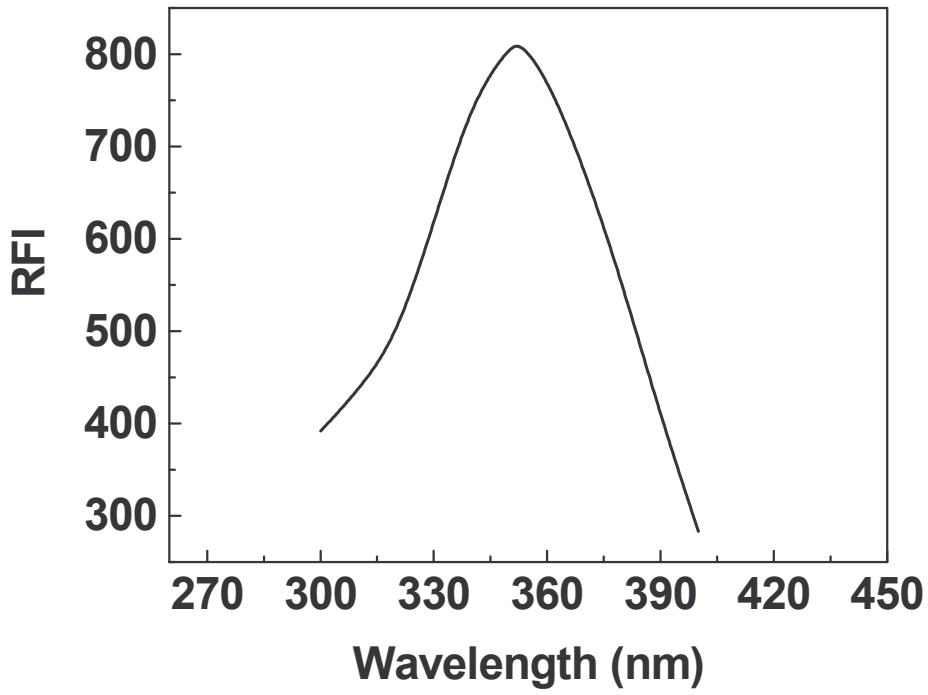

Figure 16. Conformational analysis of peptide - fluorescence

The emission spectrum of peptide was recorded from 300 – 400 nm, with excitation at 280 nm. The excitation and emission slits were at 5 and 5 nm respectively. A protein concentration of 0.05 mg/mL was used.

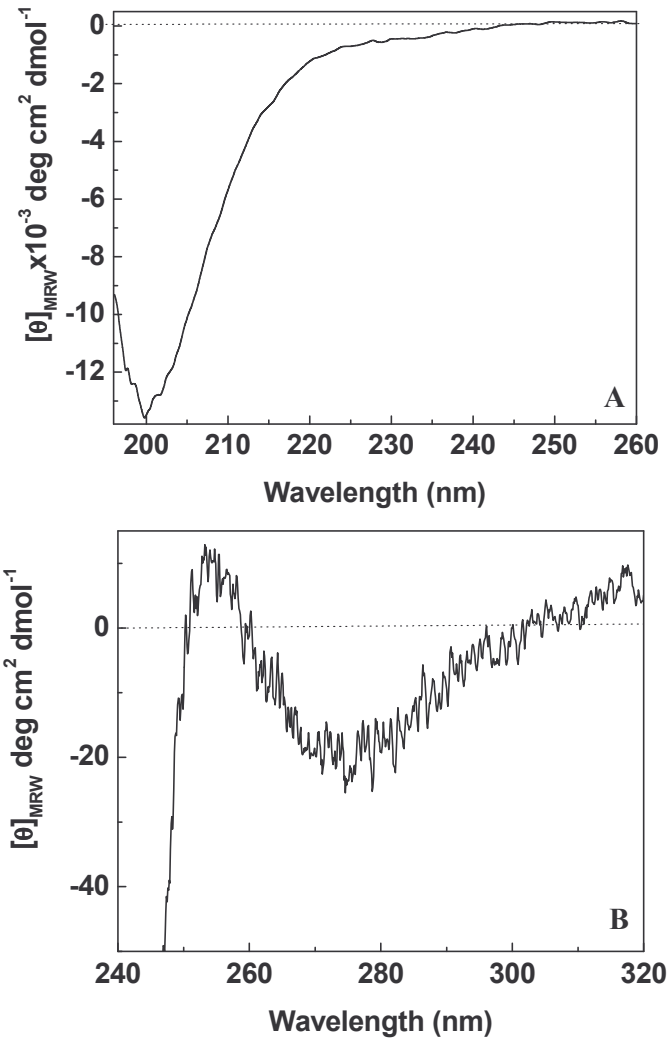

Figure 17. Conformational analysis of peptide - CD

A: Far UV CD (200 – 260 nm) spectra and **B:** near UV CD (320 – 240 nm) spectra. The spectra were recorded at a scan speed of 20-nm/ min. For far UV scans, protein (0.4 mg/ mL) in 0.02 M phosphate buffer was used. Protein concentration of 1.5 mg/mL was used in the near UV region.

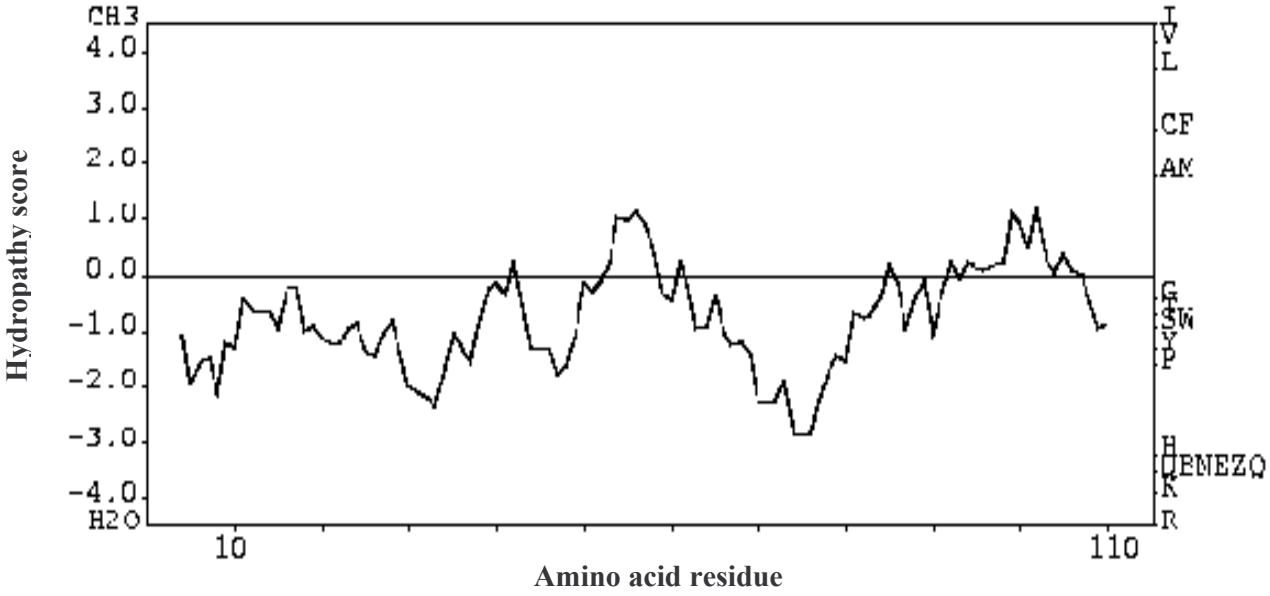

Figure 18. Hydropathy plot of napin

The Hydropathy plot of napin was constructed using Kyte and Doolittle method. The scale on the Y-axis represents the hydropathy score against amino acid residues.

Conformational analysis of napin

Napin contains a single tryptophan and tyrosine in its small and large subunits, respectively. Emission maximum is at 343 nm, suggesting the exposed nature of tryptophan in napin. The far UV CD of napin has revealed two minima at 208 and 222 nm. Intact protein is rich in α-helix (~40%).

The contribution of subunits to the conformation of napin was studied by reduction of disulfides and blocking the free thiol with iodoacetamide. The elution profile revealed two peaks and the purity of the subunits were ascertained by 15% SDS-PAGE. Secondary structures of the subunits revealed only aperiodic structure (Figure 19A). Intrinsic fluorescence showed emission maxima of 353 and 305 nm, for small and large subunits, respectively (Figure 19B). This indicated the presence of tryptophan and tyrosine in small and large subunits, respectively. The two separated subunits were also hydrophilic in nature and devoid of buried hydrophobic patches. The absorption spectra of napin and separated subunits are shown as figure 19A inset

In order to understand the interactions responsible for stability of napin, the effect of additives on the conformation of the protein was studied. The changes in surface hydrophobicity of napin were followed by fluorescent probes ANS, TNS, PRODAN and CPA.

In order to understand the effect of electrostatic and hydrophobic interactions, sodium chloride and sodium sulphate, (0 – 1 M) were used.

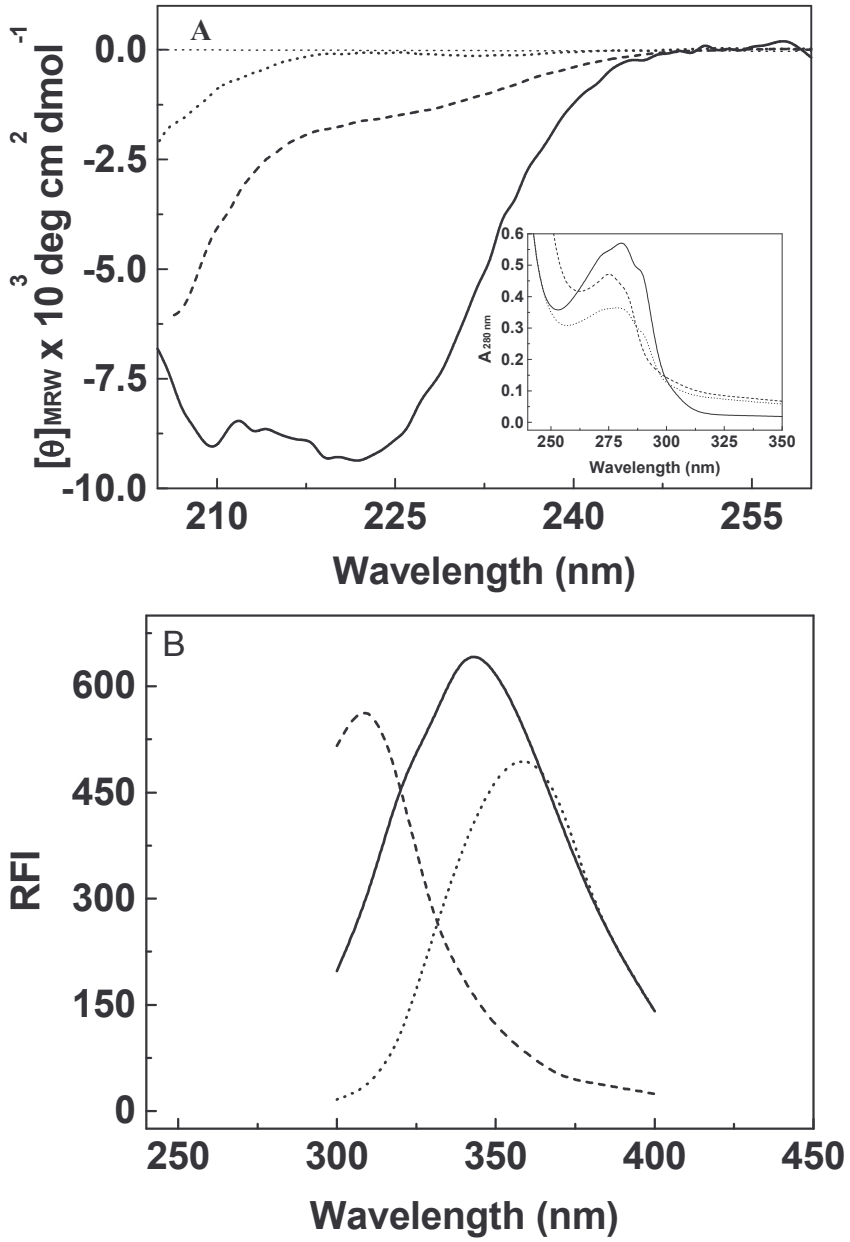

Figure 19. Charecterization of separated subunits

A: The far-UV CD of napin and separated subunits. **B:** Fluorescence emission spectra of subunits. The emission spectrum was recorded from 300 - 400 nm, when excited at 280 nm. The excitation and emission slit widths were at 5 nm. **Inset A:** Absorption spectra of napin and separated subunits recorded using Shimadzu-1602 spectrophotometer with 1cm path-length cell. (—), Napin; (...), small subunit; (- -) large subunit.

The effects of TFE, the helix promoter and monohydric alcohols on the conformation of napin were followed. Surface hydrophobicity measurements through fluorescent probes

Surface hydrophobicity can be classified into aliphatic and aromatic hydrophobicity. CPA is useful for determining the aliphatic hydrophobicity, since it is composed of aliphatic hydrocarbons and is a plant derived 18-carbon fatty acid. ANS, due to its aromatic structure, is used for determining aromatic hydrophobicity (Moro et al., 2001). TNS, a derivative of ANS, though non-fluorescent, fluoresces when bound to hydrophobic regions of protein and can be used as surface hydrophobic probe (McClure and Edelman, 1967). On the other hand, PRODAN is a neutral probe, which eliminates electrostatic contribution in the measurement of hydrophobicity.

Plots of fluorescence quenching, upon progressive addition of ANS, TNS, PRODAN and CPA, are shown in figure 20 and figure 21. The Scatchard plots are given as insets. Binding constants and number of binding sites for the protein in presence or absence of 0.5 M NaCl and 0.2 M Na_2SO_4 has been calculated and are shown in table 14; 0.5 moles of fluorescent probe bind per mole of protein indicating the hydrophilicity of napin. There is a reduction in binding constant and number of binding sites in the presence of NaCl as compared to control. The binding constant of CPA to napin is lower compared to the aromatic hydrophobic probes.

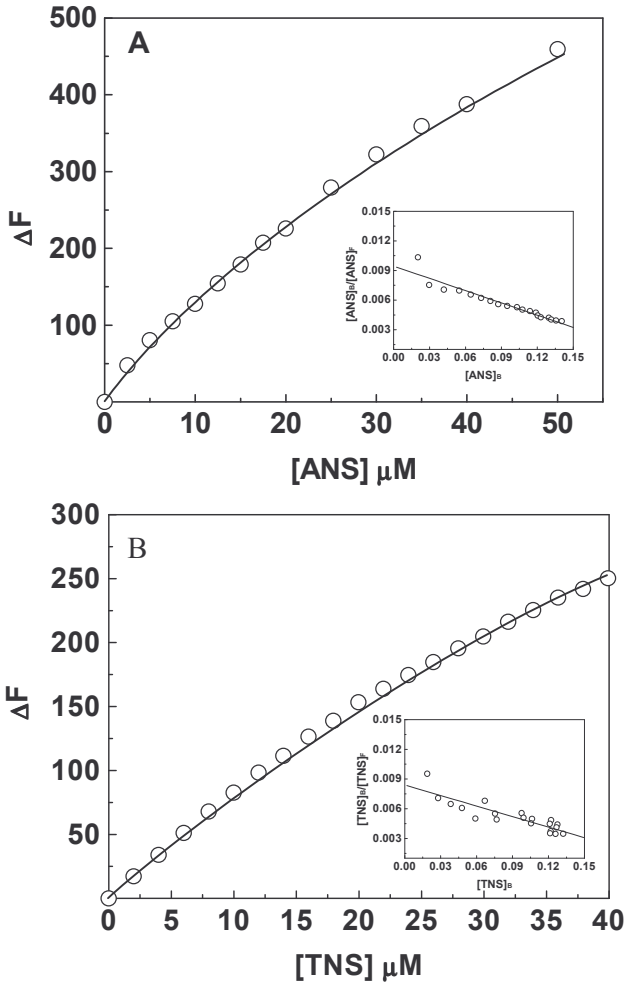

Figure 20. Surface hydrophobicity measurement of *B. juncea* napin

Plot of increase in the **A:** ANS - protein bound fluorescence (emission followed at 480 nm when excited at 375 nm); **B**: TNS - protein complex (emission at 460 nm when excited at 366 nm); **Inset**: Scatchard plots for determining the binding constants. The excitation and emission slit widths were 5 and 5 nm. Protein concentration used was 0.75 mg/mL.

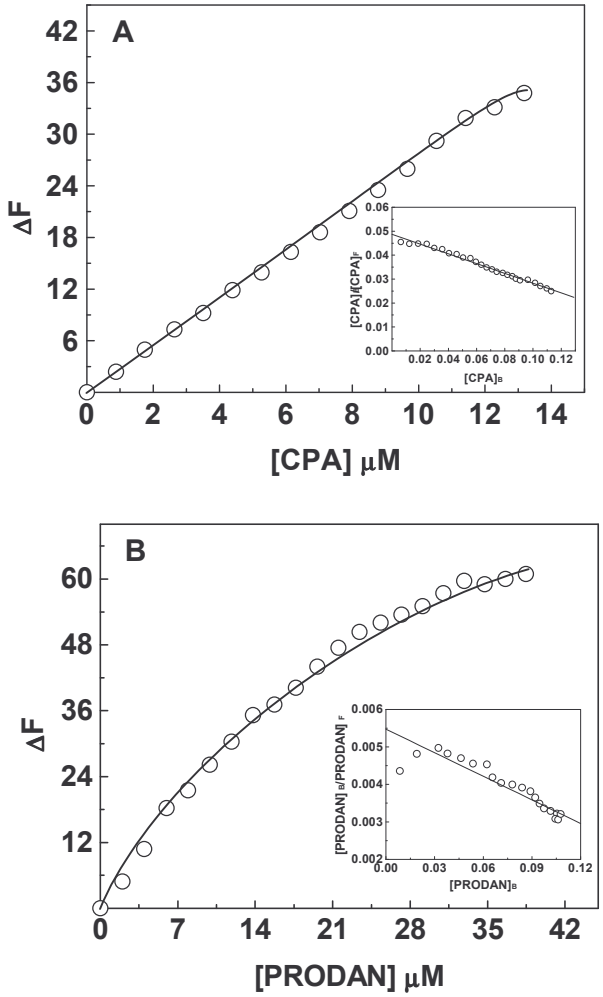

Figure 21. Surface hydrophobicity measurement of *B. juncea* napin

Plot of increase in the **A:** CPA - protein complex (emission at 420 nm when excited at 325 nm); **B**: PRODAN - protein complex (emission at 465 nm when excited at 365 nm); **Inset**: Scatchard plots for determining the binding constants. The excitation and emission slit widths were 5 and 5 nm. Protein concentration used was 0.75 mg/mL.

Table 7. Binding constants of napin with different fluorescent probes

	ANS	PRODAN	TNS	CPA
CONTROL				
No. of binding sites	0.48 ± 0.1	0.6 ± 0.1	0.53 ± 0.1	0.6± 0.1
Binding constant (M^{-1})	4.1 $x10^4$	9.5 $x10^4$	2.0 $x10^4$	0.91 $x10^4$
0.5 M NaCl				
No. of binding sites	0.21 ± 0.1	0.26 ± 0.1	0.3 ± 0.12	0.24 ± 0.1
Binding constant (M^{-1})	2.1 x 10^4	4.3 x 10^4	1.19 x 10^4	0.46 x 10^4
0.2 M Na_2SO_4				
No. of binding sites	0.5 ± 0.1	0.45 ± 0.1	0.62 ± 0.1	0.52 ± 0.1
Binding constant (M^{-1})	3.55 x 10^4	8.5 $x10^4$	1.9 x 10^4	0.89 x 10^4

Emission maximum of napin in presence of ANS was 480 nm when excited at 375 nm.
Emission maximum of napin in presence of TNS was 460 nm when excited at 366 nm
Emission maximum of napin in presence of PRODON was 465 nm when excited at 365 nm
Emission maximum of napin in presence of CPA was 420 nm when excited at 325 nm.
A protein concentration of 0.75 mg/mL was used for all the measurements. The results are average of three individual experiments.

Table 8. Surface hydrophobicity of napin with different fluorescent probes

	Surface hydrophobicity (S_o)		
	Control	**0.5 M NaCl**	**0.2 M Na_2SO_4**
ANS	22±0.1	10.6±0.1	24.04±0.8
PRODAN	44±0.6	22.2±0.3	39.11±1.2
TNS	18±0.55	5.51±0.4	15.11±1.01
CPA	12±0.1	7.2±0.5	2.2±2.0

Effect of salts on napin structure

Fluorescence measurements

The effect of salts on the tertiary structure has been studied by fluorescence emission spectra. Napin, in buffer A, was incubated with different concentrations of KCl, NaCl and Na_2SO_4, for 30 min. The relative fluorescence intensity increases with increasing salt concentration and the emission maxima shifts towards blue (-4 nm for NaCl and -1 nm for Na_2SO_4). The effect of KCl on napin is found to be similar to NaCl. Beyond 0.5 M NaCl, the fluorescence intensity remains constant, while above 0.7 M; a decrease in intensity is observed. In case of 0.2 M Na_2SO_4, maximum increase in the fluorescence intensity has been observed at 0.2 M (Figure 22 inset). Salt concentration of 0.5 M NaCl and 0.2 M Na_2SO_4 was used for the further measurements. Blue shift in the emission maximum, in presence of salt, may be due to environment around the tryptophan residue being more hydrophobic compared to native (Figure 22).

Circular dichroism measurements

Changes in the secondary structure of napin, upon salt addition, were followed by far and near UV CD spectra. The ellipticity value increased up to ~25 % in presence of 0.5 M NaCl and 3% in presence of Na_2SO_4. Beyond 1 M NaCl and 0.5 M Na_2SO_4, the ellipticity value (at 222 nm) decreased. In presence of 0.5 M NaCl, the ellipticity ratio, R, ($[\theta]_{222}/[\theta]_{208}$) increased from 1.05 to 1.25 $\pm$ 0.05, indicating a stronger inter-helical association (Figure 23A) (Lazo and Downing, 2001).

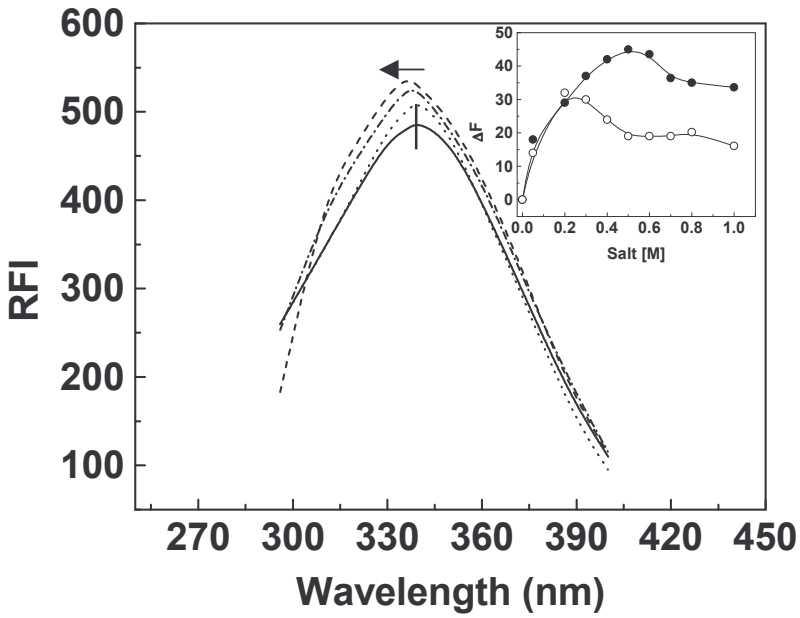

Figure 22. Salt induced conformational changes - fluorescence

The changes in fluorescence emission intensity of napin (—) napin in buffer A, (····) 0.2 M NaCl, (---) 0.5 M NaCl, (-·-) 0.75 M NaCl. **Inset**: Plot of change in the relative fluorescence intensity as a function of (●), NaCl and (○) Na_2SO_4.

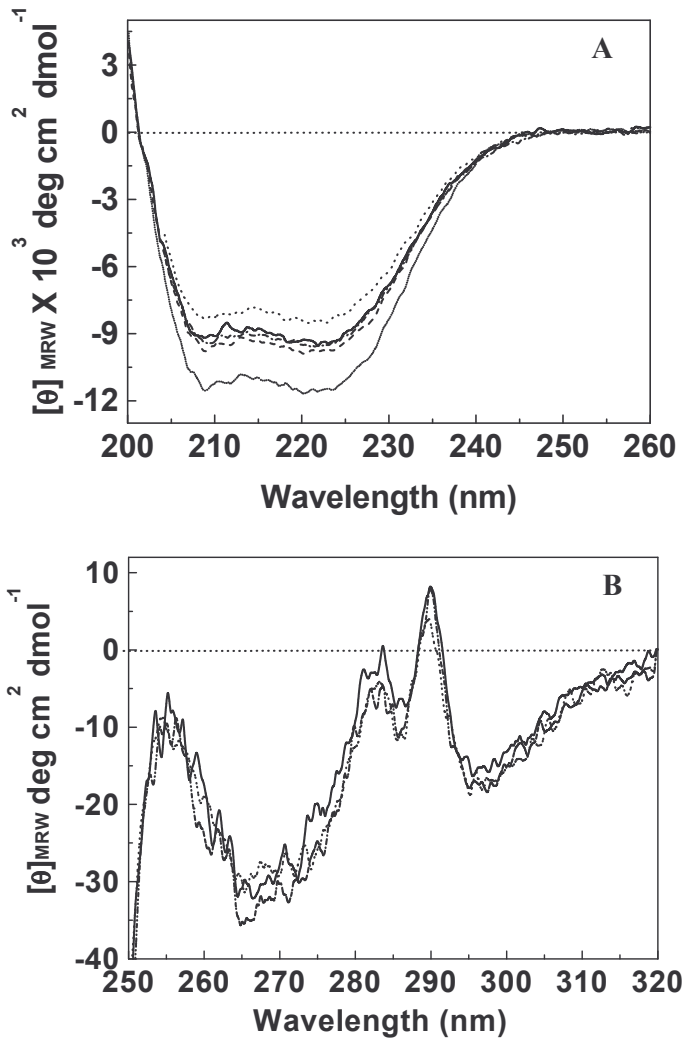

Figure 23. Salt induced conformational changes - CD

A: Far UV CD spectra. (**---**) Napin in buffer A, (····) 0.2 M Na_2SO_4, (—) 0.5 M NaCl, (-·-) 0.75 M NaCl and (–··–) 1.0 NaCl. **B:** Near UV CD spectra. (——) Napin in buffer, (…) 0.5 M NaCl and (- - -) 0.2 M Na_2SO_4. For far UV scans (200 – 260 nm), protein (0.4 mg/ mL) in buffer A was used. Protein concentration of 2.5 mg/mL was used in the near UV region (320 – 240 nm). Path-length of the cells was 1 mm and 10 mm for the far UV and near UV scans, respectively.

In presence of Na_2SO_4, the ratio was 1.07, indicating little or no change. The tertiary structure changes of napin, in presence of salts, were followed by near UV-CD, which showed no significant change in the ellipticity values at 0.5 M NaCl and 0.2 M Na_2SO_4 (Figure 23B).

Acrylamide quenching of intrinsic fluorescence

Quenching of napin fluorescence by acrylamide, a non-ionic quencher, is shown in figure 24A. The Stern-Volmer plot has been used to obtain the constant, K_{SV} (Figure 24B). The fractional accessibility of the lone tryptophan, indicative of its exposure to solvent, is 0.63 (Table 9). In presence of 0.5 M NaCl, the fractional accessibility is found to decrease to 0.5 and in presence of sulphate remains at 0.6. The decrease in the K_{SV}, in presence of NaCl, may be due to compaction of the molecule.

Gel filtration - Native napin eluted at 17 mL in buffer A. In presence of 0.5 M NaCl, the elution volume shifted to 18.2 mL indicating reduction in Stokes radius. There was no significant change in the elution volume in presence of 0.2 M Na_2SO_4.

$\boldsymbol{T_M}$ - The effect of 0.5 M NaCl and 0.2 M Na_2SO_4, on the secondary structure loss, was studied at 222 nm, in the temperature range 27- 75°C (Figure 25). In presence of 0.5 M NaCl, T_M (Transition temperature) shifted from 74°C to 88°C indicating increased protein stability.

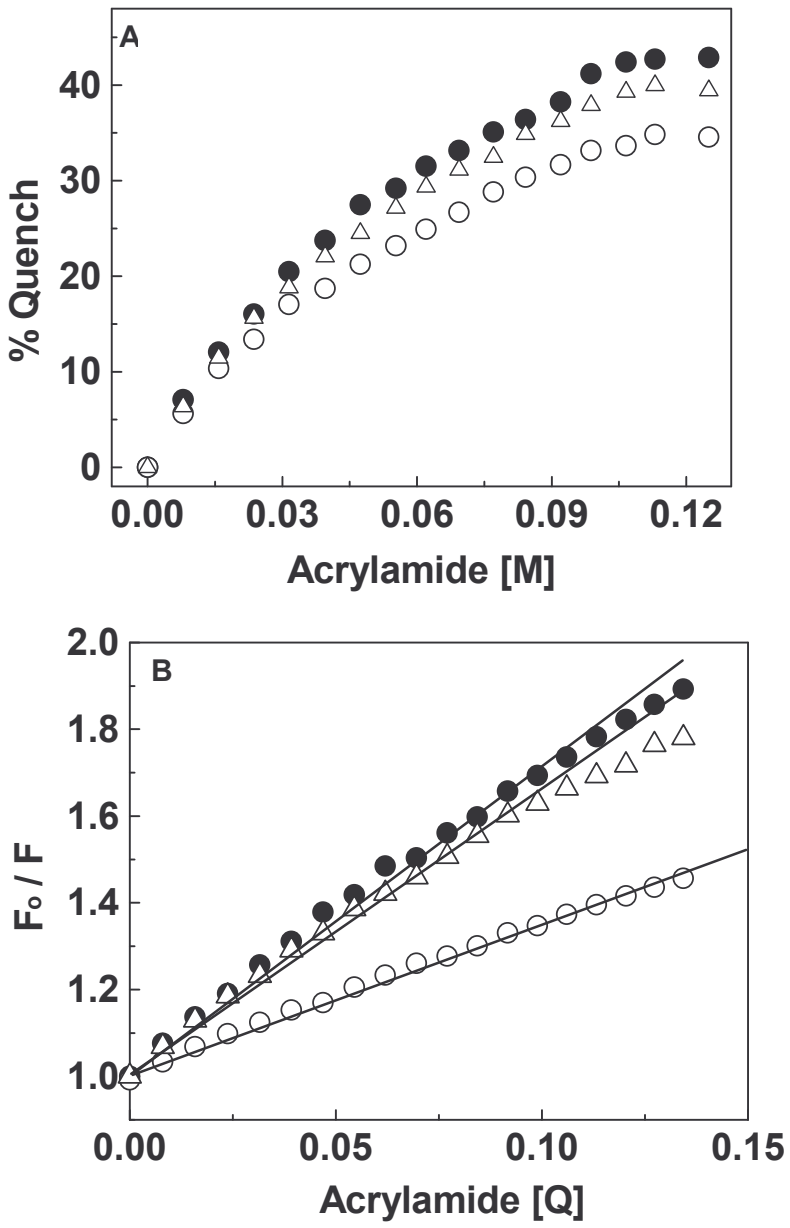

Figure 24. Intrinsic fluorescence quench of napin by acrylamide

A: Primary plot of fluorescence quench as a function of acrylamide concentration. The accessibility of tryptophan was calculated using modified Stern-Volmer equation. **B:** Stern – Volmer plot for acrylamide quenched fluorescence of napin.

(●) Napin in buffer A, (○) in presence of 0.5 M NaCl and (△), 0.2 M Na_2SO_4.

Table 9. Intrinsic fluorescence quenching by acrylamide

	Stern-Volmer constant K_{SV} (M^{-1})	Fractional accessibility
Control	6.5 ± 1.1	0.63 ± 0.14
0.5 M NaCl	3.4 ± 0.55	0.50 ± 0.1
0.2 M Na_2SO_4	6.2 ± 0.96	0.59 ± 0.11

Protein concentration of 0.12 mg/mL was used for all the measurements. The results are average of three individual experiments

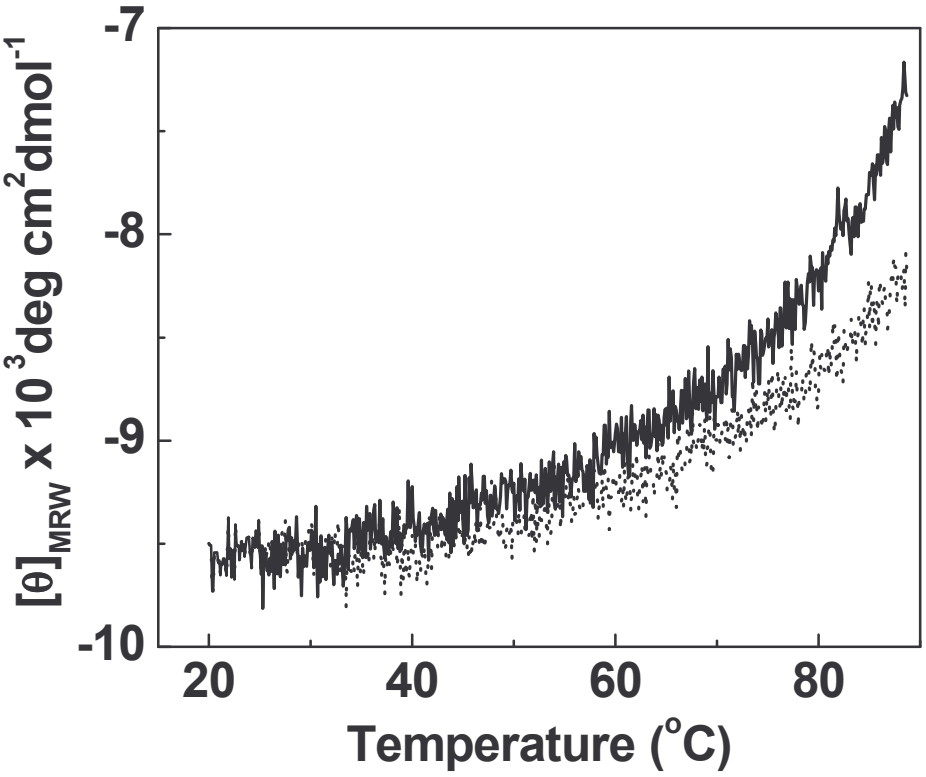

Figure 25. Temperature induced unfolding-CD

Temperature induced unfolding of napin in presence and absence of 0.5 M NaCl, monitored at 222 nm. The protein in buffer A was heated in the temperature range 27 – 75°C, at a heating rate of 1°C/min. (—), napin; (····), napin in 0.5 M NaCl. Mean residue weight of 110 was used to calculate the molar ellipticity. Protein (0.4 mg/mL) in buffer A was used for the measurements.

Effect of monohydric alcohols on napin structure

Solvents play an important role in maintaining the native structure of a protein. Structural studies of proteins in the presence of different solvent systems can provide information on their unique folded structure in solution. The propensity to form α-helix (38 %) reached maximum at 17 M methanol concentration, beyond which the protein precipitated. Napin, in presence of 8.25 M ethanol, showed 28 % increase in α-helix (Figure 26). Above 15 M ethanol concentration, protein precipitated. Similar studies, in presence of propanol and butanol, revealed increase in α-helix (20% increase in propanol and 10% increase with butanol) at 6.7 M and 3.5 M concentrations, respectively.

The change in molar ellipticity as a function of TFE is shown in Figure 26. The effect of TFE (helix promoter) on the secondary structure is shown in Figure 27. Increase in α-helix (50 %) at 10 M TFE concentration was seen. Beyond 10 M TFE, protein precipitation was observed.

Inhibition of RNase activity was used to determine the IC_{50} and K_I. (Figure 28A). The IC_{50} and K_I were found to be 12.5 μM and 1.5 μM respectively. Due to its amphipathic nature, napin -DNA interaction was confirmed by gel retardation assay. A ratio of 100: 5 DNA to protein was used. 0.8% agarose gel clearly shows the retardation in the movement of plant/ microbial DNA (Figure 28B). Protein is forming structure in presence of monohydric alcohols, TFE and SDS. Therefore, it is interesting to study the

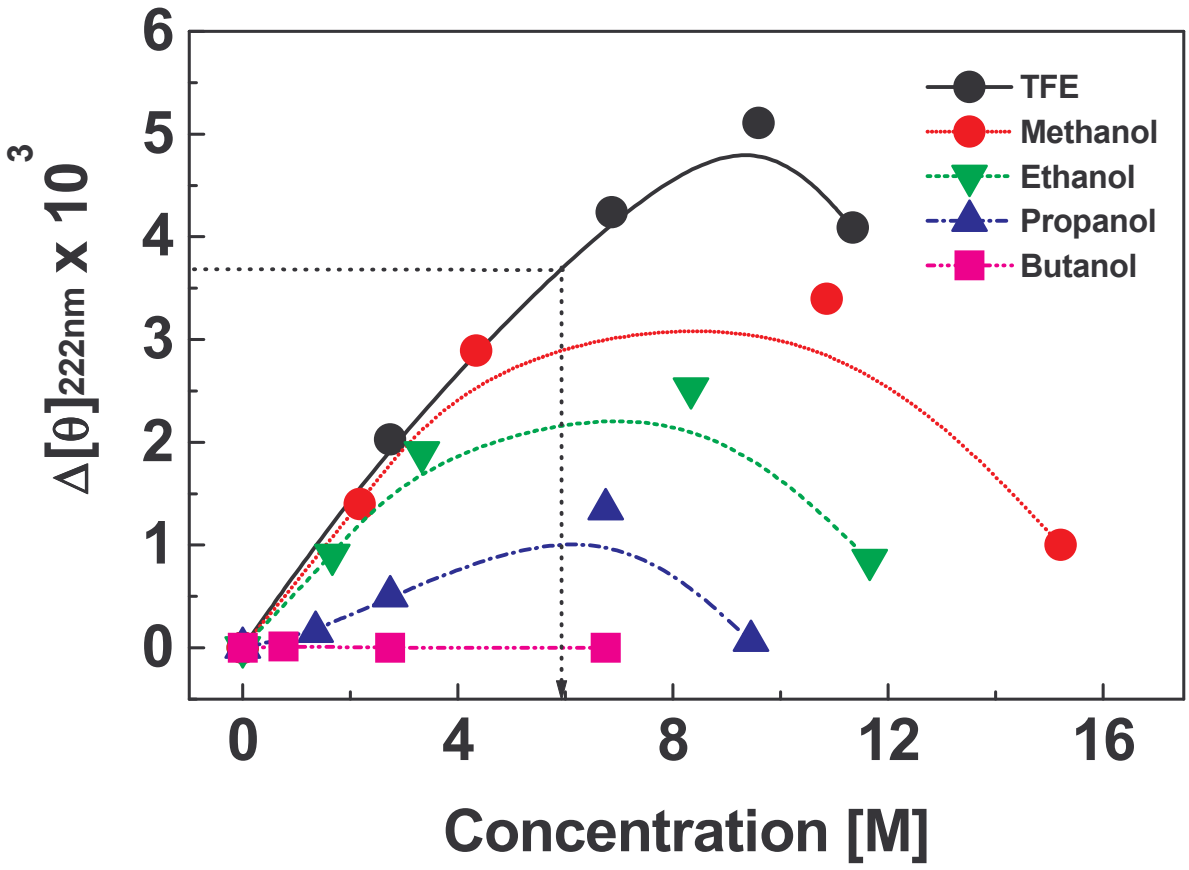

Figure 26. Monohydric alcohol induced structural changes in napin

Plot of the change in the ellipticity at 222 nm as function of monohydric alcohol concentration. Protein concentration was 0.4 mg/mL. The samples were centrifuged before recording the spectra.

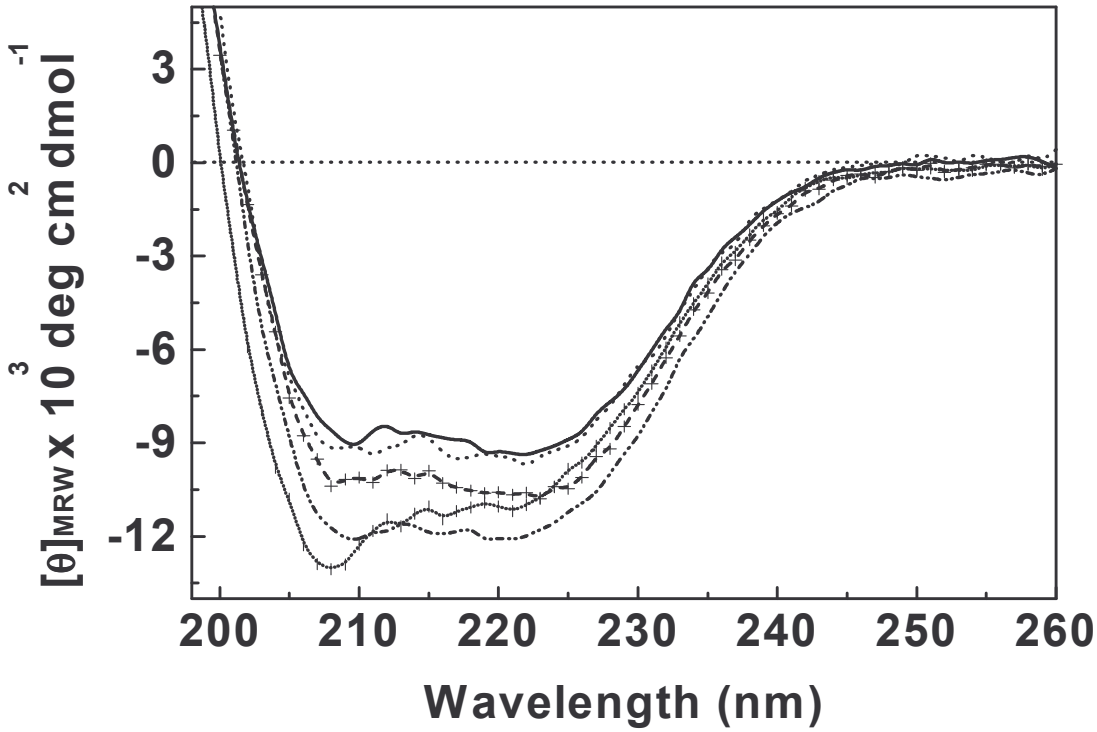

Figure 27. TFE induced structural changes in napin

Far UV CD spectra (—), napin in buffer A; (…), 3.0 M; (++), 6.0 M; (…| …), 12.0 M; (-·-·-), 12.0 M TFE. Scans were recorded in the region of 200 – 260 nm using a 1 mm pathlength cell. Protein concentration was 0.4 mg/mL. The samples were centrifuged before recording the spectra.

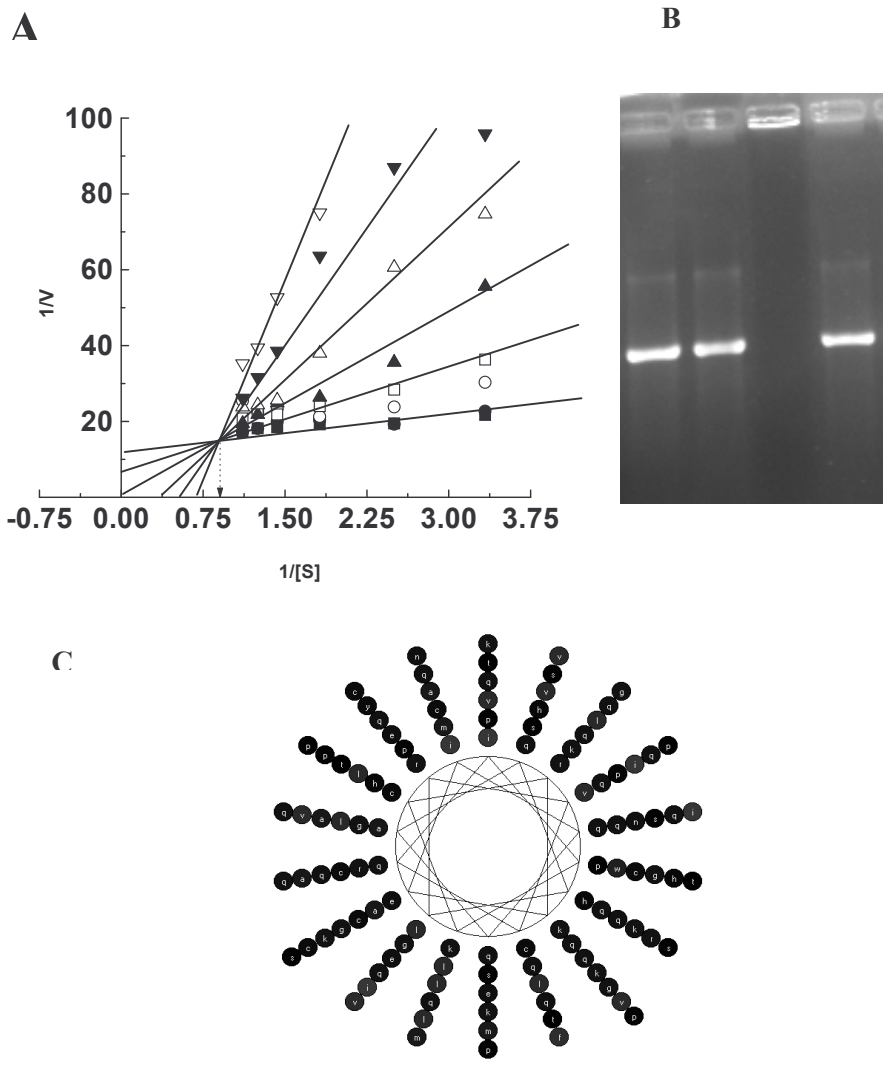

Figure 28. Napin – Nucleic acid interaction

A: Line weaver Burk plot of napin–RNA. K_I was determined using double reciprocal plot. Inhibitor (napin) concentrations used (●) control, (■) 10 μM, (○) 20 μM, (□) 30 μM, (▲) 35 μM, (△) 40 μM, (▼) 45 μM and (▽) 50 μM. **B: Gel retardation assay**: A ratio of 5 to 100 μg protein to DNA was used. The DNA in the gel was visualized by staining with ethidium bromide. Plant DNA used for the experiment. **C:** Helical wheel representation of napin was generated using *BioEdit* Sequence Alignment Editor software (ver.7.0.5.3).

amphipathic nature of napin. Amphipathic helical wheel diagram of napin was generated using software BioEdit (Figure 28C).

Discussion

Napin from mustard (*Brassica juncea* L) is synthesized as a precursor protein and translocated into endoplasmic reticulum where the intrachain disulfide bonds are formed. The proprotein is transported via secretory pathway to the vacuole where the negatively charged pro-sequences are proteolytically cleaved (Muren et al., 1996) to yield the mature napin.

Napin is found to be anti-fungal and anti-microbial (Onaderra et al., 1994). Although, mustard protein has a well-balanced amino acid profile and a favorable protein efficiency ratio, its utility as a food source of protein is limited by its allergenicity. We have investigated the contributions of the different interactions to the stability of napin.

In the present study, napin is purified and identified by comparing the amino- terminal sequence of two separated subunits to the available deduced amino acid sequence of *B. juncea* (Dasgupta et al., 1995). The protein has ~40% helix and is highly hydrophilic as shown by the Kyte and Doolittle Hydropathy plot. Napin is resistant to trypsin digestion. A peptide, rich in glutamine and cysteine, has been obtained at the end of 2 h, with most of the protein remaining intact (Figure 14). Napins from *Brassica* species are resistant to proteolysis by gastric enzymes (Pantoja-Uceda et al., 2004).

Extrinsic fluorescence probes like ANS, TNS, CPA and PRODAN have been used for determining the aromatic and aliphatic (CPA) hydrophobicity of napin. The binding constants and surface hydrophobicity for all the above probes are low (Table 7 and Table 8) with only ~0.5 moles binding to 1 mole of protein. The binding constant decreases in the presence of 0.5 M NaCl concentration. These values confirm the hydrophilic nature of the molecule. No significant change in the surface hydrophobicity is observed in presence of Na_2SO_4.

Addition of 0.5 M NaCl and 0.2 M Na_2SO_4 results in a shift of the emission maximum of 5 nm and 1 nm, respectively, towards shorter wavelength. The fractional accessibility of the single tryptophan in napin has been evaluated by following the quenching of intrinsic fluorescence by acrylamide in absence and presence of 0.5 M NaCl. Stern-Volmer constant decreases from 6.5 M^{-1} to 3.4 M^{-1}, indicating compactness in presence of NaCl. The compaction of the molecule in presence of 0.5 M NaCl is further confirmed by gel filtration.

Na_2SO_4 does not affect the secondary structure of napin. Addition of NaCl results in increase of 25% helical structure as monitored by far-UV CD spectra. The changes in the thermal transition (T_M), and elution volume could be due to compaction of protein. Based on its sequence (*GenBank* CAA46785), napin has a net positive charge of +9 at neutral pH. Hence, it is likely that the anions play a key role in the salt effect on napin. The high net positive charge coupled with low hydrophobicity suggests that napin is a rather weakly folded protein driven largely by disulfide linkages. Charge

neutralization or preferential exclusion (of the salt) from the vicinity of the protein results in compactness in presence of high salt concentrations (Gouda et al., 2003; Nishimura et al., 2001).

The propensity for napin to form structure, in the presence of intramolecular interaction enhancing organic solvents such as alcohols and TFE, has been studied. Monohydric alcohols and TFE induce structure as evidenced by increased helical content of napin. TFE is known to be an intramolecular hydrogen bond enhancer and protects solvent-exposed hydrophobic residues from aggregating. Low concentrations of monohydric alcohols on napin show the propensity to form α-helix in the presence of alcohols in the order TFE > methanol > ethanol > propanol > butanol.

The structural changes induced by alcohols are reversible. Higher concentrations of propanol (> 6.7 M) and butanol (> 3.5 M) result in protein precipitation. Recent studies have shown that at low concentrations, TFE and monohydric alcohols act by a cosmotropic mechanism to promote desolvation of the polypeptide backbone and not directly through stabilization of helical structures or strengthening hydrogen bonds (Kentsis and Sosnick, 1998).

Propensity of forming helix in presence of TFE and SDS, which mimics the membrane, may help in the prediction of napin anti fungal and anti microbial activity. The results of napin assuming more structure in presence of membrane mimicking environment led us to investigate the DNA binding ability. Gel retardation assay confirms the binding ability of napin to DNA. This also may be due to the basic (pI >10) nature of the napin.

Na_2SO_4 does not affect napin structure or stability. Addition of NaCl results in compaction of mustard napin. Electrostatic interactions play a major role in stabilizing the protein structure in addition to the presence of disulfide linkages.

Section B: Thermodynamic and structural stability of napin

Stability of napin

Resistance to proteolytic digestion - Napin is resistant to proteolytic cleavage by trypsin and chymotrypsin. The degree of hydrolysis of napin, at 27°C, was found to be 1.9 and 2.2%, respectively, with trypsin and chymotrypsin (Figure 29A inset). The protein was resistant to cleavage by trypsin and chymotrypsin at higher temperatures also (60°C).

Thermal unfolding

Circular dichroism spectroscopy - CD spectra of napin protein were obtained in the near and far UV regions (Figure 29A and 29B). Near UV CD spectra (320 – 240 nm) revealed minima at 295, 270 and 265 nm and two peaks at 290 and 255 nm in the native protein. In the far-UV region (260 – 200 nm), minima were observed at 222 and 208 nm indicating the predominance of helical structure. The experimental curve could be fitted to the presence of 43 % α- helix, 22 % β- turns and 35% aperiodic structure by the method of Yang et al. (1986). The changes in the ellipticity values either at 295 nm or 222 nm were followed in the temperature range of 27 - 77°C. There was considerable residual structure in the protein even at 77°C indicating its thermal stability. Any change observed in the far or near UV regions was completely reversible on cooling the protein.

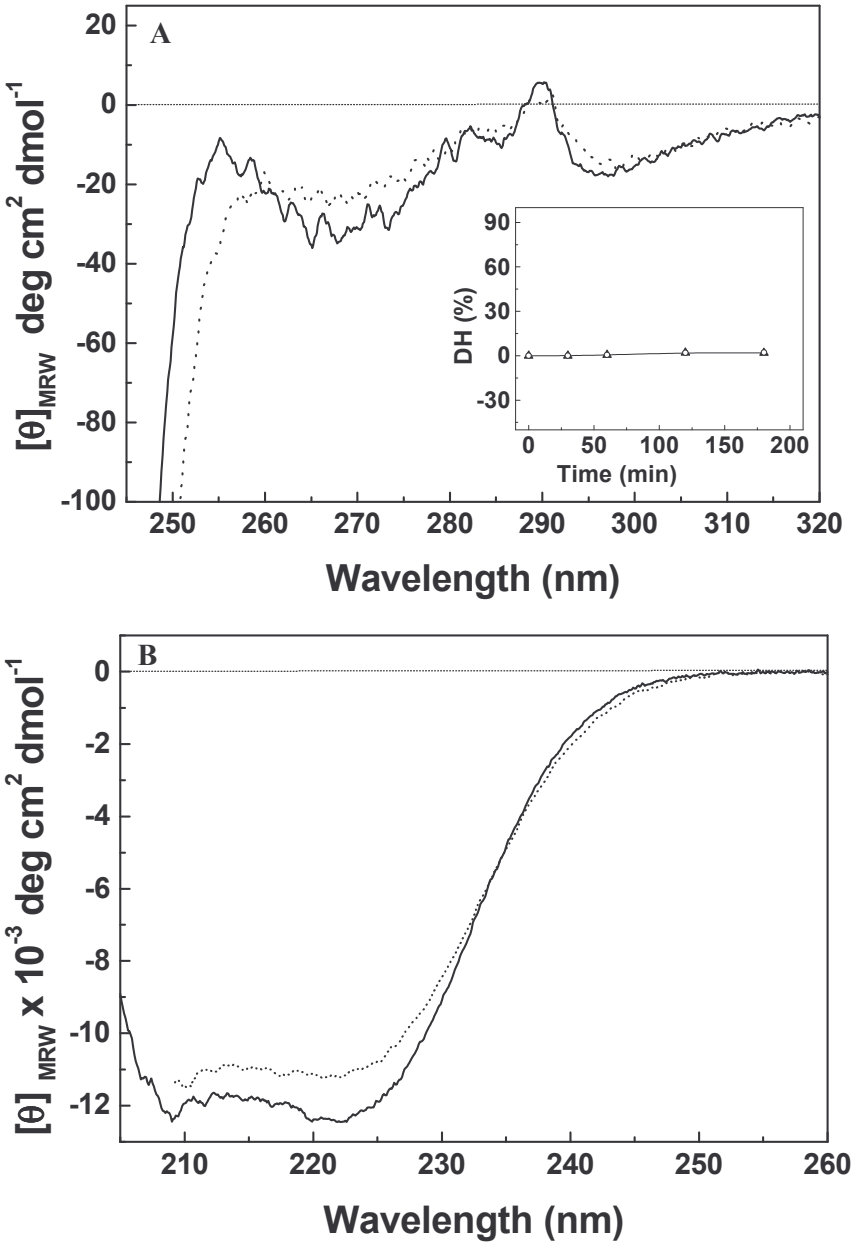

Figure 29. Thermal unfolding of *B. juncea* napin: CD analysis

A: Near UV CD spectra (240 – 320 nm) and **B:** Far UV CD spectra (200 – 260 nm). For far UV scans, protein (0.4 mg/mL) in 0.02 M phosphate buffer was used. Protein concentration of 2.5 mg/mL was used in the near UV region. (——), 27°C and (……), 75°C. **Inset A:** Resistance to trypsin and chymotrypsin digestion of napin. Napin (4.0 mg/mL) was digested with α-TPCK trypsin and α-TLCK chymotrypsin at 1:100 (37ºC). Reaction was terminated by the addition of 10μM TLCK and TPCK.

Fluorescence measurements – Napin has an emission maximum at 343 nm, when excited at 280 nm. This is typical of an exposed tryptophan residue in protein. The relative fluorescence intensity remains unchanged till 42°C suggesting little or no change in the environment around the tryptophan. However, there was 8 – 10% decrease in fluorescence intensity in the range 43 – 67°C, indicating slight change in tertiary structure in this temperature range. Beyond 67°C, no further change in the RFI was observed (Figure 30).

DSC measurements – DSC scans of napin in buffer A were carried out in the temperature range 25 - 90ºC at a scan rate of 60 K/h. The scan together with the fit of the transition peak data to a three state model are given in figure 31. Deconvolution of the transition peak reveals the existence of two kinds of entities at different temperatures. The first transition temperature (T_{M1}) was at 50.5ºC and the second transition (T_{M2}) was at 62.8ºC. Both the transitions (T_{M1} and T_{M2}) can be fitted into a least square fit (Figure 31). Rescans of the sample from 27ºC show complete reappearance of the peaks indicating that both transitions are completely reversible. Protein aggregation was observed beyond 80ºC.

The concentration and scan rate dependence of the thermodynamic parameters were studied in the protein concentration range (10 - 106 μM) and scan rates (10 - 60 K/h) (Table 10 and Table 11).

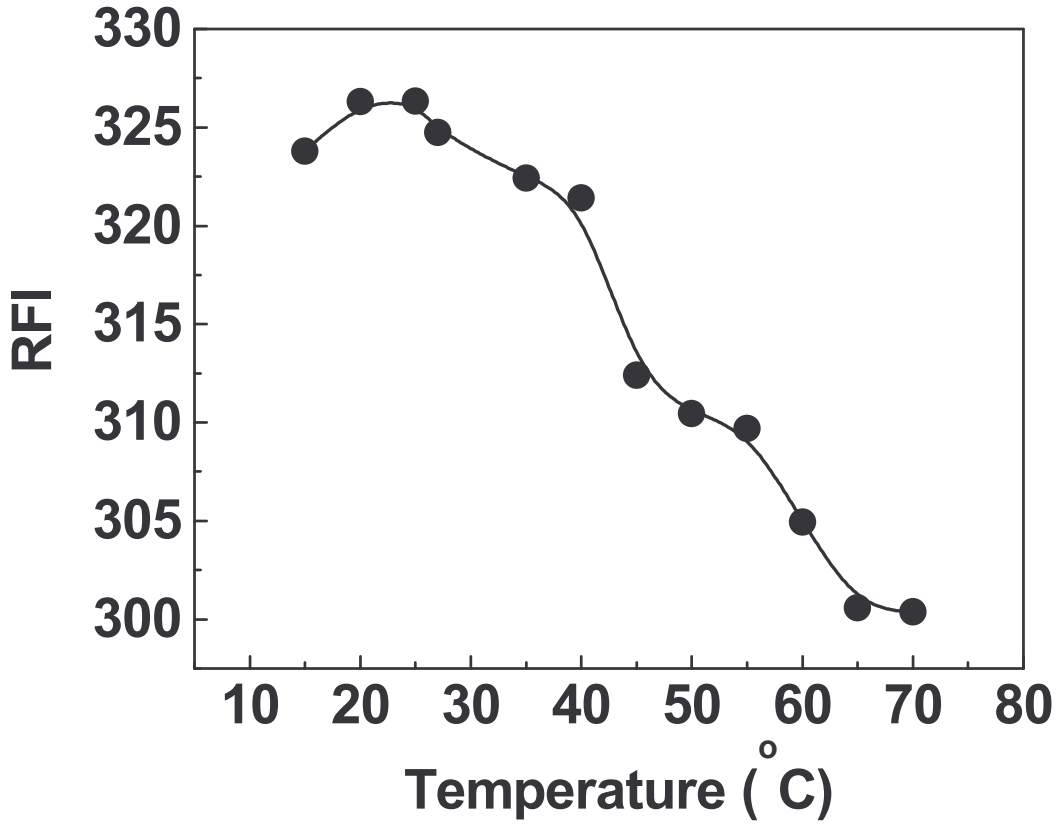

Figure 30. Thermal unfolding of *B. juncea* napin: fluorescence analysis

Fluorescence emission intensity of napin measured at 343 nm as a function of temperature. Spectra were recorded in the temperature range of 15 - 70°C. The emission spectrum of protein was recorded in the region of 300 - 400 nm after exciting at 280 nm. Protein concentrations used was 0.16 mg/mL. The bandwidths for excitation and emission monochromators were 5 and 10 nm, respectively.

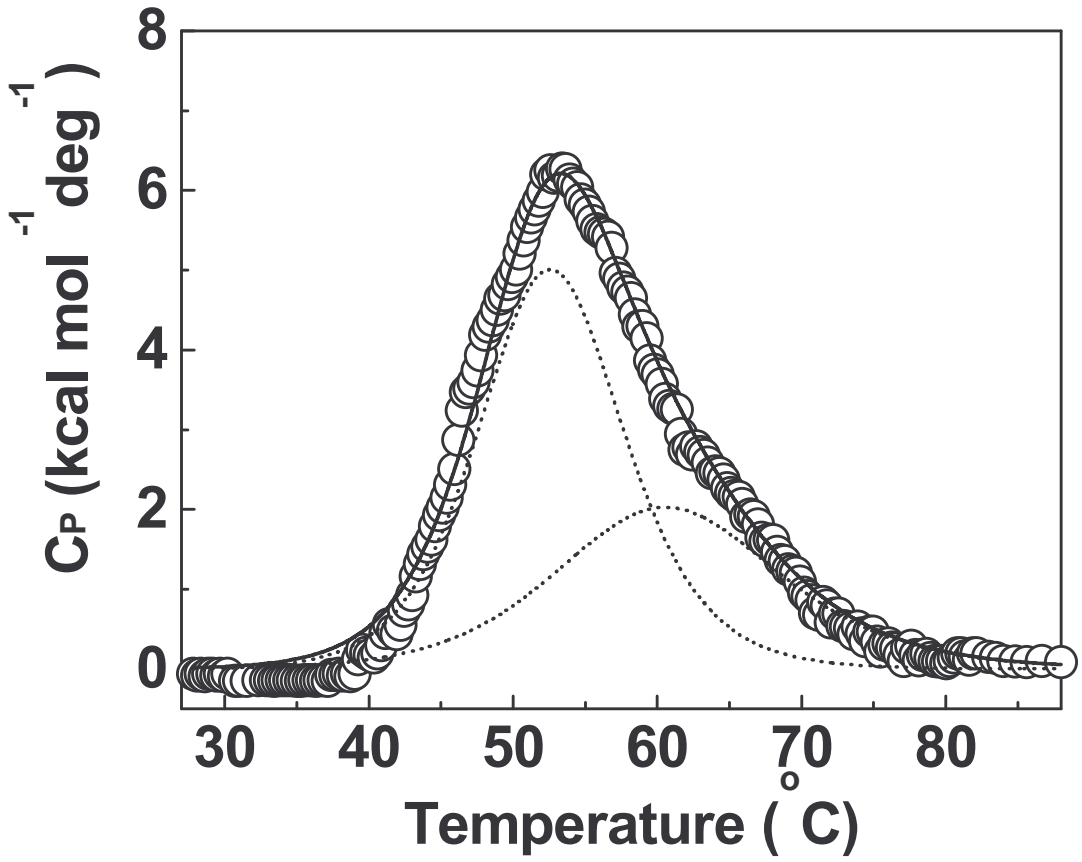

Figure 31. DSC scan of *B. juncea* napin

Typical DSC endotherm showing the apparent excess heat capacity for the thermal denaturation of napin (heterodimer) at a protein concentration of 50 μM in 0.02 M phosphate buffer (pH 7.0) and a scan rate of 60 Kh^{-1}. Samples were passed through 0.22 μ filters and degassed before loading. Resolution of the progress baseline subtracted and concentration normalized DSC curve for napin into two independent two-state curves is given: (○) experimental data points; (*Solid line*) fit obtained using three state model of ORIGIN DSC software provided by Microcal Inc. (*Dotted lines*) component curves.

Table 10. Effect of napin concentration on thermodynamic parameters

Protein Concentration (μM)	T_{M1} (°C)	ΔH_{C1} (kcal mol^{-1})	ΔH_{V1} (kcal mol^{-1})	$\Delta H_{C1}/\Delta H_{V1}$	T_{M2} (°C)	ΔH_{C2} (kcal mol^{-1})	ΔH_{V2} (kcal mol^{-1})	$\Delta H_{C2}/\Delta H_{V2}$
10	48.8±0.5	48.9±1.2	30.9±0.9	1.58	63±2.2	33.3±1.8	44.7±1.8	0.75
25	49.7±0.2	54.5±1.0	34.0±0.6	1.60	62.3±2.5	34.0±1.9	43.7±1.4	0.77
40	50.5±0.3	52.5±1.1	33.8±1.0	1.55	63.6±2.0	30.2±2.0	38.4±1.9	0.78
50	50.5±0.2	58.4±1.0	36.5±0.6	1.60	62.8±1.6	34.6±1.4	46.2±2.2	0.75
65	49.9±0.1	52.0±0.9	33.1±0.8	1.57	64.9±2.6	35.3±2.6	46.5±1.6	0.76
75	50.4±0.4	51.4±0.8	32.3±1.1	1.59	64.1±2.0	30.9±2.2	41.0±2.1	0.75
92	51.3±0.2	56.4±1.1	34.5±0.8	1.63	64.9±1.6	34.1±2.1	46.1±2.1	0.74
106	52.5±0.3	53.3±1.2	34.4±0.6	1.54	65.8±2.0	35.2±2.1	46.4±1.8	0.76

Concentration of the protein was varied from 10 -106 μM with a scan rate of 60 K/h. T_M, ΔH_C, ΔH_V and $\Delta H_C/\Delta H_V$ are transitional temperature, enthalpy, van't Hoff enthalpy and cooperativity ratio respectively for the unfolding of the first and second transition maximum. Subscripts 1 and 2 refer to the respective transitions

Table 11. Effect of scan rates on thermodynamic parameters

Rate scans (Kh^{-1})	T_{M1} (°C)	ΔH_{C1} (kcal mol^{-1})	ΔH_{V1} (kcal mol^{-1})	$\Delta H_{C1}/\Delta H_{V1}$	T_{M2} (°C)	ΔH_{C2} (kcal mol^{-1})	ΔH_{V2} (kcal mol^{-1})	$\Delta H_{C2}/\Delta H_{V2}$
10	49.52±0.4	56.4±1.2	35.9±1.1	1.57	60.9±0.5	39±1.8	49.7±2.1	0.78
20	48.36±0.2	57.2±1.4	35.4±1	1.61	61.9±0.6	43.5±1.9	56.2±2.1	0.76
30	48.94±0.5	59.5±1.2	37.8±1	1.57	59.9±0.6	34.2±1.2	47.4±2.4	0.72
40	49.52±0.6	57.4±1.6	37±0.9	1.55	61.2±0.5	36.9±1.2	47.2±1.8	0.77
50	49.32±0.5	56.2±1.8	36.3±0.9	1.55	61.3±0.5	36.8±0.8	48.3±1.9	0.76
60	50.1±0.5	58.2±1.8	36±0.8	1.61	61.6±0.6	41.9±1.0	53.1±2.0	0.78

A protein concentration of 0.8 mg/mL (50 μM) was used. The thermodynamic parameters are defined in table 10.

Neither the protein concentration (Table 10) nor the scan rate (Table 11) has a bearing on the thermodynamic quantities, ΔH_C and ΔH_V.

Thermodynamic parameters were determined at different pH (3 – 10) for calculating the excess heat capacity (ΔC_P) (Table 12). ΔC_P was obtained from the slope of the plot ΔH_V vs. T_M at different pH. The data was fitted to a straight line (Figure 32A and 32B). The estimated ΔC_{P1} and ΔC_{P2} were 2.05 kcal mol^{-1} K^{-1} and 1.40 kcal mol^{-1} K^{-1} for the two transitions at T_{M1} and T_{M2}, respectively, indicating the presence of intermediates. No significant change in the thermal transition temperature (T_M) was observed in presence and absence of 1 mM DTT (Figure 33).

State of association of napin – In order to characterize the intermediates during unfolding of napin, the state of association of protein as a function of temperature was followed by gel filtration and cross-linking (of the intermediates) with carbodiimide. Napin eluted as a single symmetric peak at 37.4 mL (molecular weight ~15,000), on Sephadex G-50, at 27°C. The column was calibrated using protein markers. Elution volume decreased with increase in temperature from 27°C to 70°C (Figure 34). At 45°C, the protein eluted at 36 mL suggesting the presence of the dimer (molecular weight 29,800). Beyond 65°C, the elution volume reduced to 34 mL, which probably relates to the unfolding of napin.

Table 12. Effect of pH on thermodynamic parameters

pH	T_{M1} (°C)	ΔH_{C1} (kcal mol^{-1})	ΔH_{V1} (kcal mol^{-1})	$\Delta H_{C1}/\Delta H_{V1}$	T_{M2} (°C)	ΔH_{C2} (kcal mol^{-1})	ΔH_{V2} (kcal mol^{-1})	$\Delta H_{C2}/\Delta H_{V2}$
3.1	55.1±0.5	78.1±1.2	49.5±1.1	1.58	64.1±0.5	40.5±1.1	54±1.2	0.75
4.1	53.2±0.4	70.5±0.9	45.5±1.6	1.55	62.0±0.4	41.6±1.8	53.4±1.1	0.78
5.1	50.1±0.5	65.2±1.4	41.8±1.2	1.56	61.7±0.6	39.2±0.9	51.5±1.0	0.76
6.2	48.6±0.5	60.2±1.5	39.2±1.2	1.54	61.2±0.5	39.8±1.1	50.5±1.0	0.79
7.1	48.7±0.6	59.8±1.2	37.9±0.8	1.58	60.3±0.5	38.8±1.1	49.6±0.9	0.78
8.1	47.4±0.6	55.8±1.2	35.8±0.9	1.56	59.6±0.7	38.6±1.3	48.9±1.2	0.79
9.2	45.1±0.5	52.6±1.3	33.1±1.0	1.59	58.9±0.4	38.3±1.2	48.5±1.2	0.79
10	ND	ND	ND	ND	ND	ND	ND	ND

A protein concentration of 0.8 mg/mL (50 μM) and scan rate of 60 Kh^{-1} was used. The thermodynamic parameters are defined in Table 10.

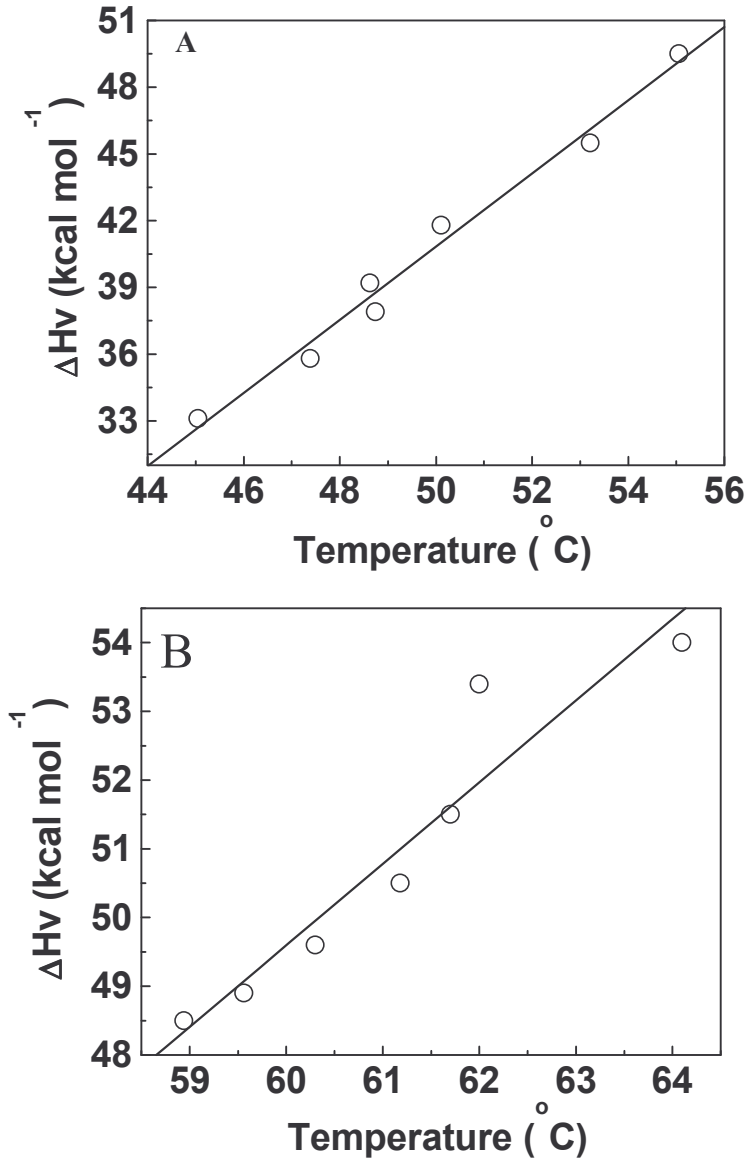

Figure 32. Determination of excess heat capacity (ΔC_P)

Plot of ΔH_V vs. T_M for the first (**A**) and second (**B**) thermal transitions. The values of ΔH_V and T_M are obtained from the linear least-squares fit. Protein concentration of 50 μM was used. pHs of the buffers used for the study was 3.12 (0.05 M glycine-HCl), 4.08 and 5.14 (0.05 M acetate), 6.18 and 7.12 (0.02 M phosphate), 8.05 and 9.16 (0.05 M glycine-NaOH). The pH was checked after degassing.

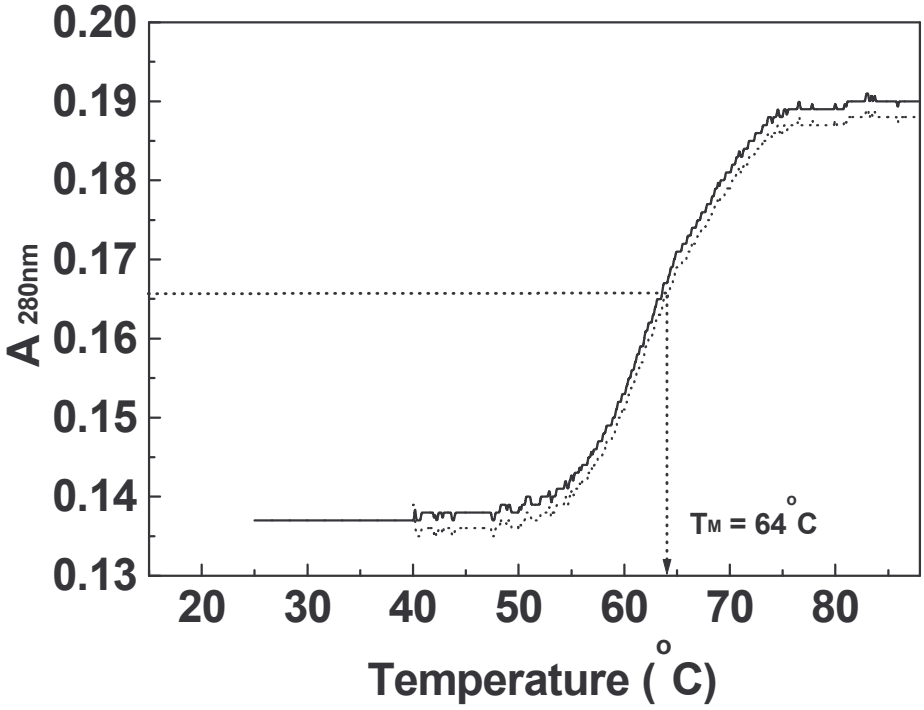

Figure 33. Determination of T_M during thermal unfolding of napin

Change in the absorbance at 280 nm was monitored in the temperature range 27 – 87°C. Napin (——), in absence and (…..), in presence of 1 mM DTT. Beyond 87°C visible aggregates was observed. Protein concentration of 50 μM was used.

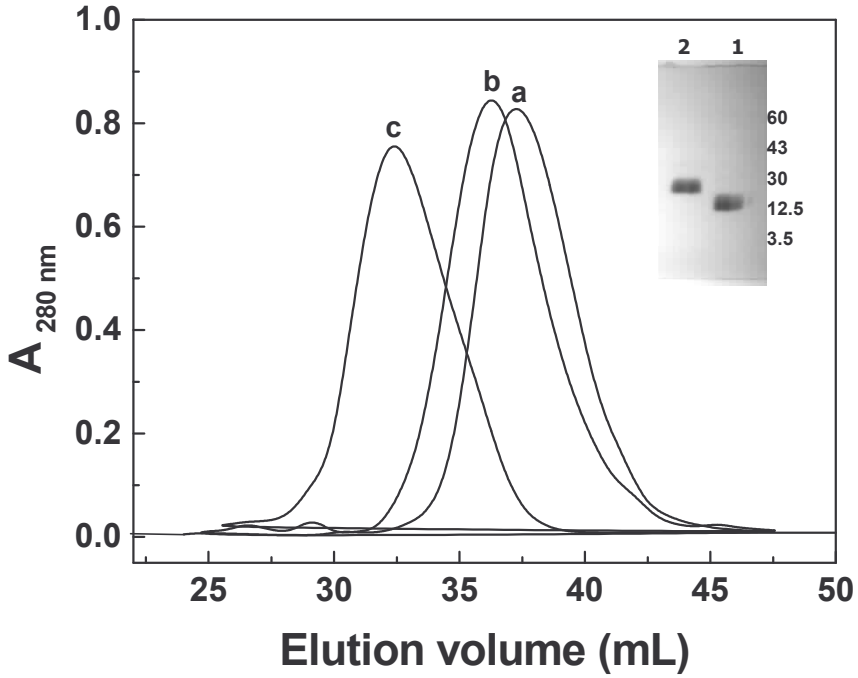

Figure 34. State of association: Gel filtration and SDS - PAGE

Gel filtration profile of napin at different temperatures. Sample (8.0 mg/mL) in 0.02 M phosphate buffer (pH 7.0) was loaded onto a water-jacketed Sephadex G-50 column. **a** – napin at 10°C, 27°C and 37°C ; **b** – napin at 45°C; **c** – napin at 60°C, 65°C and 70°C. **Inset:** Non-reducing SDS-PAGE of heated napin. Lane 1: Protein at 27°C, Lane 2: The Protein cross-linked by EDC at 45°C. 15% gel was stained by coomassie brilliant blue R-250. Concentration of the protein loaded was 2 mg/mL in case of cross-linked napin (lane 1) while 1 mg/mL was loaded in lane 2 (native napin).

When the heated samples 70°C were cooled (27°C), the elution volume reverted back to 37.4 mL, suggesting the complete reversal of state of the protein. Non-reducing SDS-PAGE (15%) of the carbodiimide cross-linked protein is shown as figure 34 inset. The associated protein has a molecular weight of 30,000 indicating possible dimerisation.

The ellipticity as a function of temperature is given in figure 35 inset. The change in ellipticity at 222 nm and its reversibility, as a function of temperature, is shown in figure 35. A steep transition is visible in the temperature region of 50 - 70°C. Thermal unfolding, as followed by DSC, gel filtration and CD, is independent of napin concentration.

Effect of DTT on thermal unfolding - Thermal unfolding of napin was followed by DSC in presence of 0.1 and 1 mM DTT as reducing agent. The profiles obtained were identical to the scans run in absence of DTT. The change in ellipticity values at 222 nm confirmed that thermal unfolding was not affected by the presence of DTT (Figure 35). The effect of DTT (1 mM) was also investigated by gel filtration on HPLC (Figure 36A and 36B). A single peak was observed at 11.849 min, which coincided with the retention time of the native protein in absence of DTT (11.851 min) indicating no change in the association of the protein under the conditions of the experiment. Thus, disulfide linkages of napin were not affected during the course of thermal unfolding, even with addition of reducing agents like DTT. Addition of DTT did not affect the association of napin during thermal unfolding. Based on native PAGE (Figure 36C), it was inferred that there is no cleavage of disulfide linkages during thermal unfolding.

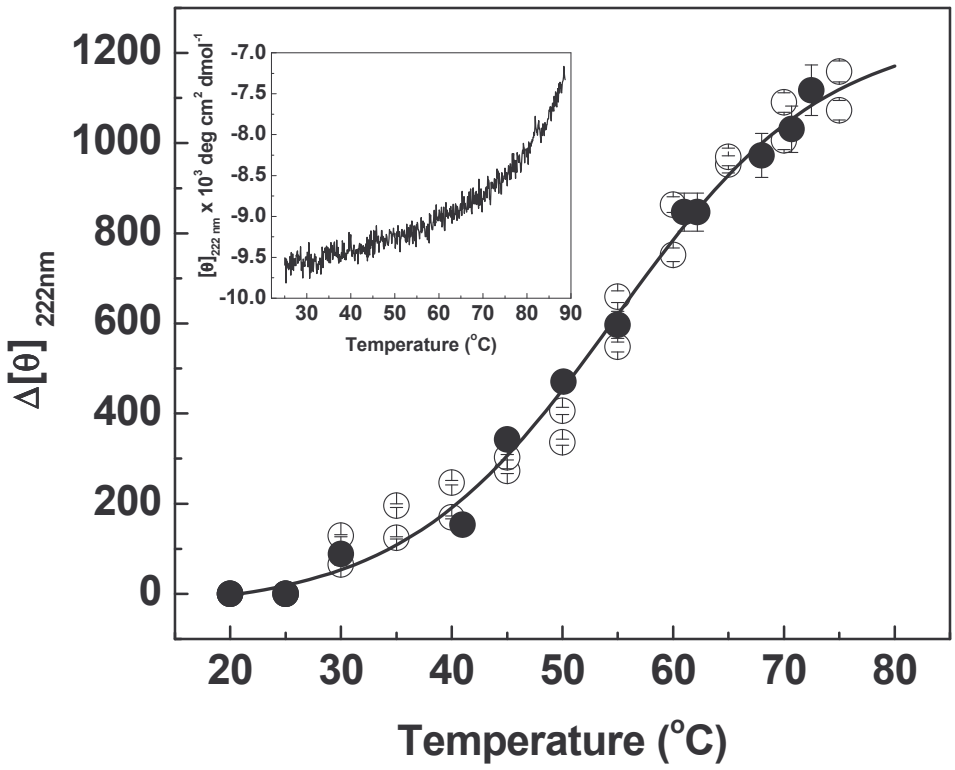

Figure 35. Thermal unfolding of napin: CD

Delta ellipticity values obtained at 222 nm vs. temperature showing loss in secondary structure of napin, (○) in absence and (●) in presence of 1 mM DTT, in the temperature range 27 – 75°C. **Inset:** Temperature induced unfolding of napin monitored at 222 nm. Mean residue weight of 110 was used to calculate the molar ellipticity at 222 nm. Protein (0.4 mg/mL) in presence or absence of 1 mM DTT in 0.02 M phosphate buffer was used.

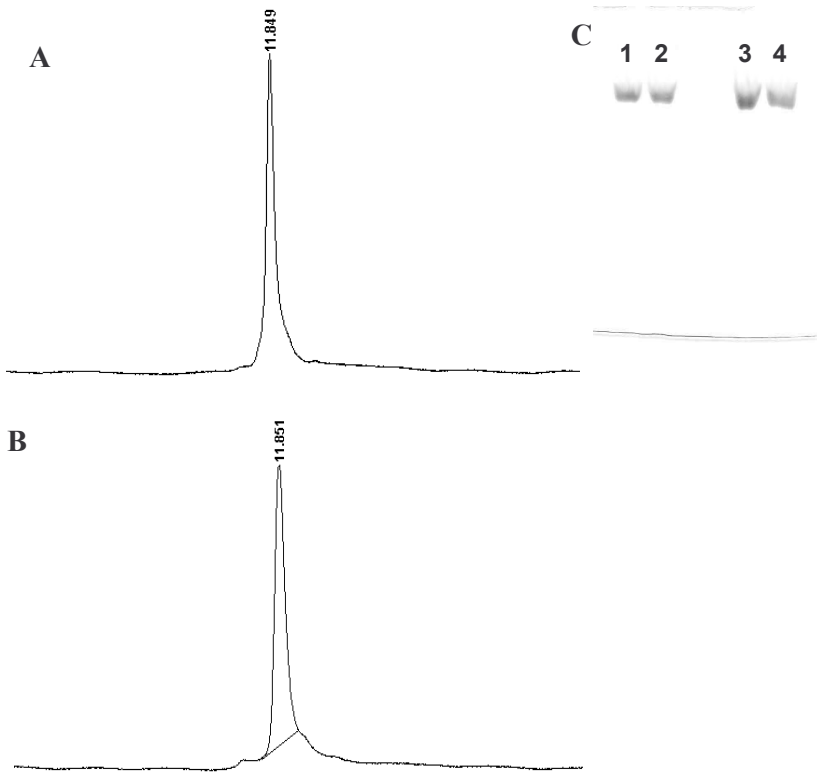

Figure 36. Size exclusion chromatography of napin in on HPLC

A: Napin in presence and **B:** Absence of 1mM DTT. Detection was at 280 nm using a photo diode array detector. Protein concentration was 1μg/μL. **C:** Native-PAGE pattern. **Lane1:** napin in absence of DTT **Lane2:** napin heated upto 75°C in absence of DTT Lane3: napin in presence of 1 mM DTT Lane4: napin heated in presence of DTT upto 75°C. The gel (10%) was stained with amido black in 7% acetic acid. The concentration of protein loaded was 1 mg/mL.

Isothermal unfolding by of napin guanidine hydrochloride

Spectroscopic measurements

Circular dichroism measurements – The Unfolding of napin by the chemical denaturant, GdnHCl was followed by measuring the ellipticity in the near and far UV region. The near UV CD spectrum (Figure 37A) revealed loss of tertiary structure as seen by disappearance of the peak at 290 nm and the minima at 270 and 295 nm. Ellipticity values at 222 nm increased at low concentrations of the denaturant (0 - 1.5 M) and remained steady thereafter up to 3.0 M. Beyond 3.0 M, ellipticity values decreased further suggesting a loss in the ordered structure before attaining a plateau at 5.0 M GdnHCl (Figure 37B).

Fluorescence studies – The emission maximum of napin in the presence of 7 M GdnHCl shifts by +12 nm from 343 to 355 nm (red shift) (Figure 38A). The emission maximum at 343 nm confirms is indicative of the partial exposure of tryptophan in the native state. In the presence of low concentrations of denaturant, (0 - 1.5 M), the emission maximum shifts towards blue, reaching 338 nm (-5 nm) at 1.5 M GdnHCl (Figure 38B). In the range 1.5 - 3.0 M GdnHCl concentrations, the protein emission maximum shifts back to 343 nm (same as native napin). Beyond 3.0 M, the fluorescence emission maxima exhibited red shift (352 nm) before attaining a plateau in the region 4.0 – 5.5 M GdnHCl.

The normalized unfolding transition curves obtained by CD data or fluorescence emission maxima are shown in figure 39.

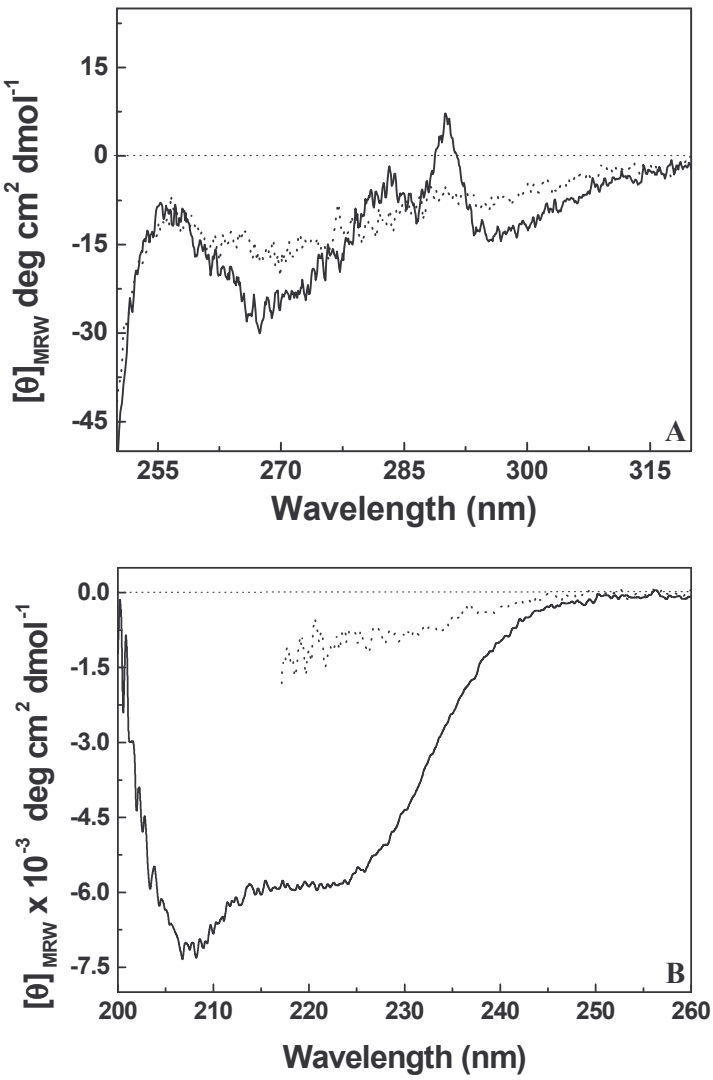

Figure 37. Isothermal unfolding of napin: CD studies

A: near UV CD and B: Far UV CD spectra for napin in (——) absence and (…..) presence of 7.0 M GdnHCl. Scans were recorded in the region of 200 – 260 nm (far UV) using a cell with 1 mm pathlength while near UV CD spectra were run in the region 320 – 240 nm with a 10 mm pathlength cell. The protein concentration was 0.4 mg/mL and 2.5 mg/mL for far and near UV, respectively.

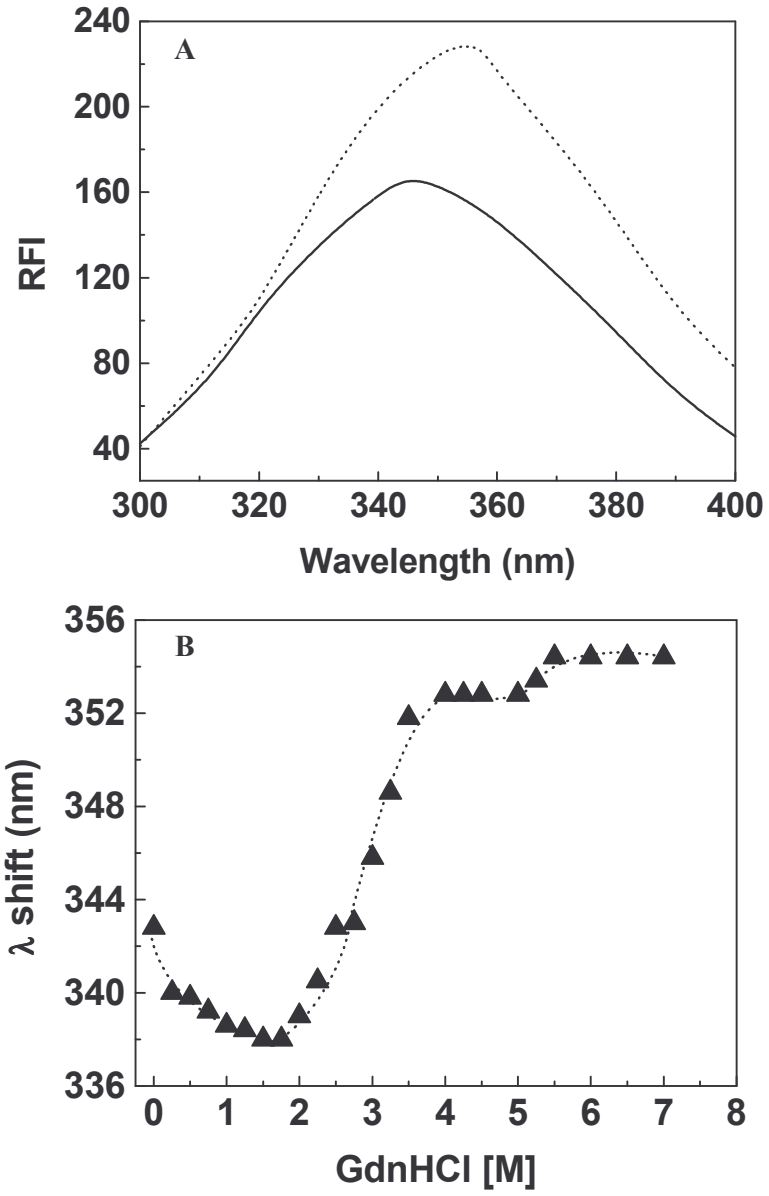

Figure 38. Isothermal unfolding of napin: fluorescence studies

A: Fluorescence emission spectra of napin in (——) absence and (…..) presence of 7.0 M GdnHCl. The temperature was maintained at 27°C through a circulating water bath. Samples (0.12 mg/mL) were incubated for 12 h at 27°C. Spectra were recorded in the range 300 – 400 nm after excitation at 280 nm. B: Shift in the fluorescence emission wavelength maxima as a function of denaturant (GdnHCl) concentration.

The curves obtained were not super imposable, suggesting the transition to be other than two state. Analysis of the data and the apparent fractional change was obtained using equation,

$$f_U = \frac{(Y_U - Y)}{(Y - Y_N)} \qquad (4)$$

where, Y is the observed value of ellipticity at 222 nm or fluorescence emission; Y_N and Y_U are the values of ellipticity at 222 nm or fluorescence emission for native and unfolded states, respectively. Values of Y_N and Y_U were obtained by linear extrapolation of the native and unfolded base lines into the transition region. The parameters for the unfolding process were obtained by the data fit to two state and three state models (Matthews and Crisanti, 1981; Beasty et al., 1986) respectively using scheme 1,

F (*folded*) ⇆ U (*unfolded*)

F (*folded*) ⇆ I (*intermediate*) ⇆ U (*unfolded*)

Scheme 1.

Marquardt-Levenberg algorithm was used to fit the unfolding data to the non-linear relationship (scheme 1). The overall K_{app} and the GdnHCl dependent equilibrium constant were defined by the following equations (5) and (6) for two and three state transition, respectively.

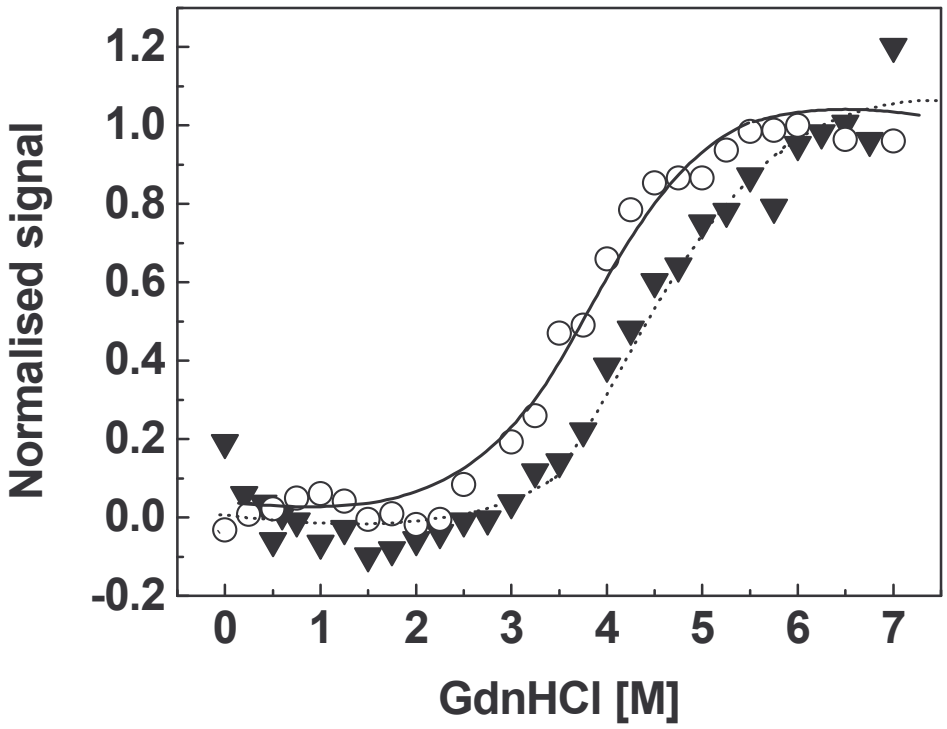

Figure 39. GdnHCl induced equilibrium unfolding of napin monitored by change in fluorescence intensity and molar ellipticity. Normalized signal of napin unfolding followed by fluorescence and CD. The increase in fluorescence intensity was followed by emission at 343 nm (○) while change in molar ellipticity was recorded at 222 nm (▼)

$$K_{app} = K_D = \exp \frac{\Delta G_{1H2O} - m_D [D]}{(-RT)} \quad (5)$$

$$K_{app} = \frac{K_1(K_2+Z)}{(1+K_1+K_1K_2)} \quad (6)$$

where K_1=exp {($\Delta G_{1H2O} - m_{1D}[D]$)/ ($-RT$)}

K_2=exp {($\Delta G_{2H2O} - m_{2D}[D]$)/ ($-RT$)}

and [D] is experimental denaturant concentration. The fractional change (Z) in the measured ellipticity value/fluorescence emission maximum for the transition from the native state to intermediate, the intercept and the negative slope of the linear extrapolation to zero GdnHCl concentration of the free energy changes associated with unfolding ΔG_{H2O}, which is measured as a function of GdnHCl, were obtained by the fit. ΔG_{1H2O}, ΔG_{2H2O}, m_1 and m_2 have the same meaning as in two-state for the individual steps in three-state model. For global fits, final analysis was made using the equation,

$$F_{app} = \frac{K_{app}}{(1+K_{app})} \quad (7)$$

The fluorescence data could be fitted adequately to a three-state model over the entire transition region.

The parameters Z, ΔG_{1H2O}, ΔG_{2H2O}, m_1 and m_2 were 0.35, 5.2 ± 0.18 kcal mol^{-1}, 5.1 ± 0.12 kcal mol^{-1}, -1.6 ± 0.04 kcal $mol^{-1}K^{-1}$ and -1.3 ± 0.02 kcal $mol^{-1}K^{-1}$, respectively (Figure 40A). Similarly, the CD data could be fitted adequately by three-state model. The values obtained were Z (0.48), ΔG_{1H2O} (5.2 ± 0.12 kcal mol^{-1}), ΔG_{2H2O} (5.1 ± 0.17 kcal mol^{-1}), m_1 (-1.8 ± 0.06 kcal $mol^{-1}K^{-1}$) and m_2 (-1.2 ± 0.02 kcal $mol^{-1}K^{-1}$) (Figure 40B), respectively.

The intermediates reached maximum concentration at 4.6 M GdnHCl. The unfolded form, which did not manifest up to 3.86 M became predominant above ~5 M GdnHCl (Table 13).

Isothermal unfolding effect on hydrodynamic radius

The effect of denaturant on hydrodynamic radius of napin was followed by size exclusion chromatography (Figure 41). Stokes radius of the native protein was determined to be 20 Å. Increase in GdnHCl concentration resulted in a decrease in the Stokes radius, suggesting a compaction of molecule at low denaturant concentrations (upto 1.5 M GdnHCl). The Stokes radius increased above 3.0 M reaching a maximum of 35 Å at 6.0 M and beyond. The presence of stable intermediates is suggested in the plateau region (4.0 – 5.0 M GdnHCl) (Figure 41 inset).

Refolding of napin

Complete reversibility of the unfolded napin, was confirmed by CD (Figure 42A), gel filtration (Figure 42B), fluorescence (Figure 43A) and ANS binding (Figure 43B) studies. Napin recovered its lost structure completely as analyzed by CD, fluorescence, gel filtration, and ANS binding ability.

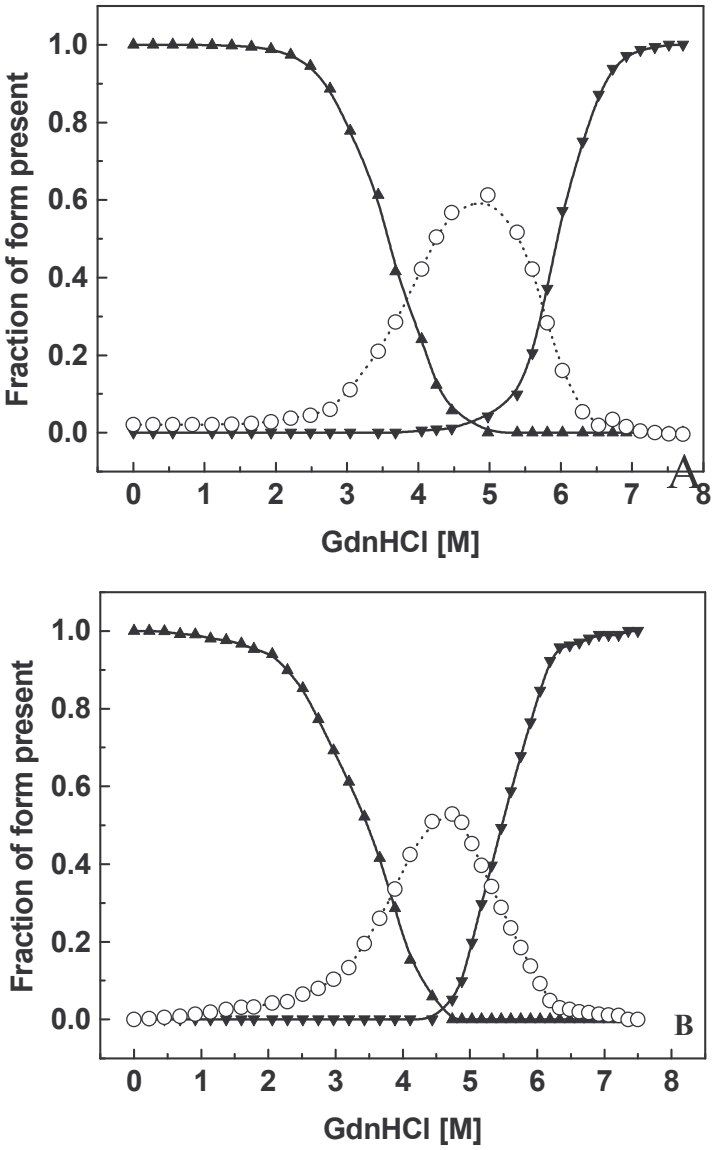

Figure 40. GdnHCl induced equilibrium unfolding of napin monitored by change in fluorescence intensity and molar ellipticity.

The experimental data was fitted using the equation (6). Calculated forms of napin (▲) native (○) intermediate and (▼) unfolded, as a function of GdnHCl concentration, followed by **A:** fluorescence emission at 343 nm and **B:** molar ellipticity at 222 nm. Fractions of form present were calculated using the parameters obtained from the three-state model.

Table 13. Free energy change during isothermal unfolding of napin

	ΔG_{1H2O} (kcal mol^{-1})	$-m_1$ (kcal mol^{-1}K^{-1})	C_{M1} (M GdnHCl)	ΔG_{2H2O} (kcal mol^{-1})	$-m_2$ (kcal mol^{-1}K^{-1})	C_{M2} (M GdnHCl)
Fluorescence (27°C)	5.24	1.63	3.21	5.107	1.32	3.9
CD (27°C)	5.22	1.75	3.0	5.075	1.20	4.2

The fluorescence and CD data could be fitted to a three-state model. The parameters Z, ΔG_{1H2O}, ΔG_{2H2O}, m_1 and m_2 were obtained from the fit. C_M is the mid point of denaturation ($\Delta G/m$).

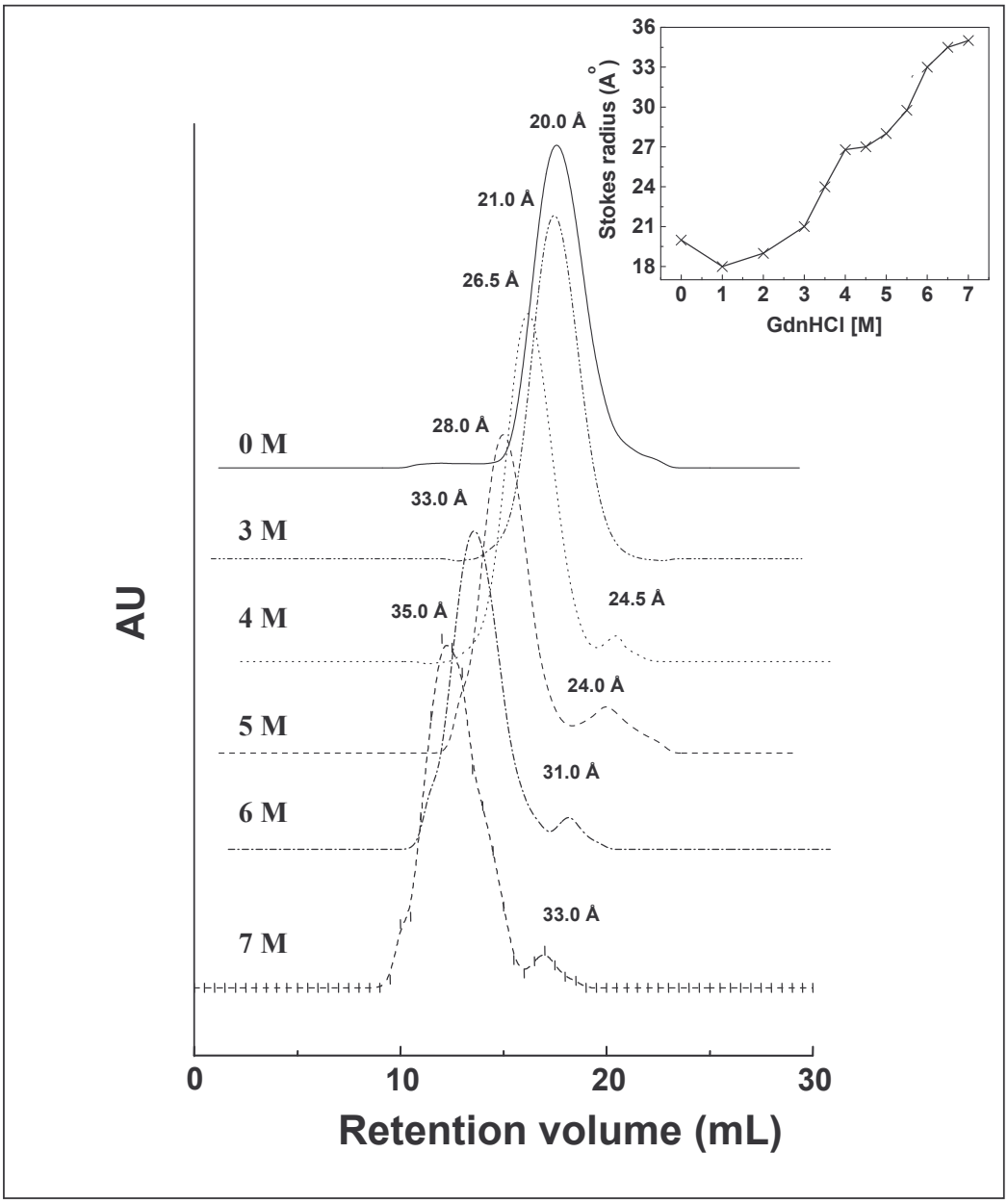

Figure 41. Gel filtration profile of napin as function of GdnHCl concentration. Samples (4.0 mg/mL) in 0.02 M phosphate buffer (pH 7.0) containing 0.002% sodium azide, were incubated in GdnHCl (0–7 M) for 12 h at 27°C and loaded on to a Bio-gel P-30 column. The denaturant concentration and Stokes radius are indicated in the profile. **Inset:** The elution volume vs. absorbance was plotted to calculate the change in Stokes radii (R_S) during unfolding.

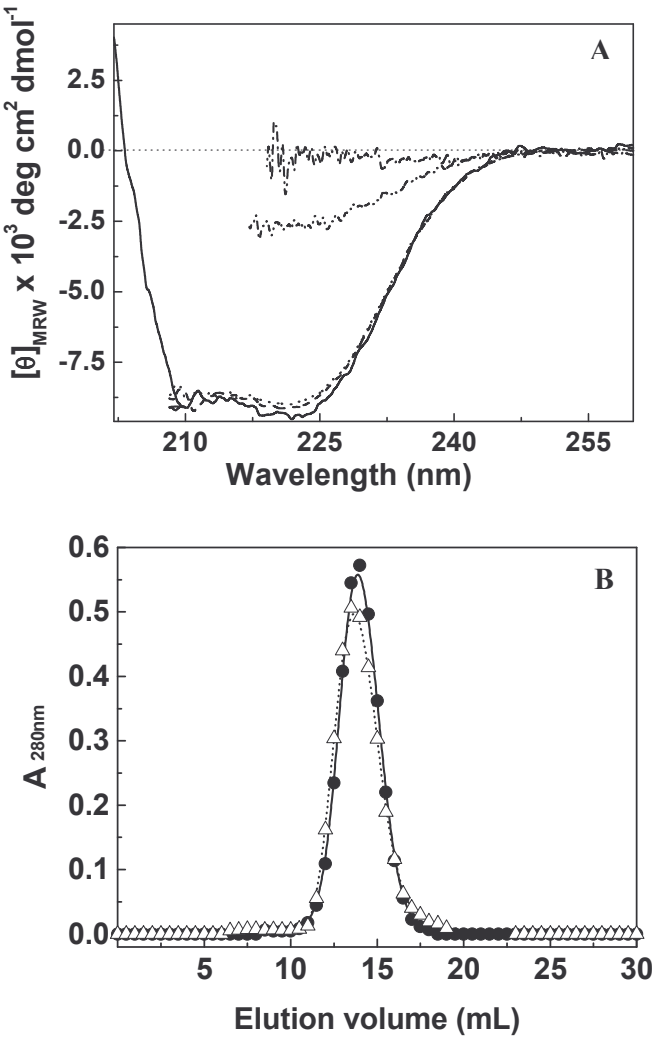

Figure 42. Refolding of napin

A: Far UV-CD of napin in, (——), 0M; (– · –), 7M; (– ·· –), 4M GdnHCl; (…), 7M refolded (– –), 4M refolded. The protein concentration was 0.4 mg/mL. B: size exclusion chromatography on sephadex G-50. (–●–), napin; (–Δ–) refolded napin (7M GdnHCl)

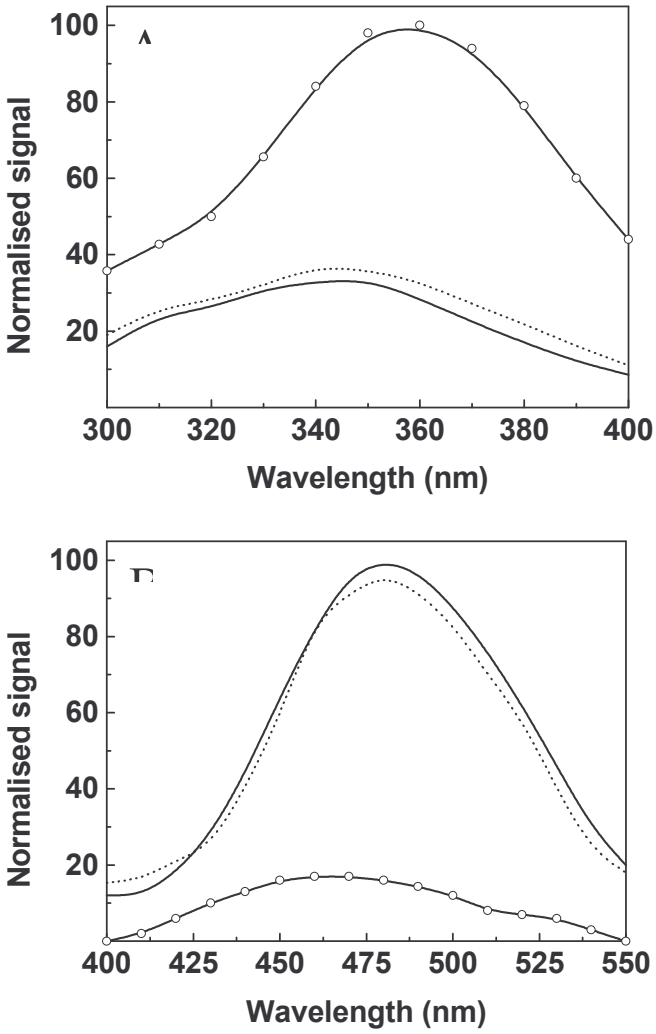

Figure 43. Refolding of napin - fluorescence

A: Fluorescence emission spectra of protein from 300 – 400 nm when excited at 280nm. B: fluorescence emission spectra of ANS - napin complex from 400 - 600 nm, excited at 375 nm. (——) 0M GdnHCl; (–o–) 7M GdnHCl; (…) refolded.

Conformation stability of napin: unfolding by GdnHCl as a function of temperature - The effect of temperature on free energy (ΔG_{H2O}) of unfolding with GdnHCl was followed by fluorescence measurements in the range 15 - 55°C. ΔG_{1H2O} and ΔG_{2H2O} at each temperature was used to calculate the change in excess heat capacity, $\triangle C_P$, using equation 8 (Nicholson and Scholtz, 1996),

$$\Delta G\,(T) = \Delta H_g\,(1 - T/T_g) + \Delta C_P\,[T - T_g - T \ln\,(T/T_g)] \qquad (8)$$

where, T_g is the temperature at which $\Delta G = 0$ and H_g is the unfolding enthalpy at T_g ; T_M is the melting temperature for the protein. The stability curves for both transitions, constructed (using equation 8) from $\triangle G_{H2O}$ vs. temperature are given in figure 44. The thermodynamic parameters obtained from the curves are given in table 14. The maximal free energy of stabilization was calculated to be 10.3 $\pm$ 0.6 kcal mol^{-1}. A comparison of the free energy of stabilization of proteins with similar molecular weights and disulfide linkages revealed that napin was more stable (Table 13).

Intrinsic stability of napin

Presence of internal repeats - In order to understand the basis of stability, the primary amino acid sequence was studied for stabilizing factors like internal repeats. The amino acid sequence analysis of napin revealed the presence of two internal repeats in the large subunit. Using the software RADAR, the segments were identified as residues 31 - 60 and 73 - 109 with ~40% similarity (Figure 45A).

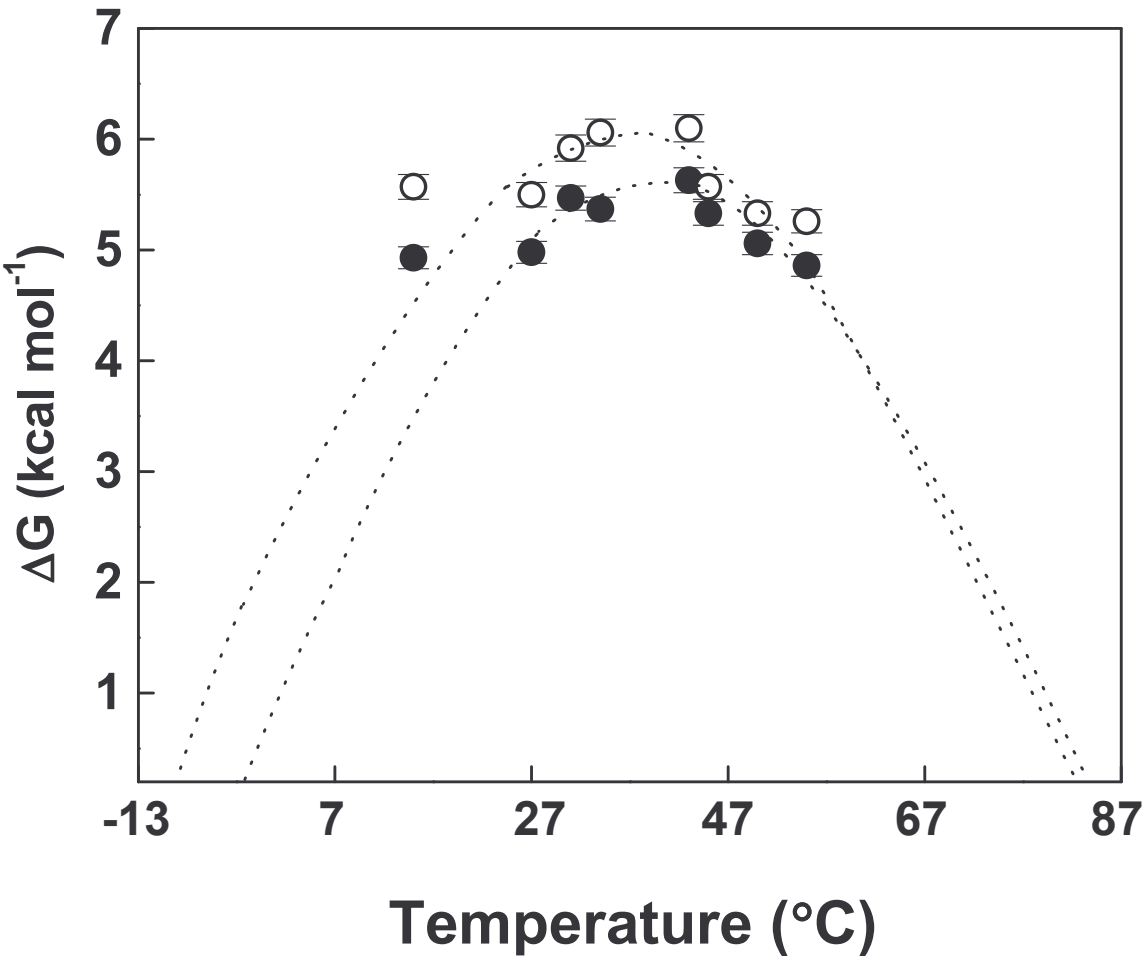

Figure 44. Determination of ΔC_P for isothermal unfolding of napin

Thermodynamic stability of napin was calculated using equation (8). Data points have been obtained from individual unfolding experiments carried out at different temperatures in the range 15 – 55°C. The broken lines passing through the points were fitted using equation (8). The first transition is depicted as (○) while the second transition is shown as (●).

Table 14. Conformational stability of *B. juncea* napin

	ΔH_g (kcal mol^{-1})	ΔC_P (kcal mol^{-1} K^{-1})	T_g (°C)
First transition	88.60 ± 10.99	1.91 ± 0.486	82.73 ± 5.09
Second transition	90.66 ± 17.73	1.84 ± 0.747	83.62 ± 7.98

Thermodynamic parameters analyzed by the stability curves using the equation 8. ΔC_P change in the heat capacity, T_g is temperature at ΔG = 0 and H_g is unfolding enthalpy at T_g.

```
31 QGPQQRPpllQQCCNELHQEE...P.LC......VCPTLK 60
   ::.::..   ::.......:..   : .:       :::..:
73 QGQQQGK...QQMVSRIYQTAthlPkVCnipqvsVCPFQK 109
```

: Indicates complete identity
. Conservative replacement

```
B.juncea        SQGPQQRPPLLQQCCNELHQEEPLCVCPTLKGASKAVKQQIQQQ-GQQ-QGKQQMVSRIYQTATHLPKVCNIPQVSVCPFQKTMPGPS
B.campestris    TQGPQQEPPLLQQCCNELHQEEPLCVCPTLKGASKAVKQQVRQQ-GQQ-QQMQQVISRIYQTSTHLPRVCNIRQVSICPFQKTMPGPS
B.rapa          TQGPQQEPPLLQQCCNELHQEEPLCVCPTLKGASKAVKQQVRQQ-GQQ-QQMQQVISRIYQTSTHLPRVCNIRQVSICPFQKTMPGPS
B.nigra         QQGPQQRPPLLQQCCNELHQEEALCVCPTLKGASKAVRQQVRQQ-GHQ-QQMQHVISRIYQTATHLPRVCNIPQVSVCPFQKTMPGPS
B.napus         PQGPQQRPPLLQQCCNELHQEEALCVCPTLKGASKAVRQQVRQQ-GHQ-QQMQHVISRIYQTATHLPRVCNIPQVSVCPFQKTMPGPS
B.carinata      PQSPQQRPPLLQQCCNELHQEEPLCVCPTLKGASKAVKQQVRQQQGQQGQQLQQVISRIYQTATHLPKVCNIPQVSVCPFQKTMPGPS
B.oleracea      PQGPQQRPPLLLQCCNELDQEEPLCVCPTLKGASKAVKQQIQQQ-GQQ-QGKQQMVSRIYQTATHLPKVCNIPQVSVCPFQKTMPGPS
                .*.***.**** ******.***.**************:**::** *:* *  *:::******:****:**** ***:***********
```

Figure 45. ***B. juncea*** **napin sequence showing internal repeats and conserved residues. A:** Presence of internal repeats in the large sub unit of napin as identified by 'RADAR'. **B:** Sequence comparison of the napins of *Brassica* species. The sequences were aligned using the CLUSTAL W (1.83) multiple sequence alignment. (✱) Indicates conserved residues, (:) indicates complete identity, (·) indicates conservative replacement. Sequences are *Brassica juncea* (CAA46785), *Brassica oleracea* (CAA46783), *Brassica compestris* (CAA46782), *Brassica nigra* (CAA46784), *Brassica carinata* (CAA52813), *Brassica rapa* (CAA46171) and *Brassica napus* (1pnb). The two internal repeats, conserved in all species are underlined for *B. juncea* sequence.

Multiple sequence alignment (CLUSTAL W ver. 1.83) of all the available sequences of *Brassica* (2S) large subunits revealed that the internal repeats are highly conserved (Figure 45B) in addition to eight conserved cysteines (involved in four disulfide bridges). The internal repeats may have a role in determining the folding behavior of napin.

Homology modeling

Napin structure was compared to the existing *Brassica napus* 2S NMR structure (Pdb id-1pnb), since the *Brassica juncea* structure data is not available. The homology model of napin is shown in figure 46A. The overall structure of the napin is all-α helix, which consists of the four-helical motif. The region of repeat amino acid sequence (colored blue) on large subunit is shown in figure 46B.

Discussion

Brassica juncea napin is a 115-residue heterodimer (molecular mass 14,724 Da), constrained by four (two inter and two intra) disulfide bridges (Ghose et al., 2001). Napin has a high content of basic amino acids and is allergenic in nature. The low degree of hydrolysis by α-trypsin and chymotrypsin indicates the inaccessibility of cleavage sites of napin. No change in the mobility is observed on SDS-PAGE when napin is heated to 70°C and cooled to 27°C. There is neither cleavage of -S-S- (disulfide) linkages nor deamidation of the protein. The protein was found to be structurally stable upto ~75°C, beyond which it aggregates.

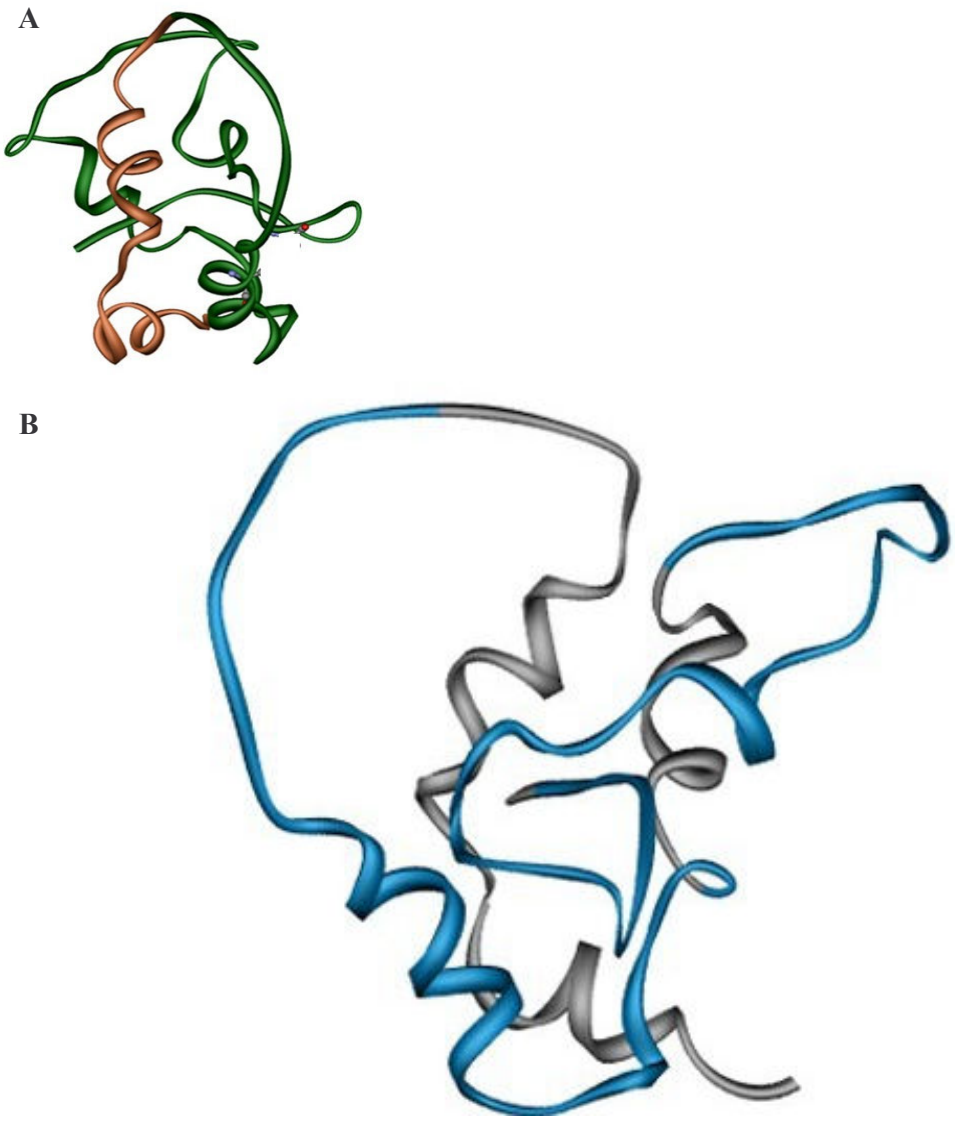

Figure 46. Model of napin showing internal repeats

A: Homology modeling of napin protein of *Brassica juncea* with *Brassica napus*. The coordinates for *B. napus* were taken from the PDB bank (pdb-1pnb). Swiss-model software was used for modeling. Large and small subunits of the protein are shown in green and orange. **B:** The two internal repeats present in the large chain are shown with blue color.

The amino terminal sequence of the first eight residues of both subunits matches with the reported deduced sequence of *Brassica juncea* (Dasgupta et al., 1995). We have characterized the thermal and isothermal (GdnHCl) unfolding of napin by DSC, fluorescence and CD spectroscopy.

Ellipticity values at 222 nm, as a function of temperature, form a sigmoidal curve with no significant change up to 50°C. The values decrease significantly in the temperature range 50 – 65°C, beyond which it remained almost, steady (Figure 35). DSC data show that the reversible unfolding of napin follows a three state transition (Figure 31). Deconvolution of the curve reveals two entities with different transition temperatures, at 52.5°C and 62.8°C, respectively. Napin from *Brassica napus*, reportedly, has a higher T_M (Krzyzaniak et al., 1988).

The thermal denaturation of several proteins with molecular weight and disulfide linkages similar to napin is available (Table 15). All these proteins (with the exception of α-lactalbumin in presence of calcium) undergo two state transition.

The cooperativity ratio of $\Delta H_V / \Delta H_C$ for the first and second transition is 1.6 and 0.75, respectively, suggesting the possible involvement of two domains in the first transition. The thermodynamic parameters, T_M, ΔH_C, ΔH_V and $\Delta H_C/\Delta H_V$ are found to be independent of concentration (Table 10) and scan rates (Table 11), implying the absence of kinetic effects such as aggregation.

Table 15. Transition temperatures of different proteins

Protein	**Molecular weight** (Daltons)	**No. Of disulfide Bridges**	T_{M1} (°C)	T_{M2} (°C)
RNASE A	13900 (Single chains)	4	64.68 (Ahmad and Bigelow, 1982)	-
α-lactalbumin (–Ca^{2+})	14178 (Single chains)	4	43.26 (Brems et al., 1995)	
α-lactalbumin (+Ca^{2+})	14178 (Single chains)	4	35.00 (Brems et al., 1995)	64.3
LYSOZYME	14300 (Single chains)	4	65.60 (Santoro et al., 1992)	
Insulin	5800 (two chains)	3	70.00 (Ewbank and Creighton, 1993)	
NAPIN	14724	4	51.00	63 (**Present work**)

The most important feature of protein unfolding is the exposure of its hydrophobic core. This is reflected by the positive change in the heat capacity, ΔC_P, the thermodynamic property, most closely linked to the hydrophobic driving force and burial of non-polar surface area of the protein during unfolding.

To determine ΔC_P of unfolding, we measured ΔH_V as a function of T_M, by DSC, in the pH range 3.0 – 10 (Table 12). Themostability of protein decreased with increase in pH (as correlated by T_M values) probably due to the ionization of the side chains of napin (Schwarz et al., 1991). The thermal unfolding data of napin could fit into a three state model in the pH range studied. ΔC_P values are pH independent over the selected range (Figure 32A and 32B). The ΔC_P estimated by the method appeared to be better in comparison with that obtained directly as the difference between the native and unfolded baseline of a single DSC scan.

ΔC_P is linearly dependent on the accessible surface area (ASA). ASA for the *Brassica napus* 2S (PDB id = 1pnb) has been calculated to be 7870.4 $Å^2$ using the software NACCESS (Hubbard, 1996). The contributions of apolar and polar region are ~52 and 48%, respectively. The ASA has been calculated for the napin using the equation (Ganesh et al., 1997),

$$ASA = 10.3\ M^{0.68} \qquad (9)$$

where M = molecular weight of the protein. ASA for napin is found to be 7032 $Å^2$, which is close to the ASA of *Brassica napus*. Although napin is highly hydrophilic in nature, the ASA is very limited compared to proteins with

similar molecular weights and disulfide bridges (RNase, lysozyme and alpha lactalbumin). Only 0.5 molecules of ANS per molecule of protein are bound due to the absence of hydrophobic core. This is probably due to presence of two intra and two inter disulfide linkages.

According to Myers et al (Myers, 1995), ΔASA is linearly dependent on the number of residues (N_{RES}) in the protein (115) and ΔC_P is linearly dependent on ASA.

$$\Delta ASA = -907 + 93\ N_{RES} \quad (10)$$

$$\Delta C_P = -119 + 0.2\ \Delta\ ASA \quad (11)$$

Hence,

$$\Delta C_P = -300.4 + 18.6\ N_{RES} \quad (12)$$

The calculated ΔC_P value is 1.84 kcal mol^{-1} K^{-1}. The larger ΔC_P 3.45 kcal mol^{-1} K^{-1} value, determined from DSC, for the thermal unfolding is probably due to the dimerisation in the temperature range 27 – 48°C. The addition of 1 mM DTT does not reveal any change in the profile and both T_{M1} and T_{M2} are identical with that obtained in absence of reducing agent. Gel filtration on HPLC and change in ellipticity values at 222 nm, in presence and absence of DTT confirm that the disulfide linkages are not affected during the course of thermal unfolding.

The gel filtration elution profile of napin as a function of temperature (10 – 37°C) reveals that the protein is a monomer in its native state, with a

molecular weight of ~15000. In the temperature range 40 – 45°C, the protein elutes as a dimer (Figure 34). The presence of dimer is confirmed by cross-linking the protein at 45°C with carbodiimide before loading on non- reducing gels (Figure 34 inset). Dissociation of subunits has not been observed when DSC scans were made in presence of 0.1 or 1 mM DTT.

Summing up our experiments on thermal denaturation of napin, we suggest that, at 48°C (first transition), the protein dimerizes and subsequently dissociates into monomers at high temperatures, followed by unfolding leading to aggregation. CD measurements, at 222 nm, as a function of temperature also indicate minimal changes in secondary structure up to 50°C indicating the absence of protein unfolding. The loss in ellipticity is greater in the temperature range of 50 – 65°C, beyond which, it remains constant (Figure 35).

The initial transition in the DSC, which is related to the dimerisation of the molecule, is reflected in $[\theta]_{222\ nm}$ values, which does not change up to 50°C. The second transition is related to unfolding of the molecule, which is reflected by loss in secondary structure. Addition of reducing agent (1 mM DTT) has no effect on the thermal transitions.

The unfolding of monomeric proteins involves only intrasubunits interactions whereas heterodimer proteins are stabilized by intersubunit interactions as well (Neet and Timm, 1994). We have studied the intersubunit interactions of napin by isothermal unfolding by GdnHCl using CD and fluorescence. Protein denaturation is observed in the range 3.0 – 6.0 M

GdnHCl. At low concentrations of denaturant (0 – 1.5 M GdnHCl), an increase in the ellipticity values at 222 nm along with a blue shift in the emission maximum is observed. CD and fluorescence data of equilibrium unfolding of napin could adequately fit a three-state model, establishing the presence of at least one stable intermediate in the unfolding process. From the statistical analysis of three-state two-step model, the predominant unfolding reaction below 3.86 M may be N↔I transition and above 3.86 M, the predominant reaction may be I↔U transition, while the intermediate form is observed at ~5 M GdnHCl (Figure 40A and 40B). The total free energy change, given by the sum of the individual ΔG_{H2O} values, is 10.3 ± 0.6 kcal mol^{-1}.

During the unfolding of a multimeric protein, a single transition indicates strong interdomain interactions and cooperative unfolding of the domains (Privalov, 1996). However, during multiple transitions, one or more relatively stable intermediates are seen, indicating the absence of strong interdomain interactions (Privalov, 1996, Jaenicke, 1999).

The hydrodynamic radius of the native napin was determined to be 20 Å, by both dynamic light scattering (Figure 12) and size exclusion chromatography. This radius decreased from 20 to 18 Å at low concentrations of GdnHCl (up to 3.0 M). Further increase in the denaturant concentration resulted in unfolding of the protein, as indicated by increase in the hydrodynamic radius. The plateau region observed in the range 4 – 5 M GdnHCl (Figure 41 inset) clearly indicates a three state transition. Refolding experiments revealed that the unfolded protein refolds back to the native state.

The temperature dependence of the free energy change for the napin denaturation is shown in figure 44. From the stability curve, it is apparent that both transitions exhibit temperature maxima at 41°C and 43°C, respectively. Thus, napin can be denatured by either raising or lowering the temperature from T_{MAX}. *T*g is found to be 83°C for both the transitions. The ΔC_P for the isothermal unfolding is 3.75 kcal mol^{-1} K^{-1}. The ΔC_P obtained from DSC measurements is 3.45 kcal mol^{-1} K^{-1}.

Proteins with similar molecular weights and disulfide linkages as napin have less stability. This is reflected by the ΔG_{H2O} values (Table 16). Further, the ΔC_P per residue is 32.6 cal (mol of residue)$^{-1}$ K^{-1}, which is considerably higher than the average value (14.5) observed for other proteins (Myers et al., 1995).

The change in excess heat capacity, ΔC_P, can be calculated using '*m*' values obtained from GdnHCl denaturation experiments using Myer's equation (Myers et al., 1995),

$$\Delta C_P = -336 + 0.66m. \qquad (12)$$

The calculated ΔC_P, 1.64 kcal mol^{-1} K^{-1}, is lower than the experimental value (3.75 kcal mol^{-1} K^{-1}). In the absence of a hydrophobic core, the other contributing factors to the higher value of ΔC_P are most probably due to the presence of disulfide linkages and internal repeats.

As the number of repeats in the protein primary structure increases, the overall stability and the sharpness of its denaturation transition also increase.

Table 16. Comparison of free energy and disulfide bonds (GdnHCl denaturation)

Protein	Molecular weight (Dalton)	No. Disulfides	ΔG_{H2O} (kcal mol^{-1})
RNase A	13900 (single chains)	4	7.3 ± 0.2 at 25ºC (Yadav and Ahmad, 2000)
α-lactalbumin	14178 (single chains)	4	4.3 ± 0.1 at 25ºC (Yadav and Ahmad, 2000)
LYSOZYME	14300 (single chains)	4	8.9 ± 0.1 at 25ºC (Yadav and Ahmad, 2000)
Insulin	5800 (two chains)	3	4.5 ± 0.5 (Huus et al., 2005)
NAPIN	14724	4	10.3±0.6 at 27ºC (present work)

In case of TPR and ANK proteins, stability increases with increasing number of repeat structures in the molecules (Main et al., 2005). The amino acid sequence analysis of napin, using the software RADAR, led to the identification of two internal repeats in the large subunit with ~40% similarity.

The two segments span from 31-60 and 73-109 residues (Figure 45A). Residues 31-60 form a right-handed α-helix, while 73-109 forms a random coil. Multiple sequence alignment with *Brassica* family 2S proteins has revealed that these internal repeats are highly conserved. The presence of these internal repeats may contribute to the enhanced stability of all napins.

Comparison of proteins with similar molecular weights and disulfide bridges also confirms the greater stability of napins (Table 15). Internal repeats stabilize the protein, by interacting with each other to form additional hydrophobic cores. The protein forming structure at low concentrations of GdnHCl may be due to the formation of ordered structure in the (otherwise unordered) internal repeat region 73 - 109.

Based on our results, we propose the following scheme (Figure 47A and 47B) for the thermal and denaturant induced unfolding of napin (Scheme 2):

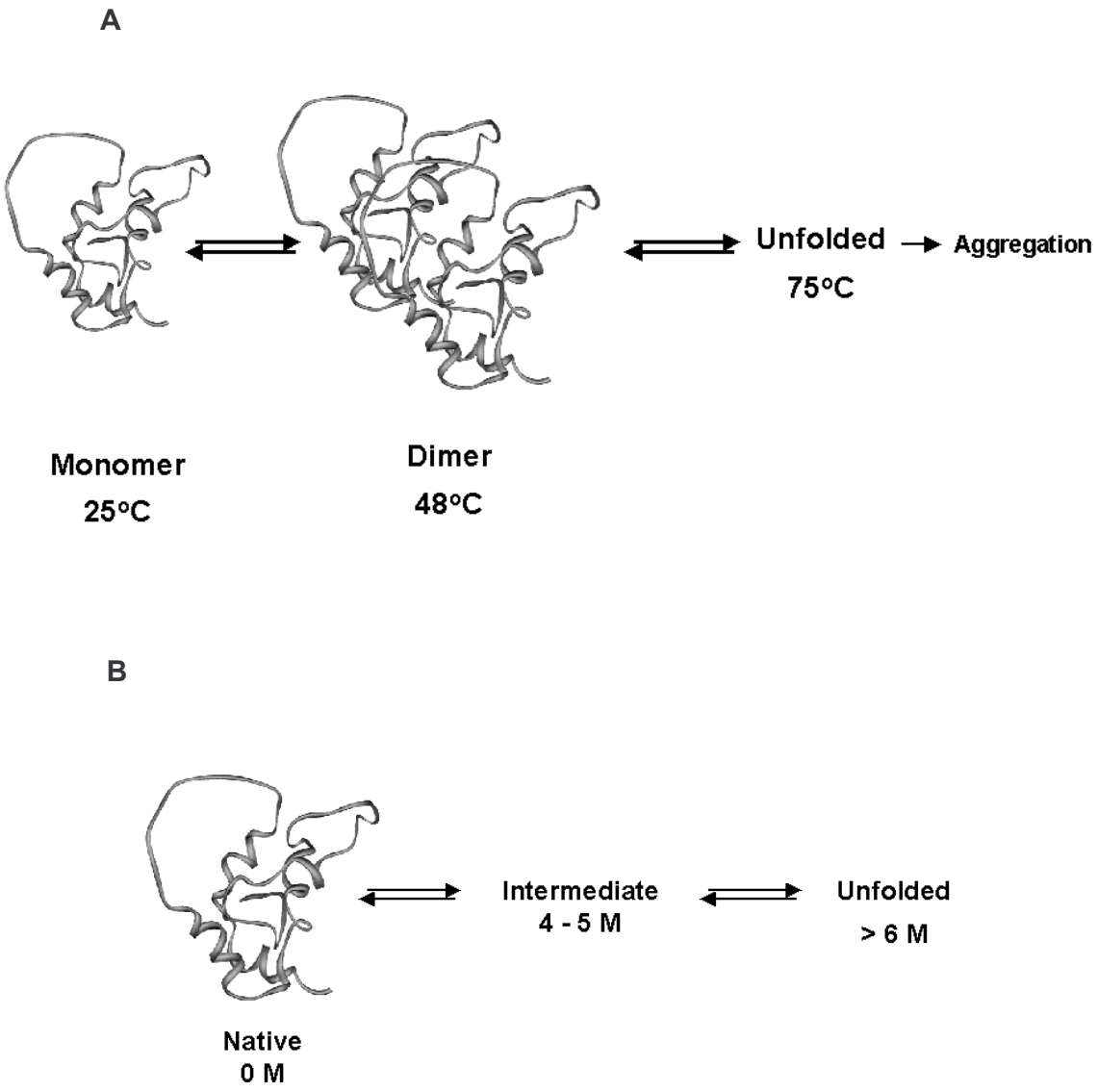

Figure 47. Schematic representation of napin unfolding (Scheme 2)

A: Thermal unfolding **B:** Isothermal equilibrium unfolding by GdnHCl.

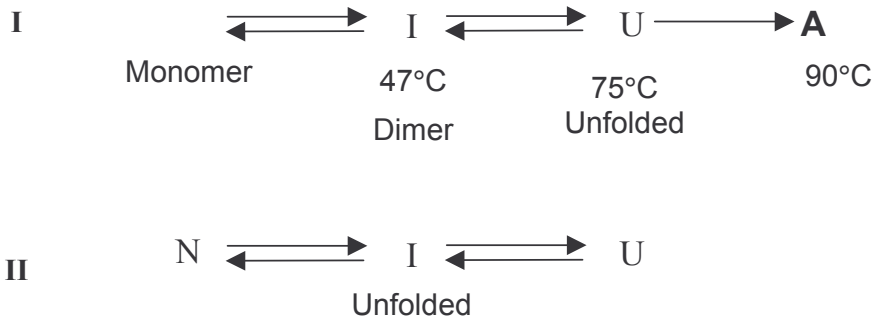

Scheme 2. Proposed mechanisms for thermal and denaturant induced unfolding. (i) Thermally induced unfolding and (ii) GdnHCl induced unfolding of napin.

N, I, U and A, represent native, intermediate, unfolded and aggregated, respectively. The end states in both thermal and chemical denaturation are different although ΔC_P values for both processes are similar. In case of thermal unfolding, the intermediate 'I' is a dimer with no observed change in the secondary or tertiary structure.

In case of unfolding by GdnHCl, the end state, 'U' does not have any residual secondary or tertiary structure. The intermediate 'I' has very limited secondary structure but no tertiary structure left. The only common element in both mechanisms is the complete reversibility of the process.

The ΔC_P values for the first transition, N ⇆ I in the thermal unfolding is higher that of the second transition i.e. I ⇆ U due to dimerisation. In case of heat shock protein, Hsp27, it has been reported that with increasing temperature, the molecule undergoes change in state of association of the

molecule (Lelj-Garolla and Mauk, 2006) The biological significance of the dimerisation of this napin is not clear. However, in case of chemical denaturation, the ΔC_P value of the first transition is almost identical with the second transition.

Unfolding studies induced by temperature and chemical denaturants such as GdnHCl establish a three-state unfolding transition. Proteins with similar molecular weight and disulfides differ significantly in their stabilities.

Section C: Interaction of napin with intrinsic ligands

Napin is rich in essential amino acids lysine (7.8%) and sulfur (9.5 %) containing amino acids (Thiyam, 2003). Binding studies of napin with intrinsic ligands helps in identification of amino acids involved in interaction and also gives the information about the structural changes upon interaction. Interaction between intrinsic ligands and napin helps in production of antinutritional free – napin. Hence, we have investigated interactions of sinapic acid, phytic acid and AIT with napin through spectroscopic methods for better utilization of mustard as food grade protein.

Sinapic acid

Sinapic acid is a major phenolic acid, which constitutes about 80% of the total phenolic of mustard meal. The absorbance spectrum showed three maxima at 321, 238 and 204 nm. The molar extinction coefficient of sinapic acid was determined and found to be 2.02 $\times$ 104 ML-1 at 321 nm, 1.84 $\times$ 104 ML-1 at 238 nm and 1.37 $\times$ 104 ML-1 at 204 nm respectively.

Napin purified on LH – 20 gelfiltration was used for the interaction studies. Napin has an emission maximum at 340 nm, when excited at 295 nm (Figure 48A). Addition of sinapic acid induces, red shift in fluorescence maxima by 4 nm. A maximum quench of 10% was observed at 40 μM of sinapic acid (Figure 48B). The Qmax = 66 $\pm$ 4 was determined from double reciprocal plot of Quench vs. concentration of sinapic acid (Figure 49A). The mass action plot shows binding constant of 3.51 $\pm$ 0.3 $\times$ 103 M-1 (Figure 49B). Modification of tryptophan reduced the interaction of sinapic acid with napin.

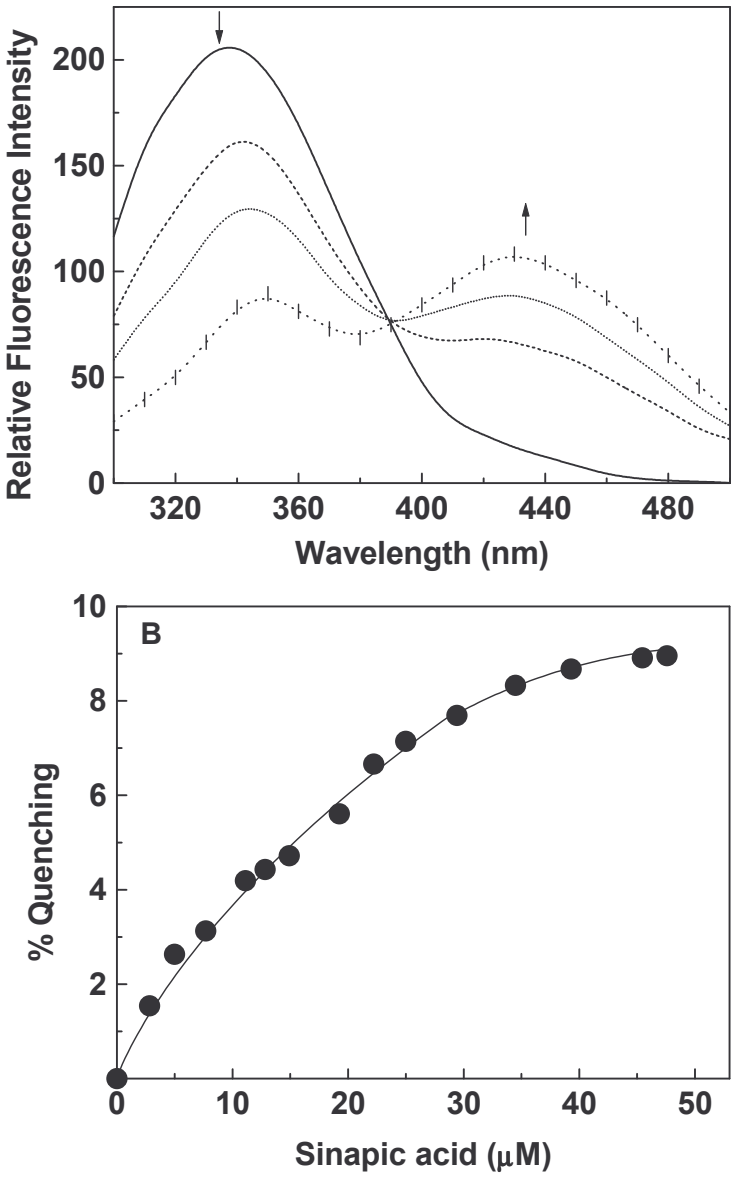

Figure 48. Interaction of napin with sinapic acid - Fluorescence

Napin was titrated with increasing aliquots of stock sinapic acid in ethanol and the percentage quench was recorded. A: Emission spectra of napin showing quench upon the addition of sinapic acid. (—) Napin, (⋆⋆⋆) 10 μM, (·····) 20 μM and (···|···) 40 μM sinapic acid. The spectra recorded from 300 – 500 nm, after exciting at 295 nm. Excitation and emission slit widths were set at 5 and 10 nm, respectively. B: Plot of decrease in the sinapic acid – Protein bound fluorescence as a function of sinapic acid concentration.

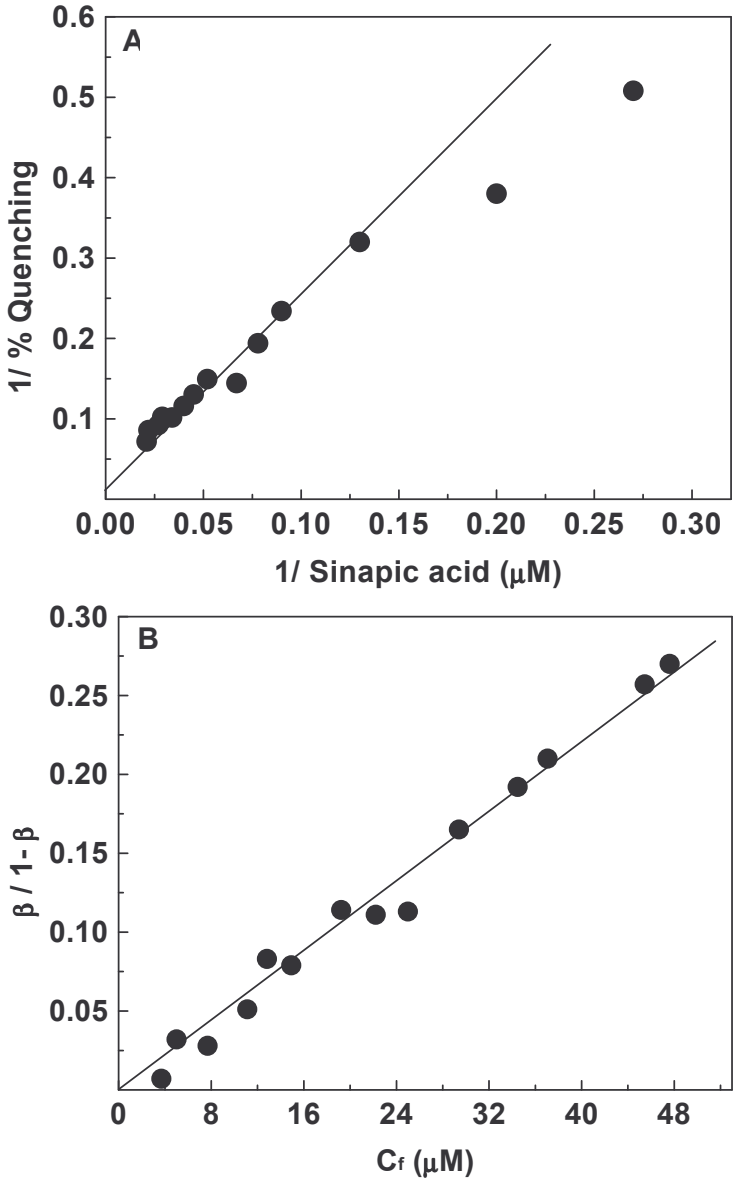

Figure 49. Quantitation napin interaction with sinapic acid-fluorescence

A: Double reciprocal plot of data 48B, and Q_{max} = 66 ± 4 B: Mass action plot of data 48B in accordance with Lee et al (1975)

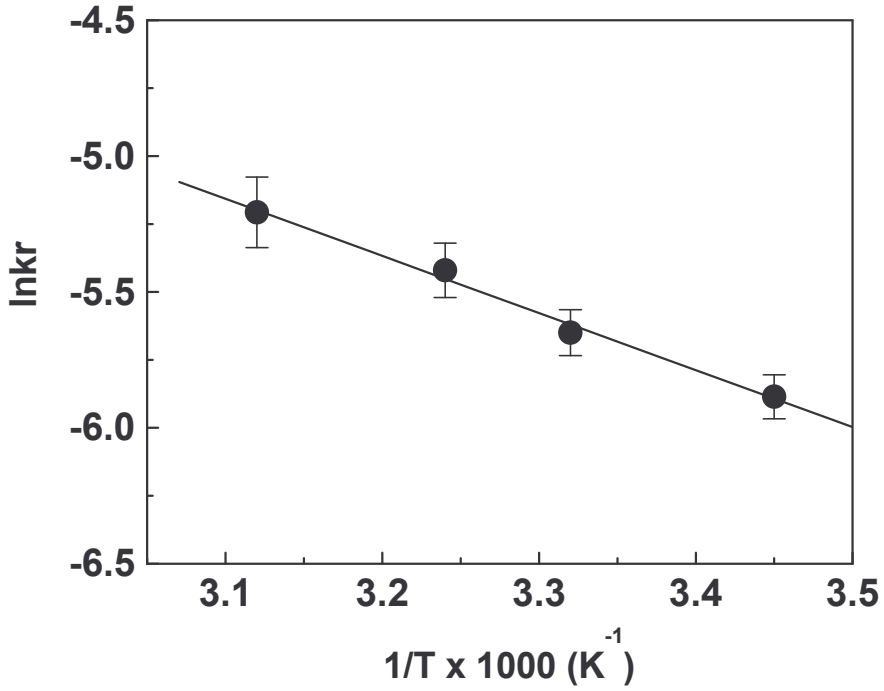

Figure 50. Interaction of napin with sinapic acid: van't Hoff plot

Effect of temperature on the binding constant of sinapic acid to napin was studied at different temperatures (17– 47 ±1°C) and the percentage quench was recorded. van't Hoff plot was constructed to obtain the thermodynamic parameters.

The effect of temperature on the interaction of sinapic acid with napin was followed in the range 17 – 47°C. The binding constant decreased in the temperature range studied. The enthalpy ΔH° and entropy ΔS° were determined to be –9.61 kcal mol-1 (Figure 50) and –15.29 cal mol-1 K-1 respectively. The free energy change ΔG° was found to be –4.95 kcal mol-1 at 27°C.

Involvement of electrostatic interactions during binding was determined by increasing the ionic strength of buffer with sodium chloride (0 – 200 mM). The binding constant decreases from 3.51 × 103 M-1 to 1.2 × 103 M-1 with increasing ionic strength suggesting the role-played by electrostatic interactions. The Stokes radius found to decrease with increase in the ionic strength from 20 Å to18 Å.

Intrinsically bound sinapic acid was determined by RP–HPLC. Figure 51A and 51B shows RP–HPLC profile of standard sinapic acid and napin-bound sinapic acid respectively. The result suggests 0.39 mole of sinapic acid bound to mole of napin. Protein content decreased considerably when treated with 1% activated charcoal. Napin treated with PVP has no effect on binding affinity.

At lower concentration of sinapic acid there was no change in secondary or tertiary structure of napin (CD). Higher concentration of sinapic acid could not be studied due to high noise/signal ratio. This may be due to the high absorption of sinapic acid.

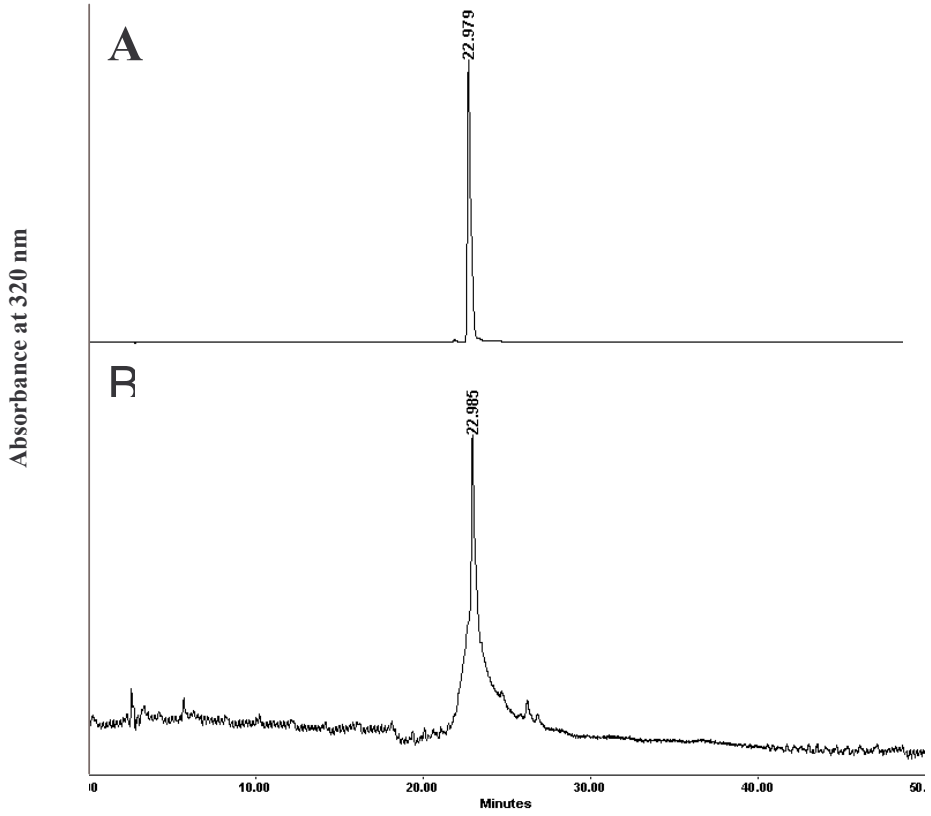

Figure 51. Determination of intrinsically bound sinapic acid

RP-HPLC was carried out using a symmetry shield ^{TM} RP_{18} (5.0 µ, 4.6 mm × 250 mm) Waters column. Elution profile was monitored at 325 nm with a flow rate of 1 mL/min at 27°C. A: chromatogram of standard sinapic acid standard (1 µg/µL). B: Sinapic acid bound to napin was extracted with 80% methanol for 3h, at 70°C, centrifuged and dried under nitrogen. Dried sample was redissolved in solvent A and injected directly to the column.

Phytic acid

Binding of phytic acid was estimated as a function of pH and concentration. Maximum binding was observed at pH 3.0 (0.02 M glycine-HCl buffer, ~85% precipitation) at a napin concentration of 6.9×10^{-5} M. Hence, all the binding studies were carried out at pH 3.0 (Figure 52). The precipitation as a function of phytic acid concentration was studied with a protein concentration of 6.9×10^{-5} and 3×10^{-3} M. As the phytic acid concentration increased concomitantly the precipitation also increased at 600 nm.

Maximum binding of phytic acid was observed at 0.28 ± 0.05 mM at protein concentrations of 6.9×10^{-5} and 3×10^{-3} M.

Figure 53 shows the HPLC chromatogram of unbound phytic acid of napin-phytic acid complex, which was precipitated from the protein (2 mg/mL) by the addition of TCA. Binding of inorganic phosphorus and phytic acid to napin was determined by Scatchard analysis figure 54 and inset. Binding constant for napin with inorganic phosphorus and phytic acid were found to be $1.0 \pm 0.8 \times 10^{5}$ and $1.51 \pm 0.6 \times 10^{5}$ M^{-1} respectively. The number of binding sites was found to be ~4 (3.95).

Change in the tertiary and secondary structure of napin upon binding to phytic acid was studied using fluorescence and CD.

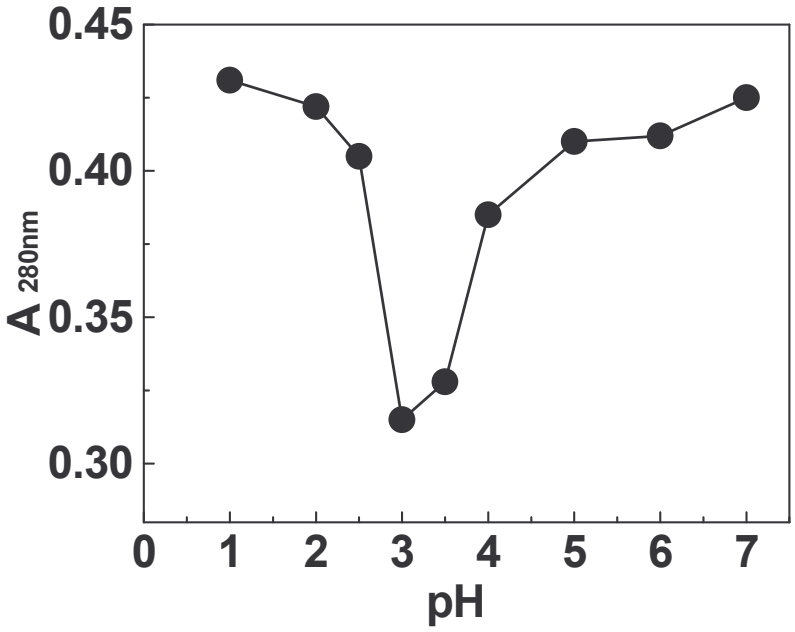

Figure 52. Effect of pH on the binding of phytic acid with napin

The effect of pH was studied in the pH range 1.0 – 7.0. Protein and phytic concentration used was 1 mg/mL and 0.2 mM respectively.

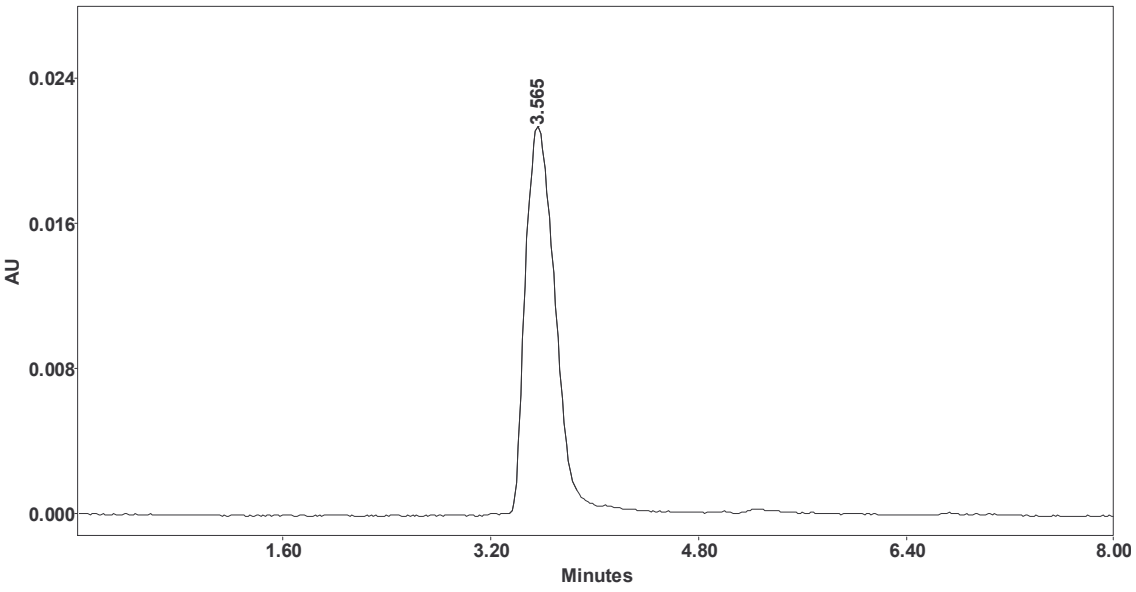

Figure 53. Quantitation of napin interaction with phytic acid

Chromatogram of unbound fraction from napin – phytic acid complex (2 mg/mL). Protein (napin-phytic acid complex) after precipitation with 3% TCA, centrifuged and supernatant injected directly on to column. Bound phytic acid was isocratically eluted using 0.005 M sodium acetate for 15 min at a flow rate of 1 mL/min. The elution of phytic acid was monitored at 254 nm (Tangendjaja et al., 1980).

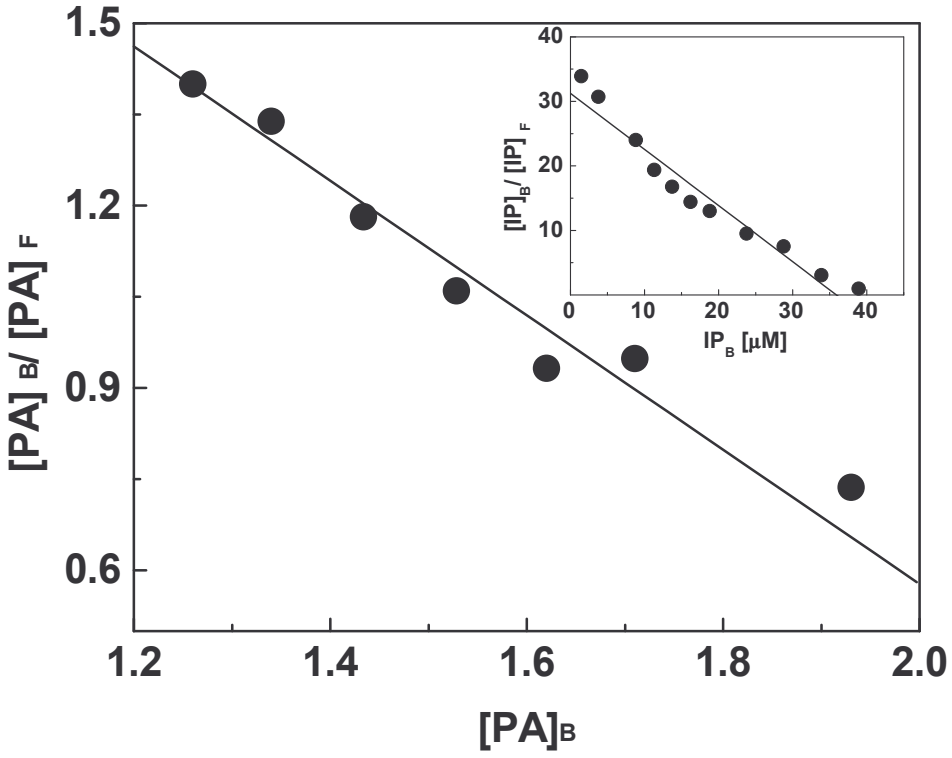

Figure 54. Determination of binding constant

Napin – phytic acid binding constant was determined by Scatchard plot. Inset: Determination of binding constant by measuring the inorganic phosphorus.

With increase in the concentration of phytic acid, the relative fluorescence intensity at 343 nm decreased by 5% and λ_{max} shifted towards blue (2 nm).

CD spectra of napin in far (Figure 55A) and near UV region (Figure 55B) in presence and in absence of phytic acid were recorded. Low concentration of phytic acid (0.07 mM) increased ellipticity upto ~12% however, at higher concentration (0.3 mM) ellipticity was decreased by 6%. Near UV CD spectra (320 – 240 nm) of native protein revealed troughs at 265, 270, 295 nm and two peaks at 250, 280, 290 nm. A slight decrease in the minima at 270 and 295 nm and significant decrease (–9) in the trough ellipticity at 255 nm was observed. These results indicate binding of phytic acid affects the conformation of napin structure. Tryptophan modification has no effect on the binding of phytic acid.

Lysine modification decreased the binding constant significantly from 15.1×10^4 M^{-1} to $5.5 \pm 0.5 \times 10^4$ M^{-1} as determined by HPLC and inorganic phosphorus measurements.

Allyl isothiocyanate

The purified protein was free from intrinsically bound AIT as confirmed by RP–HPLC. The interaction of AIT with napin was estimated by measuring the available lysine content. Effect of pH was studied in the pH range 4 – 10 with a protein concentration of 100 μM. Studies at higher pH (pH 10.0) were not carried out since the protein undergo conformational changes (Schimdt, et al., 2004).

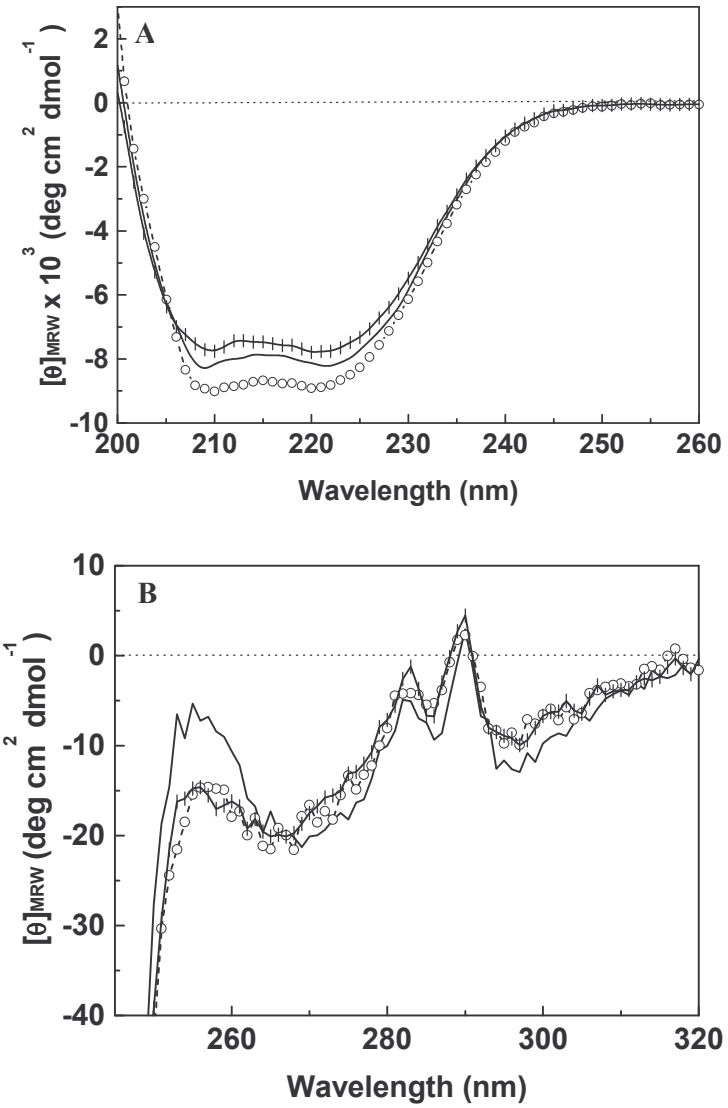

Figure 55. Phytic acid induced conformational changes

A: For far UV scans (200 – 260 nm), napin (0.4 mg/mL) in 0.02 M Glycine-HCl buffer at pH 3 was used. B: Protein concentration of 2.16 mg/mL was used in the near UV region (320 – 240 nm). (—), Napin; (oo), 0.07 mM phytic acid; (-I-), 0.3 mM phytic acid. Spectra were recorded at a scan speed of 20 nm/ min. Pathlength of the cell was 1 mm and 10 mm for the far UV and near UV scans, respectively.

The available lysine content did not change between pH 5.0 and 7.5. Maximum binding was observed at pH 7.4 hence, all AIT binding measurements were carried out in buffer A.

The binding of AIT to napin was studied by measuring the available lysine content, fluorescence, electrophoretic mobility, tyrosine ionization and structural studies by CD. Maximum binding of AIT (minimum available lysine) to napin was observed at 0.3 mM and 100 μM napin. The available lysine content decreased to 51% and remained constant (Figure 56A). The available lysine content of napin is found to be 6.3 mole/mole of napin. Earlier reported available lysine content of *B. juncea* napin is 6.7% (Aruna and Rao, 1988). The relative electrophoretic mobility on 10% native gel (Figure 56B inset) decreased with the reduction in available lysine (Figure 56B). The decrease in electrophoretic mobility (~available lysine 60%) is due to decreased positive charges on the napin. The effect of temperature on the interaction of AIT with napin was studied. Lysine content decreased from 60 – 32% with increasing temperature (Figure 57).

The fluorescence quenching has been used for AIT–napin interactions. There was no significant shift in the fluorescence maximum was observed. The extent of quenching is shown in Figure 58A. The Scatchard plot of AIT binding is given in Figure 58B. From the slope, binding constant K_a was found to be 4.6×10^5 M^{-1} with 0.8 binding sites.

The effect of AIT on the conformation of napin was studied by measuring the far and near UV CD spectra.

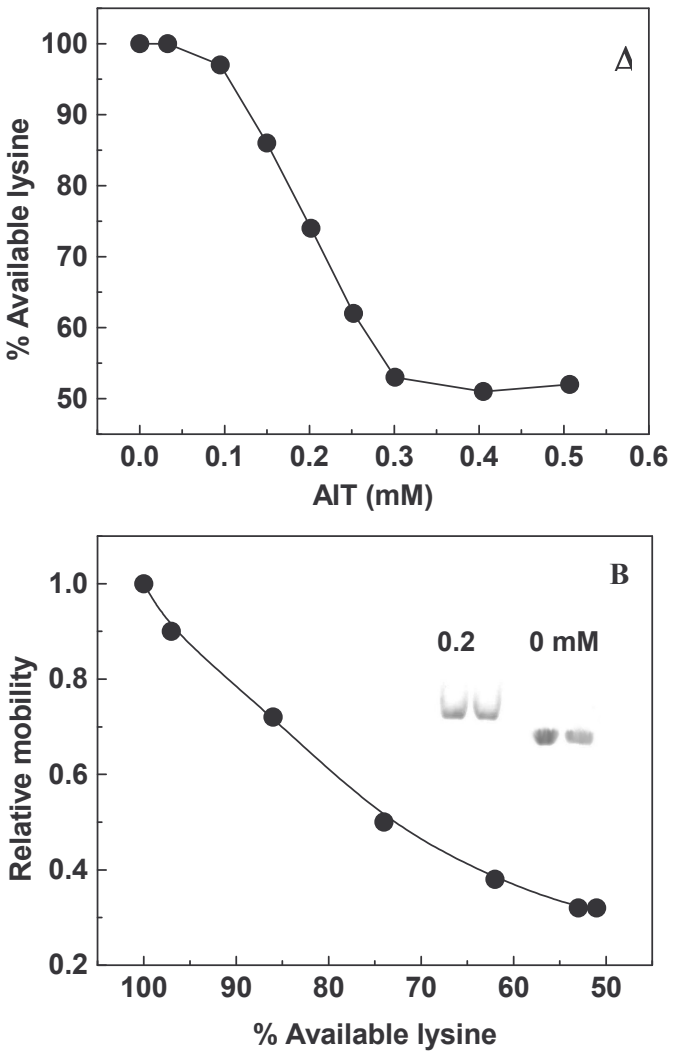

Figure 56. Quantitation napin interaction with allyl isothiocyanate

A: Effect of AIT concentration on napin available lysine content. A protein concentration of 100 μM and 0.3 mM AIT was used. B: Relative electrophoretic mobility of napin – AIT complex on 10% native gel Inset B: 10% Native gel was run in glycine – HCl (0.2 M, pH 4.0) and stained with amido black in 7% acetic acid. Polarities were reversed during the run and methylene green was used as the tracking dye. Lane 1 – napin, lane 2 – napin – AIT complex, (0.2 mM AIT).

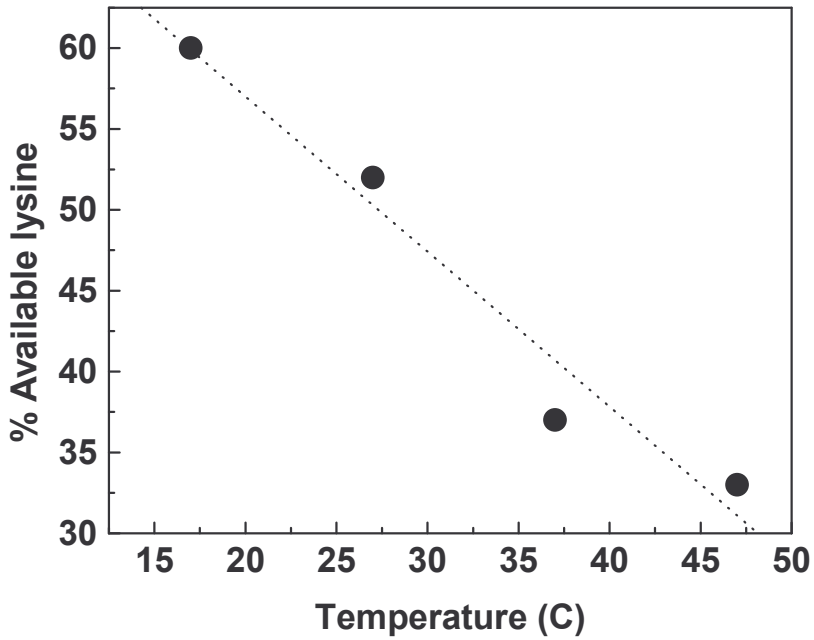

Figure 57. Effect of temperature on AIT-napin binding

Effect of temperature (17 – 47 ± 1°C) on AIT-napin binding was studied by measuring the available lysine content. A protein concentration of 100 μM and 0.3 mM AIT was used for the study.

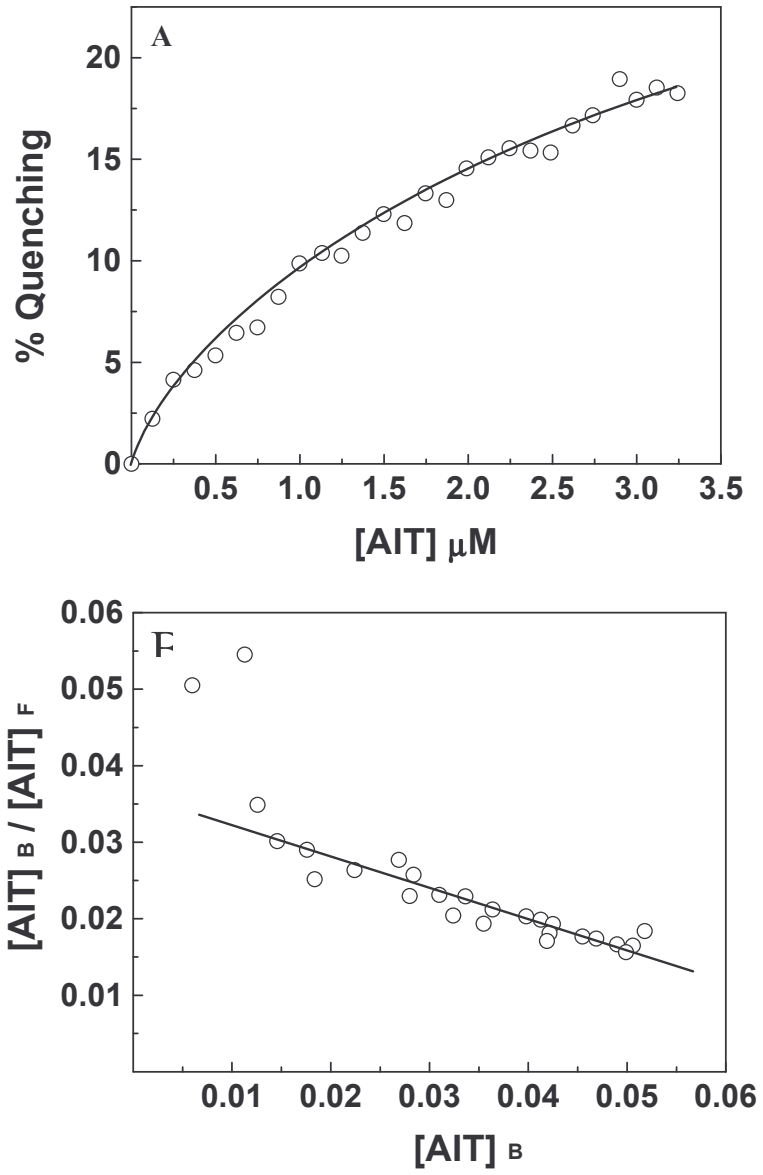

Figure 58. Interaction of napin with AIT – Fluorescence

A: Napin was titrated with increasing aliquots of stock AIT in ethanol and the percentage quench was recorded. The spectra recorded from 300 – 400 nm, after exciting at 280 nm. Excitation and emission slit widths were set at 5 and 10 nm, respectively. B: Plot of decrease in the AIT- napin bound fluorescence as a function of AIT concentration.

Neither low concentration (0.1 mM) nor high concentration (0.3 mM) of AIT affected the secondary structure of napin (Figure 59A). Disappearance of peak at 280 nm was observed in the near UV CD spectra of napin at high concentration (0.3 mM, maximum binding of AIT). Lower concentration does not affect the structure (Figure 59B).

The extent of lysine modification was determined by measuring the available content was found to be 1.8 mole/mole of napin. Modification of lysine by succinylation decreased the binding of AIT considerably.

Tyrosine ionization

The involvement of tyrosine in AIT binding was studied by tyrosine ionization in the pH range 7.0 – 11.9. The titration was carried out with napin and napin AIT complex where the available lysine content is 50% of the original. The pKa values of napin and AIT complex were 11.07 and 11.4 respectively (Figure 60).

Discussion

A number of antinutritional factors may present in food and feed products, which may adversely affect protein digestibility and amino acid availability. The naturally occurring antinutritional factors are; glucosinolates–mustard and rapeseed protein products, tannins and phenolic acid- legumes and cereals, phytates- cereals and oilseeds, gossypol- cottonseed protein products and trypsin inhibitors - hemagglutinins in legumes (Gilani, et al., 2005).

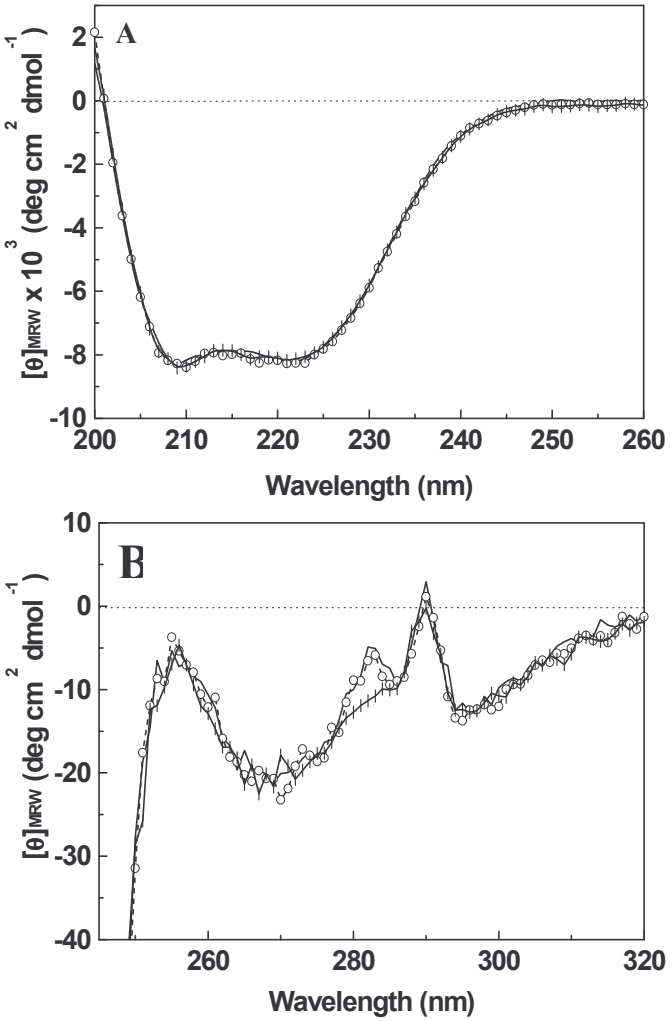

Figure 59. AIT induced conformational changes in napin structure.

A: far UV CD (200 – 260 nm) and **B:** near UV CD (320 – 240 nm) of napin-AIT complex. A protein concentration of 0.4 mg/ mL and 2.2 mg/mL in buffer A was used for far and near UV measurements respectively. (—), Napin; (oo), 0.1 mM AIT; (-I-), 0.3 mM AIT.

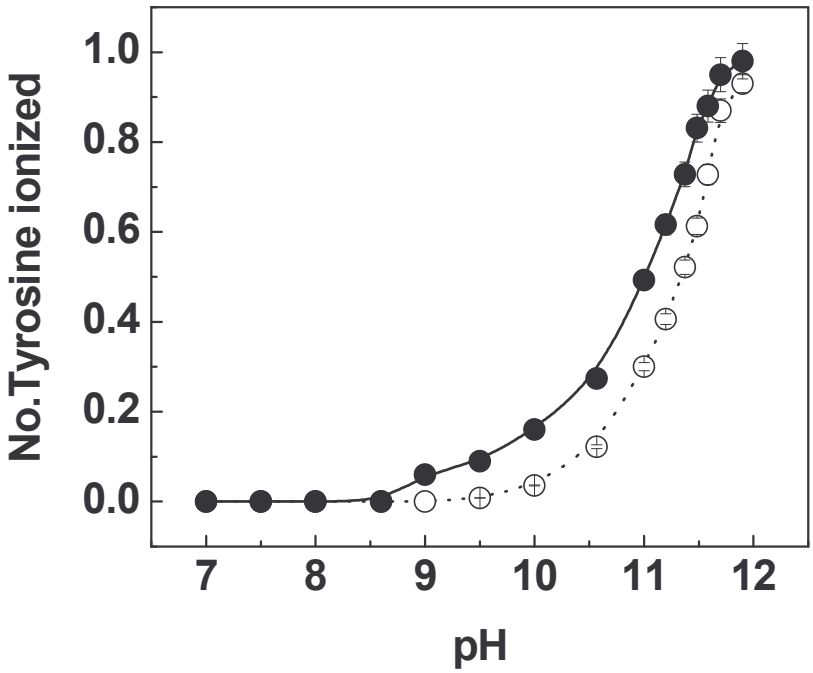

Figure 60. Tyrosine ionization

Spectrophotometric: The concentration of napin and napin – AIT complex used was 1.1 mg/mL. (●), napin and (○) napin-AIT complex. Absorption spectra were recorded using 1cm path-length cell.

Low molecular weight napin is a basic protein (Schmidt et al., 2004) and rich in lysine and sulfur containing amino acids. To produce ligand - free mustard napin, which is nutritionally rich, it is essential to know the factors responsible for binding. Hence, study has been made on the binding of anti nutritional factors of mustard such as sinapic acid, phytic acid and allyl isothiocyanate (hydrolytic product of sinigrin glucosinolates) with napin.

Results of the present study indicate that the binding of sinapic acid to napin, is characterized by low binding constant of $3.51 \pm 0.3 \times 10^3$ M^{-1} obtained from the fluorescence (Figure 49B).

Direct binding studies by equilibrium dialysis could not be carried out because of the instability of sinapic acid in buffer. There is a decrease in the binding constant with increase in temperature (Figure 50) suggests the involvement of non-covalent interactions. This was further confirmed by observed decrease in the binding constant on the addition of sodium chloride.

Phenolic acid forms complexes with protein consequently lowering - nutritional values. Zadernowski has shown the presence phenolic acid – protein complexes in rapeseed meals by subjecting it to alkaline hydrolysis (Zadernowski, 1987). Phenolic acids have a great affinity for binding with low molecular weight protein (Naczk, et al., 1998)

Napin contains a Trp and Tyr in small subunit and large subunits respectively responsible for intrinsic fluorescence. Napin contains 9 Lys and 4 Arg residues. These residues are positively charged at the pH used for study and contribute to ionic interaction with ligand. Sinapic acid has a phenolic

structure with methoxy and carboxylic group. The formation of phenol-protein complexation is usually the consequence of hydrogen bonds and hydrophobic interaction (Hagerman and Butler, 1980; Maliwal, Rao and Rao, 1985).

Presence of intrinsically bound sinapic acid makes the binding constant low. This has been confirmed by RP – HPLC of napin (Figure 49C). Gelfiltration studies at higher pH, could not resolve intrinsically bound ligand were not separated from the protein. This shows the covalent binding of sinapic acid to napin.

Maximum binding of phytic acid to napin was at pH 3.0. Sesame, casein and gluten protein also had shown maximum binding at acidic pH 3.0, 2.5 and 2.8 respectively (Rajendran and Prakash[b], 1993). Schwenke et al reported that maximum binding of phytic acid to albumin occurred below the isoelectric point, where the protein carries net positive charges (Schwenke et al., 1987).

Phytic acid carries negatively charged and may strongly interact with basic napin, which carries net positive charge, concomitantly reducing its nutritional value. At higher concentration (30 mM) of phytic acid low precipitation of protein was observed. This may be due to solubilization of complex formed by electronegative phytic acid-napin complex. At low concentration of phytic acid ($>1 \times 10^{-4}$ M), positive charges on the protein are not completely neutralized, complex has a net positive charge, which makes complex soluble (Rajendran and Prakash[b], et al., 1993). The binding of decreased significantly in presence of 0.5 M NaCl.

Taken together both the experiments have given similar binding constant for phytic acid interaction with napin. It is reported that the α- amino groups, ε- amino groups of lysine, imidazole groups of histidine and guanidine group of arginine are the reactive phytic acid binding groups of chymotrypsin (Barre and van Huot, 1965). Binding of phytic acid is also observed in human serum albumin, mustard 12S protein, soy glycinin, ovalbumin, sesame globulin, napin 2S protein from rapeseed (Kishore Kumar Murthy and Rao, 1986).

Phytic acid interaction can influence the properties of protein owing to electrostatic interaction (Maga, 1982). Hence, the changes upon binding of phytic acid to napin were studied by CD and fluorescence. The secondary and tertiary structure revealed that the aromatic environment of protein was not affected upon binding. This was further conformed by tryptophan fluorescence measurements.

At low concentration of phytic acid napin ellipticity increases. This may be due to the formation of the soluble polymer, results in more ordered structure. The similar phenomenon was also observed with apohaemoglobin (Chu and Bucci, 1979). Binding constant decreased upon modification of lysine by succinalisation. Lys, which is a positively charged essential amino acid, interacts with negatively charged phytic acid ligand. This may bring in secondary and tertiary structural changes in napin. Tryptophan modification had no affect the binding constant of phytic acid.

Because of the volatile nature of AIT, equilibrium dialysis experiments could not be performed. As the temperature increased the available lysine

content decreases. This may be due to the increased kinetic energy of the molecules with temperature.

The decrease in electrophoretic mobility is due to increased negative charge on the protein molecule (Figure 56B). ε-Amino groups of lysine that contribute positive charge to the napin are the key amino acids for decreased mobility in addition to binding. Isothiocyanates are more reactive with the uncharged $-NH_2$ groups than with the positively charged $-NH_3^+$ groups (Edman, 1970; Means and Feeney, 1971).

The decrease in UV - absorption spectra of AIT-cruciferin was observed, and which is attributed to the formation of thiourea as it absorbs strongly at 245 nm (Langer and Gschwendtova, 1969; Kishore Kumar Murthy and Rao, 1986). AIT interacts with free cysteines and forms thiourea. No increase in the absorption at 245 nm was observed with napin – AIT complex.

A positive peak at 290 nm and 282 nm of near UV CD of napin can be attributed to tryptophan and tyrosine respectively. At 0.3 mM AIT concentration, disappearance of tyrosine peak is observed. This shows the change in the environment of tyrosine residue as AIT interacts with phenolic group of tyrosyl residue of napin. Isothiocyanates are known to interact with –OH groups (Drobnica and Gemeiner, 1976). Increased in the pKa values of napin – AIT complex confirm the participation of tyrosine in binding. Involvement of tyrosine residue in binding is of AIT with mustard 12S was also reported by Kishore and Rao (Kishore Kumar Murthy and Rao, 1986).

Sinapic acid binds weakly to napin due to the presence of intrinsically bound complexes. Phytic acid interacts with napin with maximum binding at pH 3. Change in the microenvironment of tyrosine was observed upon binding of AIT to napin.

SUMMARY AND CONCLUSIONS

Summary and conclusions

Brassica juncea napin is a 115-residue heterodimer of small and large subunits, constrained by four (two inter and two intra) disulfide bridges. Napin has a high content of basic amino acids and is allergenic in nature. In the present study, the contribution of hydrophobic, electrostatic and internal repeat sequence to the structure and stability of napin has been studied. The structural stability of napin has been probed by DSC, CD, fluorescence and size exclusion chromatography after thermal and chemical denaturation. Interaction study of intrinsic ligands with napin helps to identify the binding characteristics. The following are the conclusions of this study:

- The homogeneity of purified napin from *Brassica juncea* was ascertained by SDS-PAGE, size exclusion chromatography on HPLC. The molecular weight was formed by MALDI-TOF was found to be 14724 Da.
- The pI (Isoelectric point) of napin was at pH > 10.5. The hydrodynamic radius of napin, measured by dynamic light scattering was found to be 20 Å.
- The N - terminal sequence of reduced napin

Small subunit- IPKXRKEf...

Large subunit- SQGPQQRP...

- Role of disulfide linkages, electrostatic as well as hydrophobic interactions on napin stability were investigated through different fluorescent probes, monohydric alcohols and salts.

- Kyte and Doolittle hydropathy plot confirmed the hydrophilic nature of napin. The two separated subunits were aperiodic and hydrophilic in nature but devoid of buried hydrophobic patches.
- The changes in surface hydrophobicity of napin were followed by fluorescent probes ANS, TNS, PRODAN and CPA. 0.5 moles of fluorescent probe bind per mole of protein indicating the hydrophilicity of napin. Reduction in binding constant and number of binding sites was observed in the presence of 0.5 M NaCl compared to control was observed.
- Fractional accessibility of the lone tryptophan is 0.63. The fractional accessibility, which decreased to 0.5 in presence of 0.5 M NaCl, remained at 0.6 in presence of 0.2 M sodium sulphate. Stern-Volmer constant decreased from 6.5 M^{-1} to 3.4 M^{-1}. The decrease in the fractional accessibility and K_{SV} in presence of NaCl may be due to compaction of the molecule.
- In presence of 0.5 M NaCl, the ellipticity ratio [$R=([\theta]_{222}/[\theta]_{208})$] increased from 1.05 to 1.25 $\pm$ 0.05, indicating a stronger inter-helical association. In presence of Na_2SO_4, the ratio was 1.07 indicating little or no change.
- In presence of 0.5 M NaCl, the elution volume shifted from 17 mL to 18.2 mL indicating reduction in Stokes radius. Also, T_M (Transition temperature) shifted from 74°C to 88°C, indicating increased protein stability.
- Monohydric alcohols such as methanol, ethanol, propanol, butanol and TFE induce structure as evidenced by increased helical content of

napin. Higher concentrations of propanol (> 6.7 M) and butanol (> 3.5 M) result in protein precipitation.

- Na_2SO_4 does not affect napin structure or stability, due to absence of hydrophobic core. Addition of NaCl results in compaction of mustard napin, leading to its stabilization. Electrostatic interactions play a major role in stabilizing the protein structure, in addition to the presence of disulfide linkages.
- Propensity of forming helix in presence of TFE and SDS, which mimics the membrane, may help in the prediction of napin's anti fungal and anti microbial activity. Due to its amphipathic and basic nature, napin interacts with DNA as was observed by gel retardation assay.
- Napin is resistant to proteolytic cleavage by trypsin and chymotrypsin even after 4h of digestion at 37°C. The degree of hydrolysis of napin is determined to be 1.9% (with trypsin) and 2.2% (with chymotrypsin). Napin is found to be resistant to proteolysis even at higher temperatures (60°C, 1 h).
- Digestion of napin by trypsin (100:2) was feeble, and the digest, after RP-HPLC, showed a major peptide peak at retention time of 42 min. Molecular weight of the peptide was determined to be ~ 6589 Da by MALDI –TOF.
- Peptide was found to be rich in cysteines and glutamines as determined by amino acid composition. The structure of the peptide was found to be aperiodic with fluorescence emission maxima at 352 nm.

- Thermal stability of napin was studied by measuring the changes in ellipticity values at 295 nm and 222 nm in the temperature range 27 - 77°C. There was considerable residual structure in the protein, even at 77°C, indicating its thermal stability. The structural change observed (27 - 77°C) in the far or near UV regions was completely reversible on cooling the protein.
- The relative fluorescence intensity remained unchanged till 42°C, suggesting little or no change in the environment around the tryptophan. Decrease of 8 – 10% in fluorescence intensity was observed in the range 43 – 67°C. Beyond 67°C. No further change in the RFI was observed.
- DSC scan of napin was carried out in the temperature range 27 – 90°C at a scan rate of 60 K/h. Deconvolution of the transition peak revealed the existence of two kinds of entities at different temperatures. The first transition temperature (T_{M1}) was at 50.5°C and the second transition (T_{M2}) was at 62.8 °C.
- Rescans of the sample from 27°C show complete reappearance of the transition peaks at 50 and 62.8°C, indicating that both transitions are completely reversible. Temperatures beyond 90°C resulted in napin aggregation.
- Neither the napin concentration (10 – 106 μM) nor the scan rate (10 – 60 K/h) has a bearing on the thermodynamic quantities. Ratio of the calorimetric enthalpy (ΔH_C) to van't Hoff's enthalpy ($\Delta H_C/\Delta H_V$) for the

first transition and second transition was determined to be 1.6 ± 0.05, and 0.75 ± 0.03 respectively.

- Thermodynamic parameters were determined at different pH (3.12 – 9.16) decreased with an increase in pH. ΔC_P was obtained from the slope of the plot ΔH_V vs. T_M at different pH. The estimated values of ΔC_{P1} and ΔC_{P2} were 2.05 kcal mol^{-1} K^{-1} and 1.40 kcal mol^{-1} K^{-1} for the two transitions at T_{M1} and T_{M2}, respectively.
- The intermediates during thermal unfolding of napin, the state of association of the protein as a function of temperature was followed by gel filtration and cross-linking of the intermediates with carbodiimide. The gel filtration elution profile of napin as a function of temperature (10 – 37°C) reveals the protein is a monomer with a molecular weight of ~15,000 Da. In the temperature range 40°C – 45 ± 2°C, the protein elutes as a dimer.
- The carbodiimide cross-linked protein at 45°C, run in the 15% non-reducing SDS-PAGE has a molecular weight of 30,000 Da indicating dimerisation
- Thermal unfolding studies were made in presence of reducing agent DTT. The DSC profiles obtained were identical to the scans run in absence of DTT. Addition of DTT did not affect the association of napin during thermal unfolding.
- Native PAGE, of napin heated in presence of 1 mM DTT inferred that there is no cleavage of disulfide linkages during thermal unfolding. The change in ellipticity values at 222 nm confirmed that thermal unfolding was not affected by the presence of DTT. No change in the elution of

napin, by gel filtration on HPLC, in presence and absence of DTT was observed. Disulfide linkages of napin were not affected during the course of thermal unfolding, even with addition of reducing agents like DTT.

- The calculated ΔC_P value for thermal unfolding is 1.84 kcal $mol^{-1}K^{-1}$. The larger ΔC_P 3.45 kcal $mol^{-1}K^{-1}$ value, determined from DSC is probably due to the dimerisation in the temperature range 27 – 48°C.
- The amino acid sequence analysis of napin, using the program RADAR, led to the identification of two internal repeats in the large subunit with ~40% similarity. The two segments span from 31-60 and 73 – 109 residues.
- Multiple sequence alignment with *Brassica* family 2S proteins has revealed that these internal repeats are highly conserved.
- Isothermal unfolding of napin by GdnHCl was followed using CD and fluorescence. Protein denaturation was observed in the range 3.0 – 6.0 M GdnHCl. CD and fluorescence data of equilibrium unfolding of napin could adequately fit a three-state model.
- In the three-state unfolding model, the predominant unfolding reaction below 3.86 M may be N↔I transition and above 3.86 M, the predominant reaction may be I↔U transition, while the intermediate form was observed at ~5 M GdnHCl. The total free energy change, given by the sum of the two transition ΔG_{H2O} of values, is 10.3 ± 0.6 kcal mol^{-1}.
- Isothermal unfolding of napin by size exclusion chromatography indicated increase in the hydrodynamic radius. The plateau region

observed in the range 4 – 5 M GdnHCl shows a three state transition. Refolding experiments revealed that the unfolded protein refolds back to the native state.

- The ΔC_P for the isothermal unfolding is 3.75 kcal mol^{-1} K^{-1} obtained from the stability curves for both transitions. The calculated for isothermal unfolding is ΔC_P, 1.64 kcal mol^{-1} K^{-1}, is lower than the experimental value.
- Compared to proteins with similar molecular weights and disulfide bridges i.e., RNase, Lysozyme, Lactalbumin confirms the greater stability of napins. The presence of these internal repeats may contribute to the enhanced stability of all napins.
- Sinapic acid, phytic acid bind to napin, with the binding constant of 3.5 $\pm$ 0.3 x 10^3 M^{-1} and 2.01 $\pm$ 0.6 x 10^5 M^{-1}, respectively. Tryptophan modification reduced the binding affinity of sinapic acid to napin. Modification of lysine residues decreased the binding of phytic acid.
- The binding constant decreased in the temperature range 17 - 47°C. The enthalpy $\Delta H°$ and entropy $\Delta S°$ were determined to be –9.61 kcal mol^{-1} and –15.29 cal $mol^{-1}K^{-1}$respectively. The free energy change $\Delta G°$ was found to be –4.95 kcal mol^{-1} at 27°C.
- Intrinsically bound sinapic acid to napin has been determined by RP-HPLC after extraction with 80% methanol at 70°C. 0.4 mole of sinapic acid is bound to one mole of napin. Sinapic acid binds weakly to napin due to the presence of intrinsically bound complexes.
- Maximum binding of phytic acid was observed at 0.28 $\pm$ 0.05 mM at protein concentrations of 6.9 $\times 10^{-5}$ and 3 $\times$ 10^{-3} M.

- Binding constant for napin with inorganic phosphorus and phytic acid were found to be $1.0 \pm 0.8 \times 10^5$ and $1.51 \pm 0.6 \times 10^5$ M^{-1}, respectively. The number of binding sites was found to be ~4 (3.95). Lysine modification decreased the binding constant significantly from 15 x 10^4 M^{-1} to 5.5 ± 0.5 x 10^4 M^{-1}. Tryptophan modification has no effect on the binding of phytic acid
- The available lysine content of napin – AIT decreased significantly from 6 mole/mole to 1.8 mole/mole of napin. Microenvironment of tyrosine in napin changes upon binding to allyl isothiocyanate.
- Maximum binding of AIT (minimum available lysine) to napin (1.5 mg/mL) was observed at 0.3 mM. Tyrosine pKa value of napin-AIT complex was changed to 11.07 and 11.4. Disappearance of peak at 280 nm was observed in the near UV CD spectra of napin-AIT complex (AIT = 0.3 mM, maximum binding of AIT). Increased in the pKa values of napin – AIT complex confirm the participation of tyrosine in binding.
- The decrease in the electrophoretic mobility of napin-AIT complex is due to decreased positive charges on the napin.

Napins constituting about 45-50% of the total proteins are basic proteins, rich in glutamine, lysine, and cysteine. From the above studies, it can be concluded that napin unfolds through a three-state transition. Na_2SO_4 does not affect napin structure or stability due to the absence of a hydrophobic core. Addition of NaCl results in compaction of mustard napin, thereby stabilizing it. Electrostatic interactions play a major role in stabilizing the protein structure in addition to the presence of disulfide linkages. The

compaction of napin in the presence of salts may increase our understanding of the digestibility and allergenicity of the molecule.

Unfolding studies induced by temperature and chemical denaturants such as GdnHCl shows a three-state unfolding transition. Proteins with similar molecular weight and disulfides differ significantly in their stabilities. The three state transition, could be attributed to the independent unfolding of polypeptide chains and absence of strong intersubunit interactions. The presence of internal repeat sequences probably contributes to the additional stability of the napin. The knowledge gained by investigation, on the structure and stability of these proteins, may lead to their genetic improvements for exploitation in nutrition.

BIBLIOGRAPHY

BIBLIOGRAPHY

1. Ahmad, F. and Bigelow, C. C. Estimation of the free energy of stabilization of ribonuclease A, lysozyme, α- lactalbumin, and myoglobin, J. Biol. Chem., 1982, 257, 12935 – 12938.

2. Alizadeh-Pasdar, N. and Li-Chan, E. Comparison of protein surface hydrophobicity measured at various pH values using three different fluorescent probes. J. Agri. Food. Chem., 2000, 48, 328 – 334.

3. Altenbach, S. B., Kuo, C. C., Staraci, L. C., Pearson, K. W., Wainwright, C., Georgescu, A., and Townsend, J. Accumulation of a Brazil nut albumin in seeds of transgenic canola results in enhanced levels of seed protein methionine. Plant Mol. Biol., 1992, 18, 235 – 245.

4. Altenbach, S. B., Pearson, K. W., Leung, F. W., and Sun, S. S. M. Cloning and sequence analysis of a cDNA encoding a Brazil nut protein exceptionally rich in methionine Plant Mol. Biol., 1987, 8, 239 – 250.

5. Andrade, M. A., Perez-Iratxeta, C., and Ponting, C. P. Review: Protein Repeats: structures, functions and evolution, J. Struct. Biol., 2001, 134, 117 – 131.

6. Anfinsen, C. B. and Scheraga, H. A. Experimental and theoretical aspects of protein folding. Adv. Prot. Chem., 1975, 205 – 300.

7. Appu Rao, A. G. and Cann, J. R. A comparative study of the interaction of chlorpromazine, trifluoperazine and promethazine with mouse brain tubulin. Mol. Pharmacol., 1981,19, 295 – 301.

8. Arakawa, T. and Goddette, D. The mechanism of helical transition of proteins by organic solvents. Arch. Biochem. Biophys., 1985, 240, 21 – 32.

9. Argos, P., Pederson, C., Marks, M. D. and Larkins, B. A. A structural model for maize zein proteins. J. Biol. Chem., 1982, 257, 9984 – 9990.

10. Aruna, V. and Appu Rao, A. G. Isolation and charecterization of low molecular weight protein from mustard (*Brassica juncea*), J. Agric. Food Chem., 1988, 36, 1150 – 1155.

11. Astwood, J. D., Leach, J. N. and Fuchs, R. L. Stability of food allergens to digestion *in vitro*. Nat. Biotechnol., 1996, 14, 1269 – 1273.

12. Barciszewski, J., Szymanski, M. and Haertle, T. Minireview: analysis of rapeseed napin structure and potential roles of the storage protein. J. Prot. Chem., 2000, 19, 249 – 254.

13. Barre, R. and van Huot, N. Study of the combination of phytic acid with native, acetylated and deaminated human serum albumin. Bull. Soc. Chim. Biol., 1965, 47(7), 1399 – 1417 (Fr).

14. Baszcynski, C. L. and Barciszewski, J. the biosynthesis, structure and properties of napin, the storage protein from rape seeds. J. Plant Physiol., 1999, 154, 417 – 425.

15. Batra, P., Khan Shoeb Zafar and Fakhrul Islam. Is Mustard oil toxic? SAARC OILS and FATS TODAY, 2001, 50 – 55.

16. Beasty, M., Hurle, M. R., Manz, J. T., Stackhouse, T., Onuffer, J. J. and Matthews, C. R. Effect of phenylalanine-22. fwdarw. leucine, glutamic acid-49. fwdarw. methionine, glycine-234.fwdarw. aspartic acid and glycine-234. fwdarw-lysine mutants on the folding and stability of the

alpha subunit of tryptophan synthase from E. coli, Biochemistry, 1986, 25, 2965 – 2974.

17. Becktel, W. J. and Schellman, J. A. Protein stability curves. Biopolymers, 1987, 26, 1859 – 1877.

18. Bell, J. M., and Rakow, G. F. W. Trypsin inhibitors and phytic acid in oil extracted meals from seeds of several *Brassica* species and of *Sinapis alba*. Can. J. Anim. Sci., 1996, 76, 423 – 425.

19. Bidlingmeyer, B. A., Cohen, S. A., and Tarvin, T. L. Rapid analysis of amino acids using pre-column derivatization. J. Chromatogr., 1984, 336, 93 – 104.

20. Breiteneder, H. and Ebner, C. Molecular and biochemical classification of plant – derived food allergens. J. Allergy. Clin. Immunol., 2000, 106, 27 – 36.

21. Breiteneder, H. and Radauer, C. A classification of plant food allergens, J. Allergy and Clin. Immunol., 2004, 113(5), 821 – 830.

22. Brems, D. N., Brown, P. L., and Heckenlaible, L. A., Frank, B. H. Equilibrium denaturation of insulin and proinsulin, Biochemistry, 1990, 29, 9289 – 9293.

23. Cardamone, M. and Puri, N. K. Spectrofluorimetric assessment of the surface hydrophobicity of proteins. Biochem. J., 1992, 282, 589 – 593.

24. Carnovale, E., Lugaro, E. and Lombardi-Boccia, G. Phytic acid in faba bean and pea: Effect on protein availability. Cereal Chem., 1988, 65(2), 114 – 117.

25. Cejpek, K., Valusek, J. and Velisek, J. Reactions of allyl isothiocyanate with alanine, glycine, and several peptides in model systems, J. Agric. Food Chem., 2000, 48, 3560 – 3565.

26. Chaudhari, T. K., Das, K. P. and Sinha, N. K. Surface hydrophobicity of a low molecular weight basic trypsin subtilisin inhibitor from Marine Turtle Eggwhite. J. Biochem., 1993, 113, 729 – 433.

27. Cheryan, M. Phytic acid interactions in food systems, CRC Crit. Rev. Food Sci. Nutr., 1980, 13(4): 297 – 335.

28. Chifflet, S., Torriglia, A., Chiesa, R. and Tolosa, S. A method for the determination of Inorganic phosphate in the presence of labile organic phosphate and high concentrations of protein: Application to lens ATPases. Anal. Biochem., 1988, 168, 1 - 4.

29. Chu, A. H., and Bucci, E. Interaction of human apohaemoglobin with inositol hexaphosphate, J. Biol. Chem., 1979, 254(2), 371 – 376.

30. Creighton, T. E. Disulfide bonds and protein stability. BioEssays, 1988, 8, 57 – 63.

31. Crouch, M. L., Tenbarge, K. M., Simon, A. E. and Ferl, R. cDNA clones for *Brassica napus* seed storage proteins: Evidence from nucleotide sequence analysis that both subunits of napin are cleaved from a precursor polypeptide. J. Mol. Appl. Genet., 1983, 2, 273 – 283.

32. Dasgupta, J., Dasgupta, S., Ghosh, S., Roy, B. and Mandal, R, K. Deduced amino acid sequence of 2S storage protein from *Brassica* species and their structural features. Indian J. Biochem. Biophys., 1995, 32, 378 – 384.

33. Dasgupta. S., Dasgupta, J. and Mandal, R. K. Cloning and sequence of 5´ flanking sequence from the gene encoding 2S storage protein, from two *Brassica* species. Gene, 1993, 133, 301 – 302.

34. Deechongkit, S., Nguyen, H., Jager, M., Powers, E. T., Gruebele, M., and Kelly, J. W. β-Sheet folding mechanisms from perturbation energetics. Curr. Opin. Struct. Biol., 2006, 16, 94 – 101.

35. del Mar Yust, M., Pedroche, J., Megias, C., Giron-Calle, J., Alaiz, M., Millan, F. and Vioque, J. Rapeseed protein hydrolysates: a source of HIV protease peptide inhibitors, Food Chem., 2004, 87, 387 – 392.

36. Delisle, J., Amiot, J., Goulet, G., Simard, C., Brisson, G. J. and Jones, J. D. Nutritive value of protein fractions extracted from soybean, rapeseed and wheat flours in the rat. Plant Foods Hu. Nutr. 1984, 34, 243 – 251.

37. Donovan, J. W. Spectrophotometric titration of the functional groups of the protein. Hirs, C. H. W. and Timasheff, S. N. Eds. XXVII D, Academic press, New York. Meth. Enzymol., 1973, 525 – 548.

38. Drobnica, L., Gemeiner, P. In "Protein Structure and Evolution"; Fox, J. L., Deyl, Z., Blazej, A., Eds. Marcel Dekker: New York, 105 – 115, 1976.

39. Eftink, M. R. In: J. R. Lakowicz (Ed.), Topics in fluorescence spectroscopy, 2nd ed., Plenum press, New York, 53 – 102, 1991.

40. Enami, I., Kamo, M., Ohta, H., Takahashi, S., Miura, T., Kusayanagi, M., Tanabe, S., Kamei, A., Motokii, A., Hiranoi, M., Tomo, T. and Satoh, K. Intramolecular Cross-linking of the Extrinsic 33-kDa Protein Leads to Loss of Oxygen Evolution but Not Its Ability of Binding to

Photosystem II and Stabilization of the Manganese Cluster. J. Biol. Chem., 1998, 273, 4629 – 4634.

41. Engelhard, M. and Evans, P. A. Kinetics of interaction of partially folded proteins with a hydrophobic dye: evidence that molten globule character is maximal in early folding intermediates. Protein. Sci., 1995, 4, 1553 –1562.

42. Ericson, M. L., Rodin, J., Lenman, M., Glimelius, K., Josefsson, L. G., Rask, L. Structure of the rapeseed 1.7S storage protein, napin, and its precursor. J. Biol. Chem., 1986, 261, 14576 – 14581.

43. Ewbank, J. J., and Creighton, T. E. Pathway of disulfide-coupled unfolding and refolding of bovine α- lactalbumin, Biochemistry, 1993, 32, 3677 – 3693.

44. Fenwick, G. R., Heany, R. K., Mullin, W. J. Glucosinolates and their breakdown products in food and food plants. CRC Crit. Rev. Food Sci. Nutr., 1983, 18(2), 123 – 201.

45. Fuchs, R. L. and Astwood, J. D. Allergenicity assessment of foods derived from genetically modified plants. Food Technol., 1996, 50, 83 - 88.

46. Ganesh, C., Shah, A. N., Swaminathan, C. P., Surolia, A. and Varadarajan, R. Thermodynamic Charecterization of the reversible, two-state unfolding of maltose binding protein, a large two-domain protein, Biochemistry, 1997, 36, 5020 – 5028.

47. Gehrig, P. M., Krzyzaniak, A., Barciszewski, J. and Biemann, K. Mass spectrometric amino acid sequencing of a mixture of seed storage proteins (napin) from *Brassica napus*, products of a multigene family. Proc. Natl. Acad. Sci., 1996, 93, 3647 – 3652.

48. Gerace, L. Nuclear export signal and the fast track to the cytoplasm. Cell, 1995, 82, 341 – 344.

49. Gerber, H. P., Seipel, K., Georgiev, O., Hofferer, M., Hug, M., Rusconi, S. and Schaffner, W. Transcriptional activation modulated by homopolymeric glutamine and proline stretches. Science, 1994, 263, 808 – 811.

50. Ghose, M. Mandal, S. Roy, B. Mandal, R. K. and Basu, G. Dielectric relaxation in a single tryptophan protein, FEBS Letters, 2001, 509, 337 – 340.

51. Gilani, G. S., Cockell, K. A. and Sepehr, E. Effects of antinutritional factors on protein digestibility and amino acid availability in foods. JAOAC international, 2005, 88(3), 967 – 987.

52. Gouda, M. D., Singh, S. A., Appu Rao, A. G., Thakur, M. S. and Karanth, N. G. Thermal inactivation of glucose oxidase: Mechanism and stabilization using additives. J. Biol. Chem., 2003, 278, 24324 – 24333.

53. Greiner-Stoeffele, T. and Grunow, M., Hahn, U. A general ribonuclease assay using methylene blue, Anal. Biochem., 1996, 240, 24 – 28.

54. Grimsley, G. R., Huyghues - Despointes, B. M. P., Pace, C. N., and Scholtz, J. M. Measuring the conformational stability of a protein. In: Purifying proteins for proteomics: A laboratory manual (ed. R. J. Simpson), Cold Spring Harbor Laboratory Press, Cold Spring Harbor, NY. 535 – 566, 2003.

55. Gurian – Sherman, D. and Lindow, S. E. Bacterial ice nucleation: Significance and molecular basis. FASEB J. 1993, 7, 1338 – 1343.

56. Gururaj Rao, A. Thesis: Chemical and Physico-Chemical studies Mustard seed (*Brassica juncea*) proteins, 1980.

57. Gururaj Rao, A. and Rao, M. S. N. Denaturation of the high molecular weight protein fraction of mustard (*Brassica juncea*) and rapeseed (*Brassica campestris*). by urea or guanidinium hydrochloride, J. Biosci., 1983, 5(4), 311 – 320.

58. Hagerman, A. and Butler, L. Condensed tannin purification and charecterization of tannin associated proteins. J. Agri. Food Chem., 1980, 28, 947 – 952.

59. Halpern, B. P. Glutamate and the Flavor of Foods. J. Nutr., 2000, 130, 910S – 914S.

60. Hass, L. F. Aldolase Dissociation into Subunits by Reaction with Succinic Anhydride. Biochemistry, 1964, 3, 535 – 541.

61. Heger, A. and Holm, L. Rapid Automatic Detection and Alignment of Repeats in Protein Sequences. Proteins: Structure, Function, and Genetics, 2000, 41, 224 – 237.

62. Herskovits, T. T., Gadegbeku, B. and Jaillet, H. On the structural stability and solvent denaturation of proteins. J. Biol. Chem., 1970, 245, 2588 – 2598.

63. Hirs, C. H. W. Detection of peptides by chemical methods. Meth. Enzymol., 1967, 11, 325 – 329.

64. Hsu, C. H., Chen, C., Jou, M.L., Lee, A. Y. L., Lin, Y. C., Yu, Y. P., Huang, W. T. and Wu, S. H. Structural and DNA-binding studies on the bovine antimicrobial peptide, indolicidin: evidence for multiple conformations involved in binding to membranes and DNA. Nucl. Acids Res., 2005, 33, 4053 – 4064.

65. Hubbard, S. J. NACCESS, version 2.1.1 computer program, Department of bimolecular sciences, MIST, (1996) Manchester, UK.

66. Huus, K., Havelund, S., Olsen, H. B., van de Weert, M. and Frokjaer. S. Thermal dissociation and unfolding of Insulin, Biochemistry, 2005, 44, 11171 – 11177.

67. Jaenicke, R. Stability and folding of domain protein. Prog. Biophys. Mol. Biol., 1999, 71, 155 – 241.

68. Joseffson, E. “Rapeseed-Cultivation, Composition, Processing and Utilization”; Appelqvist, L. A., Ohlson, R., Eds. Elsevier: Amsterdam. 354 – 377, 1972.

69. Jyothi, T. C., Singh, S. A., and Appu Rao, A. G. The contribution of ionic interactions to the conformational stability and function of polygalacturonase from *A.niger*. Int. J. Biol. Macromol., 2005, 36, 310 – 317.

70. Kawakishi, S. and Kaneko, T. Interaction of proteins with allyl isothiocyanate. J. Agric. Food Chem., 1987, 35(1), 85 – 88.

71. Kentsis, A. and Sosnick, T. R. Trifluoroethanol promotes helix formation by destabilizing backbone exposure: desolvation rather than native hydrogen bonding defines the kinetic pathway of dimeric-coiled coil folding. Biochemistry, 1998, 37, 14613 – 14622.

72. Kinnunen, T., Buhot, C., Narvanen, A., Rytkonen-Nissinen, M., Saarelainen, S., Pouvelle-Moratille, S., Rautiainen, J., Taivainen, A., Maillere, B., Mantyjarvi, R. and Virtanen, T. The immuno dominant epitope of lipocalin allergen Bos d 2 is sub optimal for human T cells. Eur. J. Immunol., 2003, 33, 1717 – 1726.

73. Kishore Kumar Murthy, N. V. and Rao, M. S. N. Interaction of allyl isothiocyanate with mustard 12S protein. J. Agric. Food Chem., 1986, 34, 448 – 452.

74. Kozlowska, H., Naczk, M., Shahidi, F. and Zadernowski, R. Phenolic acid and tannins in rapeseed and canola. In Canola and Rapeseed: Production, Chemistry, nutrition and Processing Technology, Ed. F. Shahidi, AVI book, New York, NY. 193 – 210, 1991.

75. Krzyzaniak, A., Burova, T., Haertle, T. and Baeciszewski, J. The structure and properties of napin-seed storage protein from rape (*Brassica napus*, L.). Nahrung, 1988, 42, 201 – 204.

76. Kumar, P. K., Appu Rao, A. G., Hariharaputran, S., Chandra, N. and Gowda, L. R. Molecular mechanism of dimerisation of Bowman-Birk inhibitor. Pivotal role of Asp^{76} in the dimerisation. J. Biol. Chem., 2005, 279, 30425 – 30432.

77. Kuntz Jr. I. D. and Kauzmann, W. Hydration of proteins and polypeptides Anfinsen. C. B. Edsall, J. T., Richards, F. M. (Eds.) Academic press. New York. In: Adv. Prot. Chem. 28, 239 – 345, 1974.

78. Kyte, J. and Doolittle, R. A simple method for displaying the hydropathic character of a protein. J. Mol. Biol., 1982, 157, 105 – 132.

79. Kyte, J. Structure in Protein Chemistry (2^{nd} edition), Publisher: Garland Science, Madison Avenue, New York, USA, 2007.

80. Laemmli, U. K. Cleavage of structural proteins during the assembly of the head of bacteriophage T4. Nature, 1970, 227, 680 – 685.

81. Langer, P. and Gschwendtova, K. Micro – estimation of major mustard oils and oxazolidinethione in small amounts of plant material. J. Sci. Food Agric., 1969, 20(9), 535 – 539.

82. Lazo, N. D. and Downing, D. T. Effects of Na_2SO_4 on hydrophobic and electrostatic interactions between amphipathic α-helices. J. Pep. Res., 2001, 58, 457 – 463.

83. Lee, C. J., Harrison, D. and Timasheff, S. N. Interaction of vinblastine with calf brain microtubule protein. J. Biol. Chem., 1975, 250, 9276 – 9282.

84. Lelj-Garolla, B. and Mauk, A. G. Self – association and chaperone activity of Hsp27 are thermally activated, J. Biol. Chem., 2006, 281, 8169 – 8174.

85. Liou, Y. C., Tocilji, A., Davies, P. L. and Jia, Z. Mimicry of ice structure by surface hydroxyls and water of a be ta-helix anti-freeze protein. Nature, 2000, 406, 322 – 324.

86. Lopez, M. M. and Makhatadze, G. I. Differential scanning calorimetry. Meth. Mol. Biol., 2002, 173, 113 –119.

87. Maga, G. A. Phytate: its chemistry, occurrence, food interactions, nutritional significance, and methods of analysis. J. Agri. Food Chem., 1982, 30(1), 1 – 9.

88. Main, E. R. G. Lowe, A. R. Mochrie, S. G. J. Jackson, S. E. and Regan, L. A recurring theme in protein engineering: the design, stability and folding of repeat proteins. Curr. Opin. Struct. Biol., 2005, 15, 464 – 471.

89. Maliwal, B. P., Appu Rao, A. G. and Rao, M. S. N. Spectroscopic study of the interaction of gossypol with bovine serum albumin. Int. J. Pep. Protein Res., 1985, 25, 382 – 388.

90. Mandal, S. and Mandal, R. K. Seed storage proteins and approaches for improvement of their nutritional quality by genetic engineering. Curr. Sci., 2000, 79, 576 – 589.

91. Mandal, S., Kundu, P., Roy, B. and Mandal, R. K. Precursor of the inactive 2S protein from the Indian mustard *Brassica juncea* is a novel trypsin inhibitor. J. Biol. Chem., 2002, 277, 37161 – 37168.

92. Marczak, E. D., Usui, H., Fujita, H., Yang, Y., Yokoo, M., Lipkowski, A. W. and Yoshikawa, M. New antihypertensive peptides isolated from rapeseed. Peptides, 2003, 24, 791 – 798.

93. Mastsushima, N., Danno, G., Takezawa, H. and Izumi, Y. Three-dimensional structure of maize alpha - zein proteins studied by small-angle x-ray scattering. Biochem. Biophys. Acta, 1997, 1339, 14 – 22.

94. Matsumura. M., Signor, G. and Matthews, B. W. Substantial increase of protein stability by multiple disulphide bonds, Nature, 1989, 342, 291 – 293.

95. Matthäus, B., and Fiebig, H. J. Simultaneous determination of isothiocyanates, indoles, and oxazolidinethiones in myrosinase digests of rapeseeds and rapeseed meal by HPLC, J. Agric. Food Chem., 1996, 44, 3894 – 3899.

96. Matthews, C. R. and Crisanti, M. M. Urea-induced unfolding of the alpha subunit of tryptophan synthase: Evidence for a multi-state process, Biochemistry, 1981, 20, 784 – 792.

97. McClure, W. O. and Edelman, G. M. Fluorescent probes for conformational states of proteins. The binding of 2-p-toluedinylnaphthalene-6-sulfanate to α-chymotrypsin. Biochemistry, 1967, 6, 559 – 566.

98. Menendez-Arias, L., Dominguez, J., Moneo, I. and Rodriduez, R. Epitope mapping of the major allergen from yellow mustard seeds, Sin a I. Mol. Immunol., 1990, 27, 143 – 150.

99. Menendez-Arias, L., Monsalve, R. I., Gavilanes, J. G. and Rodriguez, R. Molecular and spectroscopic characterization of a low molecular weight seed storage protein from yellow mustard (*Sinapis alba*). Int. J. Biochem., 1987, 19, 899 – 907.

100. Monsalve, R. I., Villaba, M., Lopez-Otin, C. and Rodriguez, R. Structural analysis of the small chain of the 2S albumin, napin nIII, from rapeseed. Chemical and spectroscopic evidence of an intramolecular bond formation. Biochim. Biophys. Acta, 1991, 1078, 265 – 272.

101. Monsolve, R. I., Gonzalez, M. A., Arias, L. M., Otin C. L., Villalba, M. and Rodriguez, R. Charecterization of a new oriental-mustard (*Brassica juncea*) allergen, Bra j IE: detection of an allergenic epitope. Biochem. J., 1993, 293, 625 – 632.

102. Moreno, F. J., Mellon, F, A., Wickham, M. S. J., Bottrill, A. R. and Clare Mills, E. N. Stability of the major allergen brazil nut 2S albumin (Ber e 1) to physiologically relevant in vitro gastrointestinal digestion. FEBS journal, 2005, 272, 341 – 352.

103. Moro, A., Gatti, C. and Delorenzi, N. Hydrophobicity of whey protein concentrates measured by fluorescence quenching and its relation with surface functional properties, J. Agric. Food. Chem., 2001, 49, 4784 – 4789.

104. Mothes, R., Schwenke, K. D., Zirwer, D. and Gast, K. Rapeseed protein-polyanion interactions. Soluble complexes between the 2S protein fraction (napin) and phytic acid Die Nahrung, 1990, 34(4) 375 – 385.

105. Muntz, K. Deposition of storage proteins. Plant Mol. Biol., 1998, 38, 77 – 99.

106. Muren, E., Ek, B., Bjork, I. and Rask, L. Structural comparison of the precursor and the mature form of napin, the 2S storage protein in *Brassica napus*. Eur. J. Biochem., 1996, 242, 214 – 219.

107. Murphy, K. P., Privalov, P. L. and Gill, S. J. Common features of protein unfolding and dissolution of hydrophobic compounds. Science, 1990, 247, 559 – 561.

108. Myers, J. K., Pace, C. N. and Scholtz, J. M. Denaturant m- values and heat capacity changes: Relation to changes in accessible surface areas of protein unfolding, Protein Sci., 1995, 4, 2138 – 2148.

109. Naczk, M., Amarowicz, R., Zadernowski, R. and Shahidi, F. Antioxidant capacity of phenolics from canola hulls as affected by different solvents. In: Phenolic compounds in foods and natural health products. Ed. Shahidi, F. and Chi Tang Ho. ACS symposium series 909. 57 – 66, 2006.

110. Naczk, M., Amarowicz, R., Sullivan, A. and Shahidi, F. Current research developments on polyphenolics of rapeseed/canola: a review. Food Chem. 1998, 62, 489 – 502.

111. Nakai, S. and Li-Chan, E. Recent advances in structure and function of food proteins: QSAR approach. CRC Crit. Rev. Food Sci. Nutr., 1993, 33, 477 – 499.

112. Neet, K. E. and Timm, D. E. Conformational stability of dimeric proteins: Quantitative studies by equilibrium denaturation, Protein Sci., 1994, 3, 2167 – 2174.

113. Neumann, G. M., Condron, R., Thomas, I. and Polya, G. M. Purification and sequencing of multiple forms of *Brassica napus* seed napin small chains that are calmodulin antagonists and substrates for plant calcium-dependent kinase. Biochim. Biophys. Acta, 1996, 1295[a], 23 – 33.

114. Neumann, G. M., Condron, R., Thomas, I. and Polya, G. M. Purification and sequencing of multiple forms of *Brassica napus* seed napin large chains that are calmodulin antagonists and substrates for plant calcium-dependent kinase. Biochim. Biophys. Acta, 1996, 1295[b], 34 – 43.

115. Ngai, P. H. K. and Ng, T. B. Isolation of a napin – like polypeptide with potent translation-inhibitory activity from Chinese cabbage (*Brassica parachinensis* cv green-stalked) seeds. J. Pep. Sci., 2003, 9, 442 – 449.

116. Nicholson, E. M. and Scholtz, J. M. Conformational stability of the *Escherichia coli* HBr protein: test of the linear extrapolation method and a thermodynamic characterization of cold denaturation, Biochemistry, 1996, 35, 11369 –11378.

117. Nishimura, C., Uversky, V. N. and Fink, A. L. Effect of salts on the stability and folding of staphylococcal nuclease. Biochemistry, 2001, 40, 2113 – 2128.

118. Nissen, J. A. Determination of degree of hydrolysis of food protein hydrolysates by trinitrobenzene sulfonic acid. J. Agri. Food Chem., 1979, 27(6), 1256 – 1262.

119. Nozaki, Y. The preparation of Guanidinium hydrochloride. Meth. Enzymol., 1972, 26, 43 – 50.

120. Ohta, Y., Takatani, K., and Kawakishi, S. Kinetic and thermodynamic analysis of the cyclodextrin - Allyl isothiocyanate inclusion complex in an aqueous solution. Biosci. Biotechnol. Biochem., 1999, 63(7), 190 – 193.

121. Onaderra, M., Monsalve, R. I., Manchero, J. M., Villalba, M., Martinez del pozo, A., Gavilanes, J.G. and Rodriguez, R. Food mustard allergen interaction with phospholipid vesicles. Eur. J. Biochem., 1994, 225, 609 – 615.

122. Osborne, T. B. The Vegetable Proteins. Monography in biochemistry (Longmans Green & Co. London). 2 nd Eds. 1924.

123. Pace, C. N. Contribution of the hydrophobic effect to globular protein stability. J. Mol. Biol., 1992, 226, 29 – 35.

124. Pantoja-Uceda, D., Palomares, O., Bruix, M., Villalba, M., Rodriguez, R., Rico, M. and Santoro, J. Solution structure and stability against digestion of rproBnIb, a recombinant 2S albumin from rapeseed: Relationship to its allergenic properties. Biochemistry, 2004, 43, 16036 – 16045.

125. Pecháček, R., Velišek, J. and Hrabcová, H. Decomposition products of allyl iso thiocyanate in aqueous solutions. J. Agric. Food Chem., 1997, 45, 4584 – 4588.

126. Polya, G. The structure and sites of action of plant defensive proteins. Recent Res. Devel. In Phytochem., 1997, 1, 95 – 110.

127. Polya, G. M., Chandra, S. and Condron, R. Purification and sequencing of radish seed calmodulin antagonists phosphorylated by calcium-dependent protein kinase. Plant physiol., 1993, 101, 545 – 551.

128. Pradeep, L., Udgaonkar, B. J. Effect of salt on the Urea- unfolded form of barstar probed by m value measurements. Biochemistry, 2004, 43, 11393 –11402.

129. Prakash, S., and Hinata, K. Taxonomy, cytogenetics and origin of crop *Brassicas*. A review. Opera Bot., 1980, 55, 1 – 57.

130. Prakash, V. and Rao, M. S. N. Physicochemical properties of oilseed proteins. CRC Crit. Rev. Biochem., 1986, 20(3), 265 – 364.

131. Privalov, P. L. and Gill, S. J. Stability of protein structure and hydrophobic interaction. Adv Protein Chem., 1988, 39, 191 – 234.

132. Privalov, P. L. and Khechinashivli, N. N. A thermodynamic approach to the stabilization of globular protein structure: A calorimetric study. J. Mol. Biol., 1974, 86, 665 – 684.

133. Privalov, P. L. Intermediate states in protein folding, J. Mol. Biol., 258 1996, 707 – 725.

134. Rajendran, S. and Prakash, V. Interaction of myoinositol hexaphosphate (MIHP) with beta – globulin from *Sesamum indicum* L. Int. J. Peptide protein Res., 1993[b], 42, 78 – 83.

135. Rajendran, S. and Prakash, V. Kinetics and thermodynamics of the mechanism of interaction of sodium phytate with alpha – globulin. Biochemistry, 1993[a], 32(13), 3474 – 3478.

136. Razvi, A. and Scholtz, J. M. Review: Lessons in stability from thermophilic proteins. Protein Sci., 2006, 15, 1569 – 1578.

137. Rico, M., Bruix, M., Gonazalez, C., Monsalve, R.I. and Rodriguez, R. ^{1}H NMR assignment and global fold of napin BnIb, a representative 2S albumin seed protein. Biochemistry, 1996, 35, 15672 – 15682.

138. Riddles, P. W., Blakeley, R. L. and Zerner, B. Reassessment of Ellman's reagent. Meth. Enzymol., 1983, 91, 49 – 60.

139. Rödin, J., and Rask, L. Characterization of the 12S storage protein of Brassica napus (cruciferin): Disulfide bonding between subunits. Physiologia Plantarum. 1990, 79(3), 421 – 426.

140. Santoro, M. M., Liu, Y., Khan, S. M. A., Li Xiang Hou and Bolen, D. W. Increased thermal stability of proteins in the presence of naturally occurring osmolytes, Biochemistry, 1992, 31, 5278 – 5283.

141. Sashidhar, R. B., Capoor, A. K. and Ramana, D. Quantitation of ε-amino group using amino acids as references standards by trinitrobenzene sulfonic acid. J. Immunol. Meth., 1994. 167, 121 – 127.

142. Scatchard, G. The attractions of proteins for small molecules and ions. Ann. NY Acad. Sci. 1949, 51, 660 – 672.

143. Schmidt, I., Renard, D., Rondeau, D., Richomme, P. and Viguier axelos, M. A. Detailed physicochemical characterization of the 2S storage protein from rape (*Brassica napus*, L.). J. Agric. Food Chem., 2004, 52, 5995 – 6001.

144. Schneuwly, S., Kuroiwa, A., Baumgartner, P. and Gehring, W. J. Structural organization and sequence of the homeotic gene antennapedia of *Drosophila melanogaster*. EMBO J., 1986, 5, 733 – 739.

145. Schwarz, F. P., Puri, K. and Surolia, A. Thermodynamics of the binding of galactopyronoside derivatives to the basic lectin from winged bean (*Psophocarpus tetrogonolobus*), J. Biol. Chem., 1991, 266, 24344 – 24350.

146. Schwenke, K. D., Mothes, R., Marzilger, K., Borowska, J. and Kozlowska, H. Rapeseed protein polyanion interactions – turbidometric studies in systems with phosphate-containing polyanions: phytic acid and octametaphosphate. Die Nahrung, 1987, 31(10), 1001 – 1013.

147. Schwenke, K. D., Schultz, M., Linow, K. J., Gast, K. and Zirwer, D. Hydrodynamic and quasi-elastic light scattering studies on the 12S globulin from rapeseed. Int. J. Pept. Protein Res., 1980, 16(1), 12 – 18.

148. Schwimmer, S. Spectral changes during the action of myrosinase on sinigrin. Acta Chem. Scand., 1961, 15, 535 – 544.

149. Shahidi, F. and Gabon J. E. Fate of sinigrin in methanol/ ammonia/ water - hexane extraction of *B. juncea* mustard seed, J. Food Sci., 1990, 55(3), 793 – 795.

150. Shahidi, F., and Naczk, M. An overview of the phenolics of canola and rapeseed: Chemical, sensory and nutritional significance. JAOCS., 1992, 69(9), 917 – 924.

151. Shaw C. H. and Ryan A. J. Genomic sequence of a 12S seed storage protein from oilseed rape (*Brassica napus*), Nucleic Acids Res., 1989, 17, 3584 – 3584.

152. Shewry, P. R. and Halford, N. G. Cereal seed storage proteins: structures, properties and role in grain utilization, J. Exprt. Bot., 2002, 53, 947 – 958.

153. Shewry, P. R. Plant storage proteins, Biol. Rev., 1995, 70, 375 – 426.

154. Shewry, P. R., Napier, J. A. and Tatham, A. S. Seed Storage Proteins: Structures and Biosynthesis. The Plant Cell, 1995, 7, 945 – 956.

155. Shofran, B. G., Purrington, S. T., Breidt, F. and Fleming, H. P. Antimicrobial properties of sinigrin and its hydrolysis products. J. Food Sci., 1998, 63(4), 621 – 624.

156. Singh, R. R. and Appu Rao, A. G. Reductive unfolding and oxidative refolding of a Bowman-Birk inhibitor from horse gram seeds (*Dolichos biflorus*): Evidence for “hyperreactive” disulfide bonds and rate limiting nature of disulfide isomerization in folding. Biochim. Biophys. Acta, 2002, 1597(20), 280 – 291.

157. Sinha, S., and Surolia, A. Oligomerization endows enormous stability to soybean agglutinin: A comparison of the stability of monomer and tetramer of soybean agglutinin. Biophys. J., 2005, 88, 4243 – 4251.

158. Sluyterman, L. A. and Wijdenes, J. An unusual type of enzyme inhibition. Biochimica et Biophysica Acta, 1973, 321, 697 – 699.

159. Smith, C., van Megen, W., Twaalfhoven, L. and Hitchcock, C. the determination of trypsin inhibitor levels in foodstuffs. J. Sci. Food Agric., 1980, 31, 341 – 350.

160. Spande, T. F., and Witkop, B. W. Determination of tryptophan content of proteins with N- Bromosuccinamide. Meth. Enzymol., 1967, 11, 498 – 506.

161. Spencer, C. M., Cai, Ya, Martin, R., Gaffney, S. H., Goulding, P. N., Magnolato, D., Lilley, T. H. and Haslam, E. Polyphenol complexation - Some thoughts and observations. Phytochem., 1988, 27, 2397 – 2409.

162. Sudharshan, E. and Appu Rao, A. G. Involvement of cysteine residues and domain interactions in the reversible unfolding of lipoxygenases - 1. J. Biol. Chem., 1999, 274, 35351 – 35358.

163. Tabe, L. M., Higgins, C. M., McNabb, W. C., and Higgins, T. J. V. Genetic engineering of grain and pasture legumes for improved nutritive value. Genetika, 1993, 90, 181 – 200.

164. Tangendjaja, B., Buckle, K. A. and Wootton, M. Analysis of phytic acid by high performanance liquid chromatography, J. Chromatogr., 1980, 197, 274 – 277.

165. Templeman, T. S., Demaggio, A. E., and Stetler, D.A. Biochemistry of fern spore germination: Globulin storage proteins in Matteuccia struthiopteris L. Plant Physiol., 1987, 85, 343 – 349.

166. Terras, F. R. G., Schoofs, H. M. E., De Bolle, M. F. C., Fred Van Leuven, Rees, S. B. Jozef Vanderleyden, Cammue, B. P. A. and Broekaert, W. F. Analysis of two novel classes of plant antifungal proteins from Radish (*Raphanus sativus* L.) seeds, J. Biol. Chem., 1992, 267, 15301 – 15309.

167. Terras, F. R. G., Sophie Torrekens, Fred Van Leuven, Osborn, R. W., Jozef Vanderleyden, Cammue, B. P. A. and Broekaert, W. F. A new family of basic cysteine - rich plant antifungal proteins from Brassicaceae species. FEBS letters, 1993, 316, 233 – 240.

168. Thiyam, U. Upcoming challenges of Indian mustard and rapeseed meal - current global perspectives. Indian Food Industry, 22(2), 2003.

169. Thompson, L. U. Reduction of phytic acid concentration in protein isolates by acylation techniques, JAOCS., 1987, 64(12), 1712 – 1717.

170. Usha, R., Maheshwari, R., Dhathathreyan, A. and Ramasami, T. Structural influence of mono and polyhydric alcohols on the stabilization of collagen. Colloids and Surfaces B: Biointerfaces, 2006, 48, 101 – 105.

171. Uversky, V. N. and Ptitsyn, O. " Partly folded" state, a new equilibrium state of protein, molecules: four-state guanidinium chloride-induced unfolding of β-lactamase at low temperature. Biochemistry, 1994, 33, 2782 – 2791.

172. Uversky, V. N. Use of fast size-exclusion liquid chromatography to study the unfolding of proteins, which denature through the molten globule. Biochemistry, 1993, 32, 13288 – 13298.

173. Velasco, L. and Möllers, C. Selection for reduced sinapic acid esters content in rapeseed, at 10th international Rapeseed congress, Canberra, Australia, 1999.

174. Vuorela, S., Meyer, A. S. and Heinonen, M. Impact of isolation on the antioxidant activity of rapeseed meal phenolics. J. Agric. Food Chem., 2004, 52, 8202 – 8207.

175. Yadav, S. and Ahmad, F. A new method for the determination of stability parameters of proteins from their heat-induced denaturation curves. Anal. Biochem., 2000, 283, 207 – 213.

176. Yang, J. T., Wu, C. S. and Martinez, H. M. Calculation of protein conformation from circular dichroism. Meth. Enzymol., 1986, 130, 208 – 269.

177. Youle, R. and Huang, A. H. C. Occurrence of low molecular weight and high cysteine containing albumin storage proteins in oilseeds of diverse species. Ameri. J. Bot., 1981, 68 (1), 44 – 48.

178. Zadernowski, R. Studies on phenolic compounds of rapeseed flours. Acta Acad. Agri. Technol. Olst., 1987, 21F, 1 – 55.